

MECHANISM OF CONFORMATIONAL CHANGES OF ARP2/3 COMPLEX IN THE
BRANCHED ACTIN NUCLEATION PATHWAY

by

MAX RODNICK-SMITH

A DISSERTATION

Presented to the Department of Chemistry and Biochemistry
and the Graduate School of the University of Oregon
in partial fulfillment of the requirements
for the degree of
Doctor of Philosophy

June 2016

DISSERTATION APPROVAL PAGE

Student: Max Rodnick-Smith

Title: Mechanism of Conformational Changes of Arp2/3 Complex in the Branched Actin Nucleation Pathway

This dissertation has been accepted and approved in partial fulfillment of the requirements for the Doctor of Philosophy degree in the Department of Chemistry and Biochemistry by:

Kenneth Prehoda	Chairperson
Bradley Nolen	Advisor
Victoria DeRose	Core Member
Kryn Stankunas	Institutional Representative

and

Scott L. Pratt	Dean of the Graduate School
----------------	-----------------------------

Original approval signatures are on file with the University of Oregon Graduate School.

Degree awarded June 2016

© 2016 Max Rodnick-Smith

DISSERTATION ABSTRACT

Max Rodnick-Smith

Doctor of Philosophy

Department of Chemistry and Biochemistry

June 2016

Title: Mechanism of Conformational Changes of Arp2/3 Complex in the Branched Actin Nucleation Pathway

Branched actin networks play an important role in cellular processes ranging from cell motility, endocytosis, and adhesion. The Actin-related protein 2/3 (Arp2/3) complex nucleates actin branches from the sides of existing actin filaments. Arp2/3 complex is highly regulated and requires association with ATP, actin monomers, actin filaments and a class of proteins called nucleation promoting factors (NPFs) to undergo an activating conformational change where the actin-related subunits, Arp2 and Arp3, arrange into a filament-like conformation that templates a new actin branch. While some progress has been made, the individual roles of each of these factors on the activating conformational change is poorly understood. In addition, it is still unclear how Arp2/3 complex is held in its inactive state, which is vital for understanding how activation occurs. In this dissertation, we dissect key interfaces in Arp2/3 complex that are responsible for holding it in an inactive state, and specifically evaluate the roles of ATP and WASP, the canonical NPF, in the activating conformational change of Arp2/3 complex.

In chapter II, we investigated the contacts made between the Arp2 and Arp3 subunits in their inactive state, and the role of ATP in stimulating the active conformation. We found that two key interfaces, the $\alpha E/\alpha F$ loop in Arp2 and the C-

terminus of Arp3, a conserved extension not present in actin, are vital for holding Arp2/3 complex in its autoinhibited state. Evaluation of the role of ATP demonstrated that binding of ATP is required for the activating conformational change and displaces the Arp3 C-terminus, an important step in destabilization of the inactive state.

In chapter III, we investigated the mechanism of WASP-induced conformational changes using an engineered crosslinking assay that only forms crosslinks when Arp2/3 is in its active conformation. We discovered that many WASP-related proteins are capable of stimulating this conformational change through a mechanism that involves displacement of the Arp3 C-terminus. Interestingly, purified Arp2/3 complex crosslinked in the active conformation was hyperactive compared to WASP-mediated activation, demonstrating that WASP activation limits nucleation and that actin monomer delivery is not required for nucleation.

This dissertation contains unpublished co-authored material.

CURRICULUM VITAE

NAME OF AUTHOR: Max Rodnick-Smith

GRADUATE AND UNDERGRADUATE SCHOOLS ATTENDED:

University of Oregon, Eugene, OR
University of Texas, Austin, TX
University of Colorado, Boulder, CO

DEGREES AWARDED:

Doctor of Philosophy, Chemistry, 2016, University of Oregon
Bachelor of Science, Biochemistry, 2011, University of Texas

AREAS OF SPECIAL INTEREST:

Biochemistry
Genetics

PROFESSIONAL EXPERIENCE:

Graduate Teaching Assistant, Department of Chemistry, University of Oregon,
Eugene, OR, 2011-2016

PUBLICATIONS:

Rodnick-Smith, M., Luan, Q., Liu, S.-L. & Nolen, B.J. (2016) The role and structural mechanism of WASP-triggered conformational changes in branched actin filament nucleation by Arp2/3 complex. *PNAS Plus* (submitted)

Rodnick-Smith, M., Liu, S.-L., Balzer, C.J., Luan, Q., & Nolen, B.J. (2016) Identification of an ATP-controlled allosteric switch that controls actin filament nucleation by Arp2/3 complex. *Nature Communications* (submitted)

Helgeson, L. A, Prendergast, J. G., Wagner, A. R., **Rodnick-Smith, M.**, & Nolen, B. J. (2014). Interactions with actin monomers, actin filaments, and Arp2/3 complex define the roles of WASP family proteins and cortactin in coordinately regulating

branched actin networks. *The Journal of Biological Chemistry*, 289(42), 28856–69.
doi:10.1074/jbc.M114.587527

ACKNOWLEDGMENTS

First, I would like to thank my advisor, Brad Nolen, for his great mentorship throughout my time as a graduate student. Brad has taught me so much about how to be a good scientist and communicator and I believe the skills I have learned under his guidance will be invaluable throughout my professional career. I want to thank the other members of the Nolen lab, past and present, particularly Luke Helgeson and Byron Hetrick for their patience and mentorship in getting me started as a graduate student. I want to thank my committee for their support and encouragement, the University of Oregon Chemistry department for giving me the opportunity to pursue this degree and my undergraduate mentors, Dr. Karen Browning and Dr. Grace Choy for taking me on as an undergraduate researcher which helped solidify my passion for biochemistry. I am very grateful to all the friendships I have made in my time here in Eugene. All the fun camping trips, hikes, soccer matches, game nights, Oregon football games and car trips have made this some of the best years of my life and I know it will be very hard to leave this city. Lastly, but certainly not least, I want to thank my family for their never-ending love and encouragement throughout my life. The values and work ethic they have instilled in me has shaped who I am today, and I would not be in the position I am in without their support.

I dedicate this work to my mother Amie, my father Larry
and my brother Zane.

TABLE OF CONTENTS

Chapter	Page
I. INTRODUCTION	1
II. IDENTIFICATION OF AN ATP-CONTROLLED ALLOSTERIC SWITCH THAT CONTROLS ACTIN FILAMENT NUCLEATION BY ARP2/3 COMPLEX.....	20
Introduction.....	20
Results.....	23
Discussion.....	41
Materials and Methods.....	45
Bridge to Chapter III.....	50
III. THE ROLE AND STRUCTURAL MECHANISM OF WASP-TRIGGERED CONFORMATIONAL CHANGES IN BRANCHED ACTIN FILAMENT NUCLEATION BY ARP2/3 COMPLEX	51
Introduction.....	51
Results.....	56
Discussion.....	75
Bridge to Chapter IV.....	82
IV. SUMMARY AND CONCLUDING REMARKS	83
APPENDICES	90
A. SUPPLEMENTARY MATERIAL FOR CHAPTER II.....	90
B. SUPPLEMENTARY MATERIAL FOR CHAPTER III.....	104

Chapter	Page
REFERENCES CITED.....	125
A. CHAPTER I.....	125
B. CHAPTER II.....	133
C. CHAPTER III.....	139
D. APPENDIX A.....	143
E. APPENDIX B.....	144

LIST OF FIGURES

Figure	Page
CHAPTER I	
1. Schematic of actin nucleation and the three classes of nucleators.....	4
2. Structure of Arp2/3 complex and conformational pathway to branch formation..	6
CHAPTER II	
1. Cartoon model of Arp2/3 complex activation	22
2. The Arp3 C-terminal tail is a conserved structural feature required for autoinhibition of Arp2/3 complex	26
3. Deletion of the Arp3 C-terminal tail causes defects in endocytic actin patches and in the uptake of FM4-64.....	28
4. The Arp3 C-terminus is required to prevent formation of the short pitch conformation	30
5. Destabilization of the splayed Arp2-Arp3 interface stimulates the short pitch conformation and activates Arp2/3 complex	33
6. The Arp3 C-terminus is an allosteric molecular switch that locks the complex in the inactive (splayed) conformation	37
7. Release of the tip of the Arp3 C-terminus from the barbed end groove stimulates formation of the short pitch conformation	40
CHAPTER III	
1. Hypothesized CA binding mode and schematic of short pitch crosslinking assay	57
2. Stimulation of the short pitch conformation is a conserved feature of WASP family NPFs.....	60
3. CA binding to both Arp2 and Arp3 is important for stimulating the short pitch conformation change.....	63
4. Locking Arp2/3 complex into the short pitch conformation bypasses the requirement for NPFs in activation	65

Figure	Page
5. The short pitch crosslinked complex is more active than WASP-activated uncrosslinked complex.....	67
6. Residues in the C region tune are important for stimulating the short pitch conformational change.....	70
7. WASP-CA fused to the C-terminus of Arp2 or Arp3 blocks binding of soluble WASP-VCA to the CA-fusion subunit.....	72
8. WASP competes with the Arp3 C-terminus for binding the barbed end groove of Arp3	76

CHAPTER I

INTRODUCTION

The Actin Cytoskeleton Plays an Essential Role in Living Cells

The cytoskeleton is an important biological network composed of hundreds of individual proteins. The cytoskeleton is a dynamic protein network, of which actin is a central component. Actin plays a role in maintaining cell shape, sensing the surrounding environment, uptake and release of chemicals through endocytosis and exocytosis respectively, cellular motility, and transporting cellular cargo, among many other processes (Welch & Mullins, 2002)(Pollard & Cooper, 2009).

Actin is a ~42kD protein that binds ATP and self-assembles into non-covalent polymers called filaments. Actin filaments are polar, where assembly is slow from the pointed or minus (-) end and more rapid from the barbed or plus (+) end (Pollard, 1986). This polarity is important for many actin binding proteins, such as transport myosins V and VI, which “walk” along filaments toward the barbed and pointed ends of filaments, respectively (Li & Gundersen, 2008). Shortly after incorporation into a filament, actin subunits rapidly hydrolyze ATP ($k_{\text{hydrolysis}}=0.3\text{s}^{-1}$) to create ADP-Pi actin and the phosphate is released slowly ($k_{\text{release}}=0.003\text{s}^{-1}$) to form ADP actin (Fujiwara et al., 2007). The nucleotide state of filaments is critical for the function of the cytoskeleton, thought to serve as a timing mechanism to determine the age of actin filaments (Le Clainche et al., 2003)(Martin et al., 2006)(Ingerman et al., 2013). Proteins such as ADF/cofilin recognize the conformational changes that occur on actin filaments during ATP hydrolysis and

phosphate release. Specifically ADF/cofilin binds and severs ADP-actin preferentially over ATP or ADP-Pi-Actin by about two-fold, enhancing filament turnover (Carrier et al., 2012).

The geometry of actin networks vary depending on the function. For example, during muscle contraction, linear actin networks are constricted by muscle myosins, where the actin filaments slide past one another to generate muscle movement (Geeves & Holmes, 1999). In contrast, actin networks are very different at the leading edge of a lamellipodia, which is a large protrusion of the membrane important for cell motility. The actin networks in this structure are highly dendritic, which is important for generating the force necessary for cell movement (Pollard, 2007). In addition to the severing of filaments by ADF/cofilin mentioned above, actin networks are tightly coordinated by over a hundred regulatory proteins. Profilin and thymosin- β 4 (T β 4) are responsible for maintaining a pool of unpolymerized actin, where T β 4 sequesters actin monomers by binding to both the barbed and pointed end of a single actin monomer, rendering it incapable of forming new filaments by preventing interactions with either ends of existing filaments (Mannherz & Hannappel, 2009). Profilin facilitates nucleotide exchange from ADP to ATP-actin and also prevents formation of new filaments, but in contrast to T β 4, only binds to the barbed end of actin monomers, allowing association of the free pointed end to the growing barbed end of actin filaments, where profilin subsequently dissociates from the actin monomer (Dominguez & Holmes, 2011). In dense branched networks, capping proteins will bind to the growing barbed ends of filaments, preventing further association of new monomers and providing the structural rigidity needed for force generation by these networks (Edwards et al., 2014). Filaments

can also be cross-linked into dense arrays by, most commonly, proteins belonging to the calponin-homology domain family like fimbrin, α -actinin, or spectrin (Gimona et al., 2002). Not only is controlling the various archetypes of actin networks very important, but controlling when and where actin polymerization is initiated is vital for cellular function and survival.

Formation of actin filaments *de novo* occurs through a process known as nucleation. During nucleation, actin monomers (globular or G-actin) must overcome a large thermodynamic barrier to form actin filaments (F-actin) due to the instability of small actin oligomers (Sept & McCammon, 2001). Despite high cellular actin concentrations favoring the filamentous state, kinetic modeling suggests that actin dimers and trimers rapidly disassemble into their monomeric forms, but once a tetramer forms, the actin oligo is stable and forms a filament to which new actin monomers can rapidly associate at a diffusion-limiting rate (Pollard, 1986)(Sept & McCammon, 2001). To control when and where actin filaments are generated, cells rely on three sets of actin “nucleators” to regulate this process; formins, tandem-WH2/V nucleators, and Arp2/3 complex (Figure 1)(Pollard, 2007)(Campellone & Welch, 2010).

Formins are proteins that form homodimers and are composed of regulatory, FH1 and FH2 domains (Pollard, 2007). Dimerization occurs through the FH2 domain, with each dimer binding two actin monomers, forming a donut-shaped hole that interacts with the barbed ends of filaments (Otomo et al., 2005). Nucleation occurs through this stable actin dimer, and the formin remains bound to the barbed end (Pruyne, 2002)(Breitsprecher et al., 2012), where it recruits profilin-bound actin monomers to the growing barbed end through its FH1 domain (Chang et al., 1997). Tandem WH2 proteins,

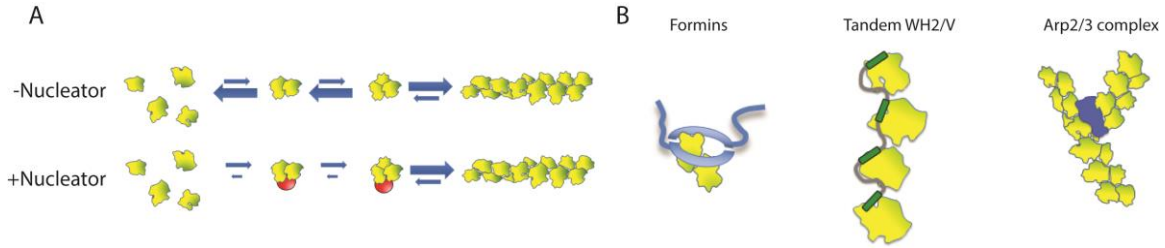


Figure 1: Schematic of actin nucleation and the three classes of nucleators.

A. Cartoon representation of actin nucleation in the presence and absence of an actin nucleator (represented by red spheres). The presence of a nucleator prevents dissociation of actin dimers and trimers, favoring formation of a new filament. **B.** Representation of the three classes of actin nucleators; formins, tandem WH2/V nucleators, and the Arp2/3 complex.

such as Spire and Cobl bind actin monomers through their WH2 regions (also called V or Verprolin-homology) and nucleate actin filaments by tethering these monomers in close proximity, speeding up the nucleation process (Campellone & Welch, 2010). The difference between tandem WH2/V nucleators and formins are that tandem WH2/V nucleators dissociate after nucleation, while formins will remain associated with the barbed end of the filament, continually adding new actin subunits and speeding up the elongation rate. These nucleators sometimes work in concert with formins. For example, *Drosophila* Spire has been shown to associate with the formin Cappuccino (Quinlan et al., 2007), where it has been proposed that one formin dimer binds two Spire molecules and nucleates 8 actin monomers. Spire then dissociates, thereby “handing off” the nucleus to Cappuccino, allowing it to processively elongate the new filament (Sitar et al., 2011). The last class of nucleators, Arp2/3 complex will be discussed in the following section.

The Arp2/3 Complex is the Key Nucleator of Actin Branches in the Cell

The Actin Related Protein 2/3 (Arp2/3) complex is unique among actin nucleators in that it normally nucleates branched actin filaments (Amann & Pollard, 2001a)(Amann & Pollard, 2001b)(Egile et al., 2005)(Wagner et al., 2013). Arp2/3 complex was initially discovered through a profilin-affinity column of *Acanthamoeba castellanii* extract where two polypeptides (associated with five other proteins), Arp2 and Arp3, contained sequence homology to yeast actins, suggesting it may have a role in regulating the actin cytoskeleton (Machesky et al., 1994). Soon after its initial discovery, homologous complexes were purified from yeast (Winter et al., 1997), mammals (Welch et al., 1997) and *Xenopus* egg extracts (Ma et al., 1998). Arp2/3 complex was shown to have nucleation activity, however these experiments required high concentrations of complex (Mullins et al., 1998). Later, groups showed that proteins such as ActA from *Listeria monocytogenes* and human Scar potently induced actin polymerization combined with Arp2/3 complex, suggesting the complex needed to be activated in order to nucleate actin (Welch et al., 1998)(Machesky et al., 1999). Electron microscopy and total internal reflection fluorescence microscopy experiments showed that Arp2/3 complex creates actin branches, confirming that it was a new class of nucleator (Amann & Pollard, 2001a)(Amann & Pollard, 2001b)(Egile et al., 2005).

The first crystal structure of *Bos taurus* Arp2/3 complex confirmed that the Arp2 and Arp3 subunits were structurally similar to actin and the five other subunits, ARPC1-5, form the scaffold that holds the Arp subunits in place (Figure 2A) (Robinson et al., 2001). Interestingly, the Arp subunits were positioned in a conformation that was neither compatible with a long pitch (end to end) nor a short pitch (side to side) conformation similar to actin dimers that have been observed in structures of actin filaments. This

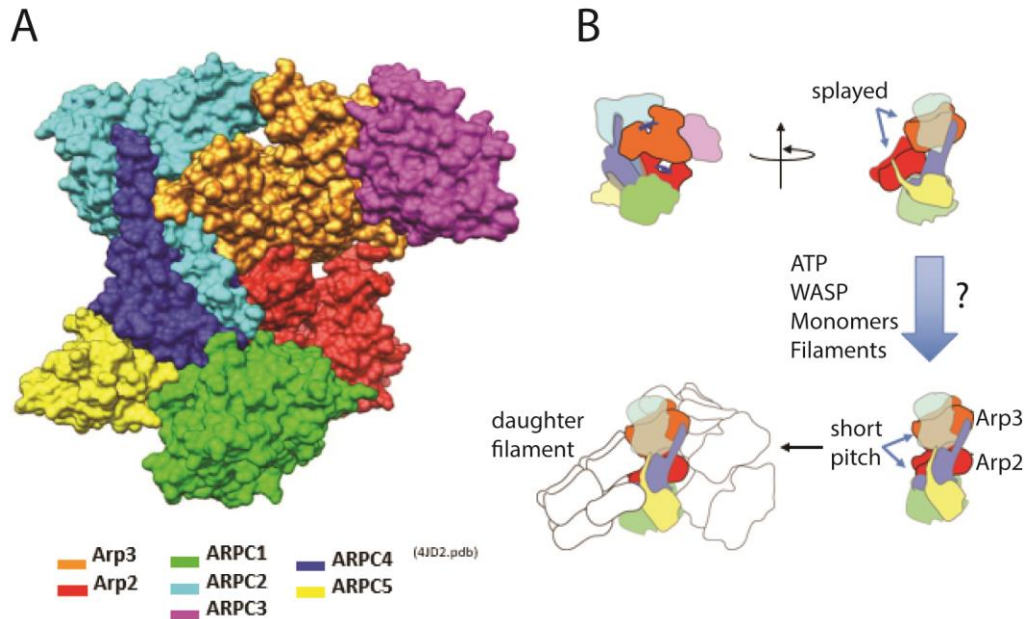


Figure 2: Structure of Arp2/3 complex and conformational pathway to branch formation.

A. Crystal structure of *Bos taurus* Arp2/3 complex with subunits distinguished by color. The structure of Arp2/3 complex with GMF (not shown) was used due to disorder of Arp2 in other structures. **B.** Cartoon of the conformational pathway for branch formation. Arp2/3 complex in the inactive, or splayed, conformation and undergoes a conformational change to the short pitch conformation at a branch junction in the presence of ATP, WASP, actin monomers and actin filaments, although the contribution of each is unknown.

conformation explained why Arp2/3 complex had no nucleation activity on its own and formed the hypothesis that the complex must undergo a large conformational change in order to nucleate an actin branch (Robinson et al., 2001). Since then, low-resolution electron microscopy reconstructions of Arp2/3 complex at a branch junction support a model where Arp2 and Arp3 move from the inactive (or “splayed”) conformation to a conformation resembling a “short pitch” actin dimer, providing the template for additional actin subunits to associate into a filament (Rouiller et al., 2008). Consistent with the hypothesis that the Arp2 and Arp3 subunits form the first two actin subunits in a

daughter filament, purified *Schizosaccharomyces pombe* Arp2/3 complex lacking the Arp2 subunit was unable to nucleate actin branches (Nolen & Pollard, 2008).

Since cells require precise control of when and where new actin filaments are generated, it is important for cells to make sure Arp2/3 complex remains in its inactive state in the absence of activating factors. Yet, how Arp2/3 complex remains in its auto-inhibited state still remains an open question. In addition to the contacts between Arp3 and subdomain 4 of Arp2, Arp2 primarily forms contacts with the ARPC1,4,5 subunits while Arp3 is mostly associated with the ARPC2,3,4 subunits (Robinson et al., 2001). Residues in Arp2 (D'Agostino & Goode, 2005)(Martin et al., 2005), ARPC2 (Rodal et al., 2005), and ARPC4 (Narayanan et al., 2011) appear to have important contacts with neighboring subunits and mutations of these residues cause increased activity of the complex. While the Arp subunits are structurally homologous to actin, Arp3 harbors a few flexible inserts that are not present in actin that regulate the activity of the complex (Dalhaimer et al., 2008)(Liu et al., 2013). In addition, molecular dynamics simulations suggest phosphorylation of a tyrosine residue on the Arp2 subunit causes conformational changes of the complex, suggesting that the phosphorylation could also contribute to relieving autoinhibition (Narayanan et al., 2011).

We now know that Arp2/3 complex requires interactions with ATP, actin monomers, actin filaments and a class of proteins called nucleation promoting factors (NPFs), such as ActA, Scar and WASP, in order to relieve autoinhibition and form actin branches (Figure 2B)(Machesky & Insall, 1998)(Machesky et al., 1999)(Dayel et al., 2001)(Amann & Pollard, 2001b). Identifying and characterizing the various types of

NPFs has been an exciting development in the field of studying branch formation by Arp2/3 complex.

NPFs are Composed of Diverse Classes of Proteins that Activate Arp2/3 Complex

The intrinsic inactivity of Arp2/3 complex is a conserved feature across many of the forms so far studied. Throughout evolution, many unique NPFs have arisen and can generally be divided into classes called Type I NPFs, Type II NPFs, and the more recently-discovered WISH/DIP/SPIN90 family of proteins (Pollard, 2007)(Campellone & Welch, 2010)(Wagner et al., 2013). Type I NPFs, the most commonly known and characterized being the WASP and Scar (also called WAVE) family of proteins, share a minimal functional region located at the C-terminus referred to as the VCA region which is necessary and sufficient to activate the Arp2/3 complex *in vitro* (Machesky et al., 1999)(L Blanchoin et al., 2000)(Marchand et al., 2001). The VCA region is comprised of three discrete regions, which are called the Verprolin-homology, Central and Acidic regions, each conferring a unique role in the activation of Arp2/3 complex.

The CA region interacts with the Arp2/3 complex, with the acidic region comprising of the bulk of the affinity, a mode dependent on a conserved tryptophan at the C-terminal part of the region (Marchand et al., 2001). The role of the acidic residues is less well-defined since addition or removal of acidic residues from type I NPFs either increases or decreases the activity of the complex, depending on which NPF has been studied (Zalevsky et al., 2001)(Smith et al., 2013). The central region alone does not have significant affinity for Arp2/3 complex, however removal of the central region from a CA peptide reduced the affinity for Arp2/3 complex 5 to 8-fold (Marchand et al., 2001)(Kelly

et al., 2006). Despite its weak affinity, the central region has an important function in activation of the complex. Upon binding to the complex, it forms an amphipathic helix that is thought to bind the barbed end grooves of the Arp subunits and promote activation of the complex (Panchal et al., 2003). The central region is comprised of several conserved hydrophobic residues and a conserved arginine residue. Mutation of the hydrophobic residues had varying effects on VCA-mediated activation of Arp2/3 complex, ranging from none to severe (Marchand et al., 2001)(Panchal et al., 2003)(Kelly et al., 2006). Mutation of the conserved arginine to lysine in WASP (R477K) has been observed in patients with Wiskott-Aldrich Sndrome (the disease from which WASP gets its name)(Derry et al., 1995) and has diminished activity in polymerization assays (Marchand et al., 2001)(Panchal et al., 2003).

The V region is the defining characteristic of type I NPFs. The V region forms an α -helix that interacts with the barbed end groove of actin monomers (Chereau et al., 2005), and delivers them to Arp2/3 complex, which is thought to stabilize the actin nucleus and allow faster branch formation (Higgs et al., 1999). This activity is vital for Arp2/3 complex activity, as the CA region alone provides little to no activation of the complex (Marchand et al., 2001)(Kelly et al., 2006). Interestingly, the number of V regions in type I NPFs varies to some degree, with the majority containing one V region N-terminal to the CA region, however some NPFs contain multiple V regions like N-WASP and WHAMM (two V regions) or JMY (three V regions)(Zuchero et al., 2009)(Dominguez, 2009)(Campellone & Welch, 2010). Increasing the number of V regions is thought to speed up actin nucleation by stabilizing larger actin oligomers, which is thought to be the

mechanism of tandem WH2 nucleators such as Spire, which nucleates linear actin filaments through four consecutive WH2 regions (Quinlan et al., 2005)(Sitar et al., 2011).

Type II NPFs are characterized by their ability to bind actin filaments, rather than monomers (Goley & Welch, 2006). All type II NPFs contain an acidic region that is capable of binding Arp2/3 complex, however some fungal type II NPFs, such as coronin, Myo3p and Myo5p also contain C regions (Evangelista et al., 2000)(Humphries et al., 2002)(Liu et al., 2011). One of the most well characterized type II NPFs is cortactin (Urano et al., 2001)(Urano et al., 2003)(Helgeson & Nolen, 2013)(Helgeson et al., 2014), which is present in metazoans and localizes to many Arp2/3 complex-containing actin networks, most notably invadopodia which are protrusions of the membrane often associated with cancer cells that are involved in degradation of the extracellular matrix (Ayala et al., 2008). The mechanism for activation by type II NPFs varies. Due to their actin filament binding properties, type II NPFs are believed to activate Arp2/3 complex by recruiting them to the sides of filaments (Goley & Welch, 2006). However, experiments suggest that by themselves, type II NPFs are weak activators of Arp2/3 complex. Cortactin fails to activate Arp2/3 complex to a significant degree by itself (Urano et al., 2001)(Urano et al., 2003)(Helgeson & Nolen, 2013)(Helgeson et al., 2014). Yeast coronin produces some activation at low concentrations, but inhibits at high concentrations, possibly due to saturating the sides of filaments, preventing Arp2/3 complex from binding (Humphries et al., 2002)(Liu et al., 2011). Yeast proteins Myo5p and Abp1 either fail to or weakly produce any activation of Arp2/3 complex (Sun et al., 2006)(Goode et al., 2001). Despite this weak activity, type II NPFs can often indirectly activate the complex. While cortactin is unable to activate the complex on its own, potent

synergistic activation of Arp2/3 complex is achieved upon addition of dimeric NPF constructs due to cortactin enhancing the slow dissociation step of these NPFs (Urano et al., 2001)(Urano et al., 2003)(Helgeson & Nolen, 2013)(Helgeson et al., 2014). Yeast myosins also activate the complex by binding to verprolin, which recruits actin monomers to the complex, allowing activation. Consistent with the inability of type II NPFs to directly recruit actin monomers, addition of V regions to cortactin caused activation of Arp2/3 complex, although not as strongly as VCA (Helgeson et al., 2014).

The WISH/DIP/SPIN90 family of proteins has only been recently classified as an activator of Arp2/3 complex, however this family is very unique among NPFs in that these proteins recruit Arp2/3 complex to generate linear filaments (Wagner et al., 2013). Unlike type I or type II NPFs, these proteins bind neither actin filaments nor monomers, and lack the canonical acidic region containing the conserved tryptophan thought to be required for all NPFs (Wagner et al., 2013). Instead, WISH/DIP/SPIN90 proteins utilize a leucine-rich domain that has not been observed in other NPFs, making this family of proteins an intriguing target for further mechanistic studies.

In addition to all of the classes of NPFs described among eukaryotes, bacterial pathogens have developed novel NPFs of their own in order to hijack their host's cytoskeleton in order to promote movement within in the cell, including, but not limited to, ActA from *Listeria monocytogenes* (Welch et al., 1998) and VopL from *Vibrio parahaemolyticus* (Liverman et al., 2007). Due to the vast variety of NPFs, determining the mechanisms of how these proteins coordinate the regulation of branched actin networks is an important and challenging goal for understanding cytoskeletal dynamics.

Individual Roles of ATP, WASP, Actin Monomers and Actin Filaments in the Branched Actin Nucleation Pathway

Although it is known that ATP, WASP, monomers and filaments are required to form actin branches, the specific contributions of each are not well understood. ATP hydrolysis by the Arp subunits, like with actin, provides a timing mechanism to determine the age of actin branches, aiding in actin branch disassembly (Le Clainche et al., 2003)(Martin et al., 2006)(Ingerman et al., 2013). Hydrolysis of ATP in actin promotes disassembly by the actin filament-severing protein cofilin (Blanchoin et al., 2000). Similarly, the ADF/cofilin homolog GMF, which severs filaments at the branch junction rather than the sides of the filament, possibly acts through an analogous mechanism with Arp2 (Gandhi et al., 2010)(Luan & Nolen, 2013).

In addition to providing a timing mechanism, ATP binding to Arp2/3 complex is important for initial branch formation. In crystal structures of Arp2/3 complex, the nucleotide-free state shows the nucleotide cleft in Arp3 to be in an open conformation and upon nucleotide binding, constricts into a more closed form (Robinson et al., 2001)(Nolen et al., 2004). Subdomains 1 and 2 of Arp2 are disordered in these structures, however a recent structure of Arp2/3 complex with ATP and GMF bound caused ordering of these domains and the nucleotide cleft of Arp2 was observed to be closed (Luan & Nolen, 2013). The effect of ATP binding on the short pitch conformation was investigated with labeled ARPC1 and ARPC3 subunits and caused an increase in FRET, but due to the low resolution of this technique, the exact structural changes are unclear (Goley et al., 2004). In molecular dynamics simulations, ATP binding caused release of the Arp3 C-terminus from its barbed end groove, which is thought to be an important

regulatory element in Arp2/3 complex activation and could explain the conformational changes observed in the FRET experiments (Dalhaimer et al., 2008). Consistent with these simulations, the C-terminus becomes more disordered in crystal structures when ATP and other nucleotides are bound (Robinson et al., 2001)(Nolen et al., 2004)(Nolen & Pollard, 2007).

Unlike ATP, much less is known of the nature and effects of WASP binding to the complex. Experiments using analytical ultracentrifugation (Padrick et al., 2011)(Hetrick et al., 2013) and isothermal titration calorimetry (Ti et al., 2011)(Boczkowska et al., 2014) have supported binding of two VCA molecules to Arp2/3 complex. Additionally, dimeric VCA constructs bind the complex with ~100-180-fold higher affinity (Padrick et al., 2008). WASP-related proteins have not been shown to dimerize in isolation, however they are believed to act as oligomers in cells due to clustering on the plasma membrane (Padrick et al., 2008)(Gohl et al., 2010)(Suetsugu, 2013). Chemical crosslinking studies have suggested that one of the VCA peptides binds to Arp3, while the other spans Arp2 and ARPC1 (Kreishman-Deitrick et al., 2005)(Padrick et al., 2011)(Liu et al., 2011)(Ti et al., 2011). The acidic region is believed to bind to Arp3 between subdomains 3 and 4, based on crystal structures containing Arp2/3 and WASP showing weak electron density in this region (Ti et al., 2011)(Jurgenson & Pollard, 2015), while the other acidic region is believed to bind ARPC1, since this subunit binds CA in isolation (Pan et al., 2004). The ITC experiments have shown that the two binding sites have roughly a 9 to 25-fold difference in affinity, suggesting that there might be an importance of one binding site over the other (Ti et al., 2011)(Boczkowska et al., 2014). Indeed, there has been some debate as to which binding

site is first targeted by VCA. Low resolution structures of VCA and VCA crosslinked to actin monomers bound to the complex have suggested that the first binding site is on Arp3 or Arp2, respectively (Xu et al., 2012)(Boczkowska et al., 2008), although it is possible that the preference of binding for the high affinity site can be influenced by the presence of actin monomers.

While the exact effects of the individual WASP binding sites have not been fully elucidated, studies have supported a model where WASP stimulates a conformational change in Arp2/3 complex that adopts a more “filament-like” conformation. Addition of WASP caused a large increase in the FRET assay described above (Goley et al., 2004) and single-molecule particle EM reconstructions show that addition of WASP to Arp2/3 complex caused the complex to adopt a more “closed” conformation (Rodal et al., 2005), suggesting WASP stimulates the short pitch conformation. Lastly, engineered cysteine mutations in the Arp2 and Arp3 subunits that only crosslink the two subunits together in the expected “short pitch” conformation in the presence of BMOE, an ~ 8 Å crosslinker, show an increase in crosslinking upon the addition of N-WASP-VCA, an effect that is reduced upon addition of the Arp2/3 complex inhibitor CK-666, demonstrating that this inhibitor blocks the activating conformational change induced by WASP (Hetrick et al., 2013). Determining precisely how WASP induces this conformational change is an important unanswered question in the field.

The role of VCA-recruited actin monomers has long been assumed to stabilize the nascent nucleus, speeding up the slow nucleation step (Higgs et al., 1999). Like VCA binding, the importance of delivering actin monomers to either the Arp2 or the Arp3 site is still uncertain. A peptide-linked diVCA construct did not show any preference in

binding of the N or C-terminal VCA portion, however in the presence of actin monomers, displayed asymmetric binding (Padrick et al., 2011). Removal of the C-terminal V region, which preferentially delivers actin monomers to the Arp3 site, caused a more dramatic loss of VCA activity versus removal of the N-terminal V region, suggesting delivery of monomers to the Arp3 site is more important (Padrick et al., 2011). However, it is unclear if the asymmetric binding still holds in the absence of actin monomers at these sites. A low resolution small-angle X-ray scattering (SAXS) structure suggests that a single actin monomer crosslinked to VCA puts the actin monomer at the barbed end of Arp2, however this structure could not discern if Arp2/3 complex was in the splayed or short pitch conformation (Boczkowska et al., 2008). Additional evidence that the first actin monomer was delivered to Arp2 came from ITC experiments demonstrating that GMF, which binds to the barbed end of Arp2 (Luan & Nolen, 2013), did not bind to a 1:1:1 Actin:VCA:Arp2/3 complex (Boczkowska et al., 2014). While the effects of actin monomer delivery to the Arp2 versus the Arp3 site are still unclear, recent experiments using the dual-cysteine crosslinking assay revealed that addition of actin monomers with WASP to the reaction caused an increase in crosslinking over WASP alone, demonstrating that actin monomers aid in stimulation of the short pitch conformation (Hetrick et al., 2013). This result was surprising because it suggests that WASP alone cannot fully populate the short pitch conformation, and that actin monomer delivery is required for the maximal stability of the short pitch conformation. This experiment was conducted under saturating VCA+actin conditions, so the individual role of delivery to Arp2 versus Arp3 is still unclear. A structural argument for the importance of delivery of actin to Arp3 can be made. The inactive structure of Arp2/3 complex shows that the

barbed end of Arp3 is blocked by Arp2 (Robinson et al., 2001), suggesting that an actin monomer delivered to this site would prevent Arp2 from transitioning back to the splayed conformation. Testing this hypothesis will be important for understanding the role of monomer recruitment in Arp2/3 complex activation.

Since Arp2/3 complex is a branched actin nucleator, the field has assumed that actin filaments cooperate with WASP and actin monomers to stabilize the short pitch conformation, although this role has not been directly tested. The dual-cysteine crosslinking assays suggest that WASP and actin monomers alone are capable of potentially stimulating the short pitch conformation, suggesting the role of actin filaments could be more nuanced (Hetrick et al., 2013). WASP and actin monomers appear to stabilize the short pitch conformation, yet filaments are required for branch formation. Mutations of the predicted actin filament binding interface, as determined by molecular docking simulations, reduced the activity of Arp2/3 complex in pyrene actin polymerization assays and affected the stability of branches that actually formed (Goley et al., 2010). These mutations did not affect ATP and CA-induced conformational changes as measured by FRET, indicating their role is for the binding and stability of Arp2/3 complex to actin filaments (Goley et al., 2010).

One possible clue for the role of filaments comes from a model of an actin filament generated by x-ray fiber diffraction (Oda et al., 2009). In crystal structures of actin monomers alone, the nucleotide cleft in subdomains 2 and 4 of actin are closed with the two regions in a “twisted” conformation (Kabsch et al., 1990). In the F-actin model, the nucleotide cleft remains closed, but the subdomains untwist into a more “flattened” conformation (Oda et al., 2009). Indeed, in the EM reconstruction of Arp2/3 complex at

the branch junction, the Arp subunits appear to be in a more closed state, presumably the “flattened” conformation (Rouiller et al., 2008). This flattened conformational change is expected to initiate ATP hydrolysis as actin monomers are incorporated into the elongating filament (Oda et al., 2009). In one study, WASP and actin monomers alone were not able to stimulate hydrolysis of ATP in Arp2, however once WASP, monomers and filaments were mixed together, hydrolysis did occur (Dayel & Mullins, 2004). One interpretation of this result could be that WASP and actin monomers stimulate the short pitch conformation, but that this is not enough to nucleate a new filament. Once this assembly binds to a mother filament, the flattened conformation in Arp2 and Arp3 is stimulated and then an actin branch can form. Due to the lack of evidence for the role of actin filaments, testing if actin filaments stimulate flattening or other important steps in the pathway is essential to understanding why Arp2/3 complex exclusively forms branched actin networks.

In chapter II, we investigated how Arp2/3 complex is held inactive in the absence of activating factors. From previously published high resolution crystal structures (Robinson et al., 2001)(Nolen et al., 2004)(Nolen & Pollard, 2007) and molecular dynamics simulations (Dalhaimer et al., 2008), we hypothesized that the Arp3 C-terminal tail plays an important role in stabilizing the inactive state, with the N-terminal portion (or “base”) forming contacts with subdomain 4 of Arp2 and the C-terminal portion (or “tip”) wedged in the barbed end groove of Arp3. We found that removal of the C-terminal region in *S. pombe* and *S. cerevisiae* Arp2/3 complexes caused NPF-independent hyperactivity and affected actin patch dynamics *in vivo*. We show that removal of the C-terminus causes a potent increase in formation of short pitch crosslinking, suggesting the Arp3 Δ C complex

more closely resembles the active conformation. Mutational analysis of subdomain 4 of Arp2, specifically the $\alpha E/\alpha F$ loop, shows that this region provides important contacts in the inactive conformation, as these mutants displayed NPF-independent activity in actin polymerization and crosslinking assays. Since crystal structures showed that ATP causes an allosteric effect, where closing of the Arp3 nucleotide cleft correlates with disorder of the C-terminal tail, we hypothesized that ATP is required for stimulation of the short pitch conformation. Using mutations of the nucleotide binding clefts of Arp2 and Arp3, we show that ATP binding is required for crosslinking, demonstrating why ATP is required for activation. Lastly, we show that destabilization of the tip of the C-terminal tail also causes NPF-independent hyperactivity, supporting a “tail release” model where ATP binding causes release of the tip of the tail from the barbed end groove of Arp3 causing destabilization between the base of the tail and Arp2, thereby stimulating the short pitch conformation.

In chapter III, we specifically investigated the role of WASP proteins in the short pitch conformational change. Using the crosslinking assay, we demonstrate that stimulation of the short pitch conformation is a conserved feature of WASP-related proteins. Mutational analysis of N-WASP shows that while residues in both the C and A regions are important for activity in polymerization assays, only residues in the C region are important for stimulation of the short pitch conformation, as demonstrated by crosslinking. To determine the importance of binding of WASP either the Arp2 or Arp3 site, we use WASP-Arp chimeras where the CA is fused to the C-terminus of either Arp2 or Arp3 to demonstrate that binding of WASP to both sites is important for full stimulation of the short pitch conformation. To determine the precise role of the short

pitch conformation on branch formation, we purified Arp2/3 complex crosslinked into the short pitch conformation and, remarkably, found that it is much more active compared to WASP-activated complex. We show that this is likely due to WASP release limiting nucleation rates, as CA inhibited the short pitch crosslinked complex in polymerization assays. Finally, using the Arp3 Δ C strain described in chapter II, we show that binding of WASP's C-region to the barbed end groove of Arp3 competes with the C-terminal tail, supporting our "tail release" model where WASP and ATP cooperate to displace the Arp3 C-terminal tail to promote the short pitch conformation.

The work presented in chapter II has been submitted to the journal Nature Communications and was coauthored with Su-Ling Liu, Connor J. Balzer, Qing Luan and Brad J. Nolen. The work presented in chapter III has been submitted to the journal PNAS and was coauthored with Qing Luan, Su-Ling Liu and Brad J. Nolen.

CHAPTER II

IDENTIFICATION OF AN ATP-CONTROLLED ALLOSTERIC SWITCH THAT CONTROLS ACTIN FILAMENT NUCLEATION BY ARP2/3 COMPLEX.

AUTHOR CONTRIBUTIONS

B.J.N. and M.R.-S. designed the experiments and interpreted the data. B.J.N., M.R.-S., and C.J.B wrote the manuscript. B.J.N., M.R.-S., S.-L.L., C.J.B, and Q.L. generated reagents and carried out experiments.

INTRODUCTION

Arp2/3 (Actin-related protein 2/3) complex is a seven-subunit protein assembly that plays a key role in regulating the actin cytoskeleton. By nucleating branched actin filaments in response to cellular signals, it controls the assembly of dendritic actin networks required for a broad range of cellular processes, including endocytosis, protrusion of invadopodia and lamellipodia, and positioning of the meiotic spindles¹⁻³. In the absence of activating factors, Arp2/3 complex is held in an inactive or low activity state. Activation typically requires interactions with several activating factors, including preformed actin filaments, actin monomers, ATP, and a class of proteins called nucleation promoting factors (NPFs)⁴⁻¹⁰. The nucleation activity of Arp2/3 complex must be tightly regulated by these factors for cells to properly control the dynamics and architectures of actin networks¹¹⁻¹³. Despite the importance of ensuring that the complex

does not nucleate filaments in the absence of activators, the molecular basis by which the complex is held in an autoinhibited state is not understood.

Several high-resolution structures of autoinhibited/inactive Arp2/3 complex are available¹⁴⁻¹⁷. In this conformation, the two actin-related subunits in the complex, Arp2 and Arp3, align roughly end-to-end in a conformation referred to as “splayed” (Fig. 1). Activation is thought to require a substantial structural change in which Arp2 moves ~20 Å into position side-by-side with Arp3, creating an Arp2-Arp3 “short pitch” heterodimer that mimics two consecutive actin monomers within a filament. The short pitch conformation is hypothesized to provide the nucleus to template a new filament¹⁴. While this hypothesis has never been directly tested, several lines of evidence indicate that activating factors stimulate movement of Arp2 and Arp3 into the short pitch conformation, suggesting this conformational change may be a key activation step^{7,18-22}. Therefore, controlling the conformational switch from the splayed to the short pitch state could be a critical aspect of Arp2/3 complex regulation. However, despite the availability of high-resolution structures of the inactive complex and several mutational studies, the structural features of the complex that stabilize the splayed/autoinhibited state in the absence of activators have yet to be clearly identified. Activating mutations on four Arp2/3 complex subunits (Arp2, Arp3, ARPC2, and ARPC4) have been identified either in screens or in targeted mutational analysis, but the mechanism by which these mutations influence the conformation of the complex is unknown^{7,13,20,23-26}. Identification and structural dissection of autoinhibitory features would not only reveal how nucleation is prevented in the absence of activating factors, but would provide a framework for understanding how activators stimulate nucleation.

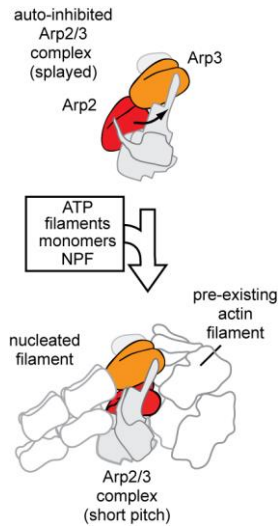


Figure 1 | Cartoon model of Arp2/3 complex activation.

Activation of Arp2/3 complex is thought to require movement of the actin-related subunits Arp2 and Arp3 from an inactive “splayed” conformation to an active conformation that mimics a filament-like short pitch actin dimer. ATP, actin monomers, actin filaments, and an NPF protein are typically required for activation.

Multiple inputs (NPFs, actin monomers, actin filaments and ATP) are required for activation of the complex. Mounting evidence indicates that each of these inputs plays an important role in regulating the dynamics and architectures of Arp2/3-nucleated actin networks *in vivo*^{4,10,27-29}. For instance, NPFs such as the WASP family proteins link Arp2/3 complex to cellular signaling pathways, while the requirement for preformed filaments ensures that the complex creates exclusively branched actin filaments^{4,10}. Likewise, bound ATP provides a built-in timer that controls branch lifetimes, since hydrolysis of ATP occurs on the complex following nucleation and stimulates debranching^{28,30,31}. Like WASP, ATP binding causes conformational changes in the complex, but how these changes are linked to activation is not known. In x-ray crystal structures, ATP binding causes the nucleotide cleft of Arp3 to close, moving subdomain 4 of Arp3 closer to subdomain 2^{15,16}. ATP binding increases FRET in Arp2/3 complex

tagged with fluorescent proteins, providing additional evidence for ATP-induced structural changes²¹. A precise understanding of these changes and how they are linked to activation is critical, both to determine how the ATP-binding requirement is structurally encoded into the branching nucleation mechanism and to uncover the molecular bases for regulating branched actin network dynamics.

Here we identify interactions at the Arp2-Arp3 splayed interface as key autoinhibitory features of the Arp2/3 complex. We show that destabilizing this interface stimulates population of the short pitch conformation and activates Arp2/3 complex nucleation activity. We identify the Arp3 C-terminal tail as a switchable molecular element that controls the activity of the complex *in vitro* and *in vivo* by controlling the stability of the Arp2-Arp3 splayed interface. Specifically, our data indicate that engagement of the Arp3 C-terminal tail with the Arp3 barbed end groove helps hold the complex in the inactive splayed conformation, while release of the tail destabilizes the splayed interface to stimulate the short pitch conformation. ATP binding stimulates the short pitch conformation, likely through an allosteric connection between the nucleotide binding cleft and the barbed end groove that triggers release of the Arp3 C-terminus. Therefore, this work reveals a molecular mechanism by which ATP contributes to activation and provides a structural framework to understand how activators of Arp2/3 complex can relieve autoinhibition to activate branching nucleation.

RESULTS

The C-terminus of Arp3 is required to keep Arp2/3 complex inactive in the absence of activators

Both Arp2 and Arp3 contain several conserved inserts/extensions relative to actin, suggesting that in addition to mimicking actin during nucleation, the actin-related subunits play additional structural roles in the function of the complex^{24,32}. Consistent with this hypothesis, we recently discovered two insertions within the Arp3 subunit that harbor complex-specific functions, one in controlling interactions with actin filaments and another in stabilizing attachment of a non-actin related subunit to the complex²⁴. These observations led us to wonder if other insertions/extensions could be directly involved in the response of the complex to its regulators. Our analysis led to one promising candidate, a conserved extension in Arp3 termed the C-terminal tail, which wedges into a cleft between subdomains 1 and 3 called the barbed end groove (Fig. 2a). The surface of the barbed end groove is largely hydrophobic, and two conserved non-polar residues within the Arp3 C-terminus pin it into the groove in some structures (Fig. 2b)^{14,16}. Molecular dynamics simulations suggested the engagement of the C-terminal tail with the barbed end groove could allosterically influence the conformation of the Arp3 nucleotide binding cleft³³, so we reasoned that the tail could be important for controlling the conformation and activity of the complex. To test this, we created a budding yeast strain expressing an *arp3* mutant (*arp3* Δ C) lacking 10 residues from its C-terminus as its sole copy of Arp3. The Arp3 Δ C complex was purified from budding yeast and its activity measured in a pyrene actin polymerization assay (Fig. 2c,d, Fig. S1). The C-terminal truncation potently increased the NPF-independent activity of Arp2/3 complex. In reactions containing 50 nM Arp2/3 complex the maximum polymerization rate increased ~20-fold upon deletion of the Arp3 C-terminus. These data demonstrate that the Arp3 C-terminus plays a critical role in keeping the complex inactive in the absence of activators.

To determine if the autoinhibitory function of the Arp3 C-terminus is conserved, we truncated the homologous residues from the C-terminus of *S. pombe* Arp3. To accomplish this, we used the homologous recombination method of Bahler *et. al.*, to introduce a premature stop codon in *ARP3* at its endogenous locus in *S. pombe*³⁴. We then purified and assayed the mutant complex. As observed with budding yeast Arp3, deletion of the C-terminus of *S. pombe* Arp3 increased the NPF-independent activity of the complex (Fig. 2e,f). In the absence of nucleation promoting factors, 200 nM *S. pombe* Arp3 Δ C increased the maximum polymerization rate almost two-fold over actin alone in a pyrene actin polymerization assay. Under the same conditions, wild-type Arp2/3 complex showed only a ~16% increase in the maximum polymerization rate over reactions with actin alone. These data demonstrate that the C-terminus of Arp3 has a conserved role in autoinhibiting Arp2/3 complex.

The C-terminus of Arp3 is required for proper assembly and function of endocytic actin structures in yeast

We next asked if deletion of the C-terminus has functional consequences *in vivo*. Specifically, we tested whether Arp3 C-terminal tail deletion influences the assembly or dynamics of *S. pombe* actin patches, cortical actin networks required for plasma membrane invagination during endocytosis^{7,23,35-38}. To monitor actin patch dynamics, we used GFP-tagged Fim1, an actin crosslinking protein that binds actin filaments in the patches and shows the same accumulation and disassembly kinetics as actin^{39,40}. Actin patches in the *arp3* Δ C strain were similar in quantity and overall appearance to wild type patches (Fig. 3a,b). In wild type cells, the Fim1-GFP signal typically accumulated at the

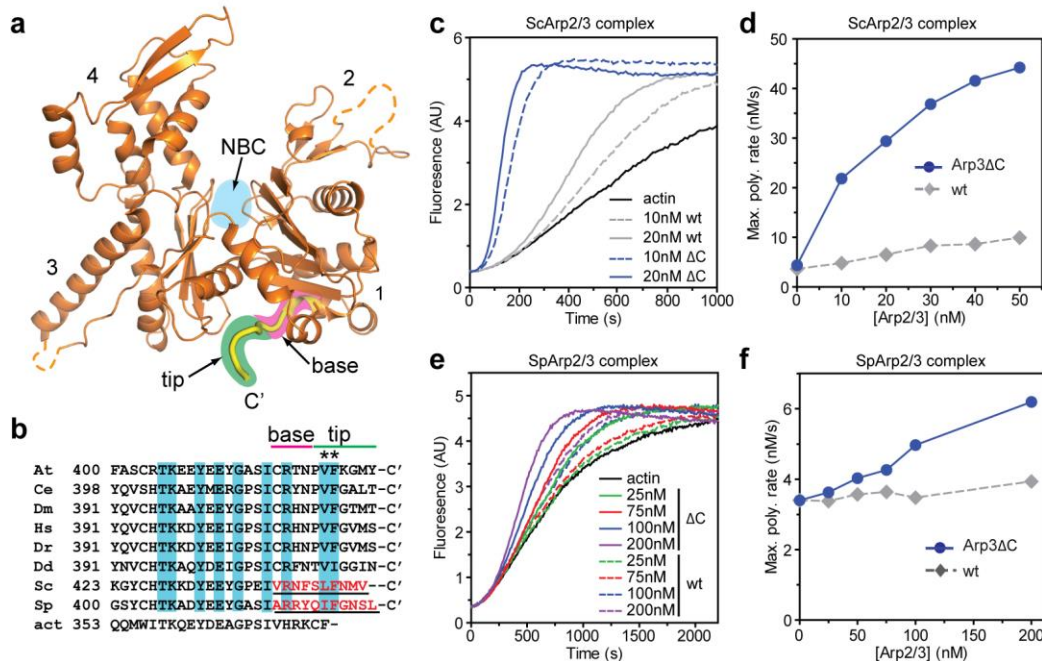


Figure 2 | The Arp3 C-terminal tail is a conserved structural feature required for autoinhibition of Arp2/3 complex.

(a) Ribbon diagram of Arp3 from crystal structure of *Bos taurus* Arp2/3 complex (1K8K) showing the position of the Arp3 C-terminus (yellow)¹⁴. Subdomains 1-4 are numbered and the ATP binding site in Arp3 is indicated with cyan circle. The base and tip of the Arp3 C-terminus are highlighted in pink and green, respectively. (b) Sequence alignment of the C-terminus of Arp3 from diverse species. At: *Arabidopsis thaliana*; Ce: *Caenorhabditis elegans*; Dm: *Drosophila melanogaster*; Hs: *Homo sapiens*; Dr: *Danio rerio*; Dd: *Dictyostelium discoideum*; Sc: *Saccharomyces cerevisiae*; Sp: *Schizosaccharomyces pombe*; act: rabbit skeletal muscle actin. Residues underlined and in red are deleted in Arp3 Δ C mutants. Cyan boxed residues are conserved in Arp3 sequences. Asterisks mark conserved hydrophobic residues that pin the C-terminal tail into the barbed end groove in some crystal structures. (c) Time course of pyrene actin polymerization with 3 μ M 15 % pyrene-labeled actin showing constitutive activity of Arp3 Δ C mutant compared to wild-type *S. cerevisiae* (Sc)Arp2/3 complexes. (d) Maximum polymerization rate versus concentration of wild-type or Arp3 Δ C *S. cerevisiae* complex for conditions described in C. (e) Time courses of pyrene actin polymerization as measured in (b), but with *S. pombe* (Sp)Arp2/3 complexes. (f) Maximum polymerization rate versus concentration of wild-type or Arp3 Δ C *S. pombe* complexes for conditions described in (e).

cortex and then moved inward as it disappeared, consistent with previous studies^{41,42}.

Importantly, actin patches in the *arp3* Δ C strain frequently failed to internalize, with only 51 % of actin patches (n = 114) moving off of the cortex compared to 76 % of the patches

tracked in wild type cells (n = 113, Fig. 3c). Actin patches in the *arp3ΔC* strain also had longer lifetimes than wild type patches (Fig. 3d, Supplementary Movie 1 and 2). To determine whether the increased lifetimes were caused by decreased patch assembly or disassembly rates, we measured Fim1-GFP intensity throughout the patch lifetime in both wild type and *Arp3ΔC* mutant cells. Both assembly and disassembly were slowed, and the total intensity of Fim1-GFP was less in the mutant (Fig. 3e). This result was unexpected, since increases in Arp2/3 complex activity might be expected to accelerate actin patch assembly (see discussion). We next asked if the actin defects influenced endocytosis by pulsing cells with the lipophilic dye FM4-64. In wild type cells, the dye was immediately internalized from the plasma membrane, and stained endosomes and other internal membranes even at the first imaging time point, similar to previous reports²⁴ (Fig. 3f). In contrast, uptake was delayed in the *arp3ΔC* strain, with strong FM4-64 staining of the plasma membrane 5 min after the initial pulse. By comparison, the delay was more pronounced in a *wsp1Δ* strain⁴³, where strong staining was visible at the plasma membrane up to 20 min after the pulse. The observed defects in both actin patch dynamics and endocytosis indicate that the C-terminal tail of Arp3 is required to properly regulate Arp2/3 complex *in vivo*.

The Arp3 C-terminus is required to prevent formation of the Arp2-Arp3 short pitch dimer

Our data show that the Arp3 C-terminal tail plays a critical role in keeping the complex inactive in the absence of activators. We analyzed the available x-ray crystal structures to determine how the tail could influence activity. The N-terminal portion of

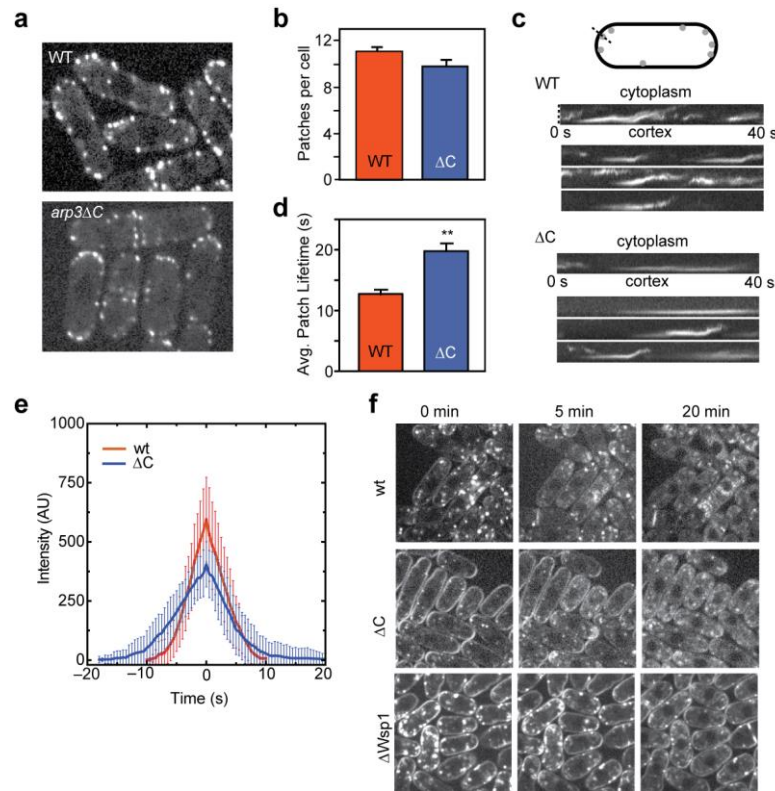


Figure 3 | Deletion of the Arp3 C-terminal tail causes defects in endocytic actin patches and in the uptake of FM4-64.

(a) Spinning disk confocal fluorescence micrographs of wild type and mutant *S. pombe* cells expressing Fim1-GFP. Images are taken through the middle of the cells. (b) Average number of patches per cell ($n \geq 50$ cells). Error bars show standard error. (c) Kymographs of four actin patches for wild type and Arp3ΔC strain. (d) Average patch lifetime for wild type and Arp3ΔC strain. Error bars show standard error. (e) Quantification of Fim1-GFP intensity in wt and Arp3ΔC *S. pombe* cells. Data show average intensity and standard deviation from measurements of patches from wt ($n=30$ patches) and Arp3ΔC ($n=30$) strains, respectively. The zero time point was taken to be the frame of maximum Fim1-GFP intensity during the lifetime of each patch. (f) FM4-64 endocytosis assay showing that Arp3ΔC strain exhibits slowed dye uptake compared to the wild type strain.

the tail, which we refer to as the “base” of the tail, wraps around the bottom of subdomain 1, fills the back end of the barbed end groove, and directly contacts subdomain 4 of Arp2 at the splayed interface¹⁴⁻¹⁶. The C-terminal end of the tail, which we will refer to as the “tip”, wedges into the front portion of the barbed end groove and is pinned into position by L445 and F446 (Fig. 4a). In some x-ray crystal structures, the tip

engages the groove while in others, it is disengaged and disordered¹⁴⁻¹⁶. Because the base of the Arp3 C-terminal tail occupies a critical position at the Arp2-Arp3 splayed interface and the tip adopts multiple conformational states, we hypothesized that the Arp3 C-terminus could be a switchable structural element that allows activating factors to influence the stability of the Arp2-Arp3 splayed interface.

To test this, we first asked if the Arp3 C-terminal tail is required to hold the complex in the splayed conformation. We used a previously described crosslinking assay in which engineered cysteines on Arp2 and Arp3 can be crosslinked by the 8 Å crosslinker bismaleimidoethane (BMOE) only when the complex is in the short pitch conformation²² (Fig. 4b). The Arp3 C-terminal deletion is not predicted to significantly influence either the solvent accessibility or the pKa of the engineered cysteine residues, ensuring that changes in short pitch crosslinking efficiency are due to the conformational change and not the chemical reactivity of the thiol groups (Supplementary Table 1). Deletion of the Arp3 C-terminal tail in the context of the dual cysteine *S. cerevisiae* Arp2/3 complex potently stimulated crosslinking between the engineered cysteines (Fig. 4c,d). A thirty second reaction with 25 μM BMOE, 200 μM ATP and no NPF yielded 31 ± 6 % crosslinking with the Arp3ΔC complex, while a negligible amount of the wild type complex was crosslinked under the same conditions. These data indicate that the C-terminal tail of Arp3 is a critical autoinhibitory structural feature that prevents the complex from adopting the short pitch conformation in the absence of WASP proteins. We note that analysis with the program X-walk showed that minimal crosslinking length required to bond the engineered cysteines when the complex is in the short pitch conformation (Cβ to Cβ) is between 8.0 and 11.3 Å, very close to the maximum expected

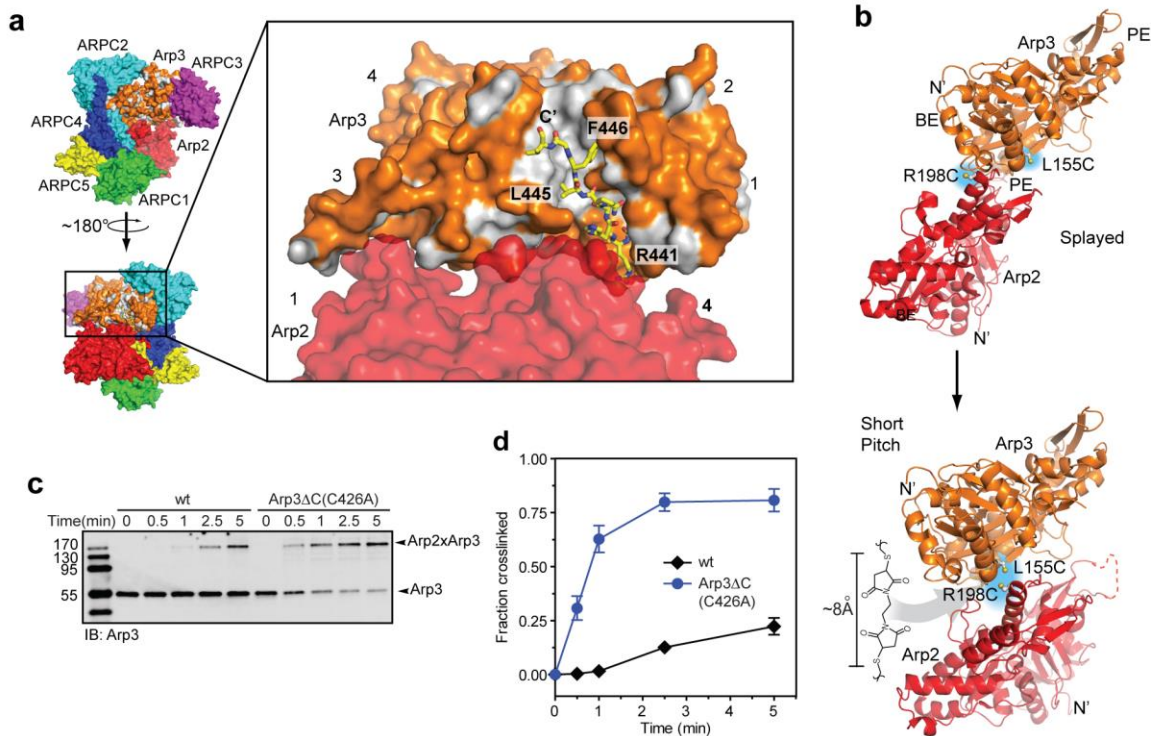


Figure 4 | The Arp3 C-terminus is required to prevent formation of the short pitch conformation.

(a) Surface representation of BtArp2/3 complex (4JD2) showing the barbed end of Arp3, the barbed end groove and Arp3 C-terminal tail (yellow stick representation). Residues in Arp3 are colored according to hydrophobicity, with polar residues orange and non-polar residues grey. Residues are labeled based on the *S. cerevisiae* Arp2/3 complex sequences. (b) Ribbon diagrams of Arp2 and Arp3 showing the position of engineered cysteines (Arp3(L155C), Arp2(R198C)) in the splayed and short pitch conformations and the structure of the chemical crosslinker (BMOE) used in the short pitch crosslinking assay. Structure 4JD2 was used to make both panels. In the right panel, the Oda, et. al. actin filament structure was used to move Arp2 into the short pitch conformation⁷⁰. The solvent accessible crosslinking distance between engineered cysteines is 32.5 Å in the splayed conformation, and ranges from ~8-11.3 Å in different models of the short pitch conformation (see Fig S3)⁴⁴. (c) Anti-Arp3 western blot of 1 minute crosslinking reactions containing 1 μM wild type (wt) or Arp3ΔC ScArp2/3 complexes in 200 μM ATP, 1 mM MgCl₂, 50 mM KCl, 20 mM Imidazole pH 7.0, and 1 mM EGTA. Both complexes harbor the dual engineered cysteine residues. The Arp3ΔC complex also contains the C426A mutation to eliminate the non-short pitch crosslinking product (see Fig. 7). (d) Quantification of reaction described in panel (c). Error bars show standard error for three reactions.

crosslinking distance of BMOE (~8 Å from sulfur to sulfur)⁴⁴. Therefore, the crosslinked complex is held in or very near the short pitch conformation. For simplicity, we refer to

the crosslinked complex as being in the short pitch conformation in the sections that follow, though it is important to note that we cannot currently eliminate the possibility that Arp2 and Arp3 could deviate somewhat from a perfect filament-like arrangement and still form the engineered crosslink.

Destabilization of the splayed Arp2-Arp3 interface activates Arp2/3 complex

The base of the Arp3 C-terminal tail directly contacts Arp2 at the splayed interface, suggesting the tail prevents adoption of the short pitch conformation by stabilizing the splayed conformation (Fig. 4a). However, some residues in the Arp3 C-terminal tail are near the Arp2-Arp3 short pitch interface in the electron tomography model of a branch junction⁴⁵ (Fig. S2), so it is also possible that the C-terminal truncation influences the conformation of the complex by stabilizing short-pitch contacts between Arp2 and Arp3. To investigate these possibilities, we first sought more conservative mutations to test if destabilization of the splayed Arp2-Arp3 interface is sufficient to stimulate the short pitch conformation. We initially considered R441 and N442 in the base of the Arp3 C-terminus. These residues contribute to the splayed Arp2-Arp3 interface, but are also close to the predicted short pitch interface (Fig. 4a, Fig. S2). In contrast, the $\alpha E/\alpha F$ loop in subdomain 4 of Arp2 contributes several residues to the Arp2-Arp3 splayed interface, and none of them are predicted to contribute to the short pitch interface (Fig. 5a,b, Fig. S3)⁴⁵. Therefore, we constructed budding yeast strains expressing Arp2 $\alpha E/\alpha F$ loop mutants as their sole copy of Arp2, then purified and characterized the mutant complexes (Fig. 5c). At Arp2 position 207 we changed the wild type alanine to bulkier amino acids to disrupt contacts of the $\alpha E/\alpha F$ loop with Arp3. In

addition, we mutated Arp2 F203 to Tyr. F203Y is one of two mutated residues found in an Arp2 mutant isolated in a genetic screen, *arp2-7*, that confers increased NPF-independent activity to the complex^{13,23,46,47}. Because of its position in the Arp2 $\alpha E/\alpha F$ loop, we reasoned that the F203Y mutation could also destabilize the Arp2-Arp3 splayed interface. To determine if these mutations influence the conformation of the complex, we used the short pitch crosslinking assay. We found that three of the splayed interface mutations increased formation of short pitch crosslinks (Fig. 5d,e, Supplementary Table 2). In one minute reactions, the Arp2-A207W, A207C and F203Y mutants increased crosslinking 5, 6 and 12-fold compared to the wild type complex, respectively. These results demonstrate that the Arp2-Arp3 splayed interface is critical for holding the complex in the inactive conformation. Furthermore, they show that destabilizing the splayed interface potently stimulates the short pitch conformation. We note that the Arp2(A207I) mutant complex was prone to degradation, but when isolated showed similar behavior in the crosslinking assay as wild type complex, indicating not all mutations of residue 207 can stimulate the short pitch conformation.

To determine if the splayed interface mutations increased the NPF-independent activity of the complex, we tested the mutants in pyrene actin polymerization assays. The Arp2(A207C), Arp2(A207W) and Arp2(F203Y) mutant complexes each showed increased NPF-independent nucleation activity compared to wild type Arp2/3 complex, consistent with their increased propensity to adopt the short pitch conformation (Fig. 5f,g). The A207C and F203Y mutations showed the most potent activation, and at 100 nM increased the maximum polymerization rate 3.6- and 2.6-fold over the wild type complex, respectively. The A207W mutant showed a more modest 1.8-fold increase in

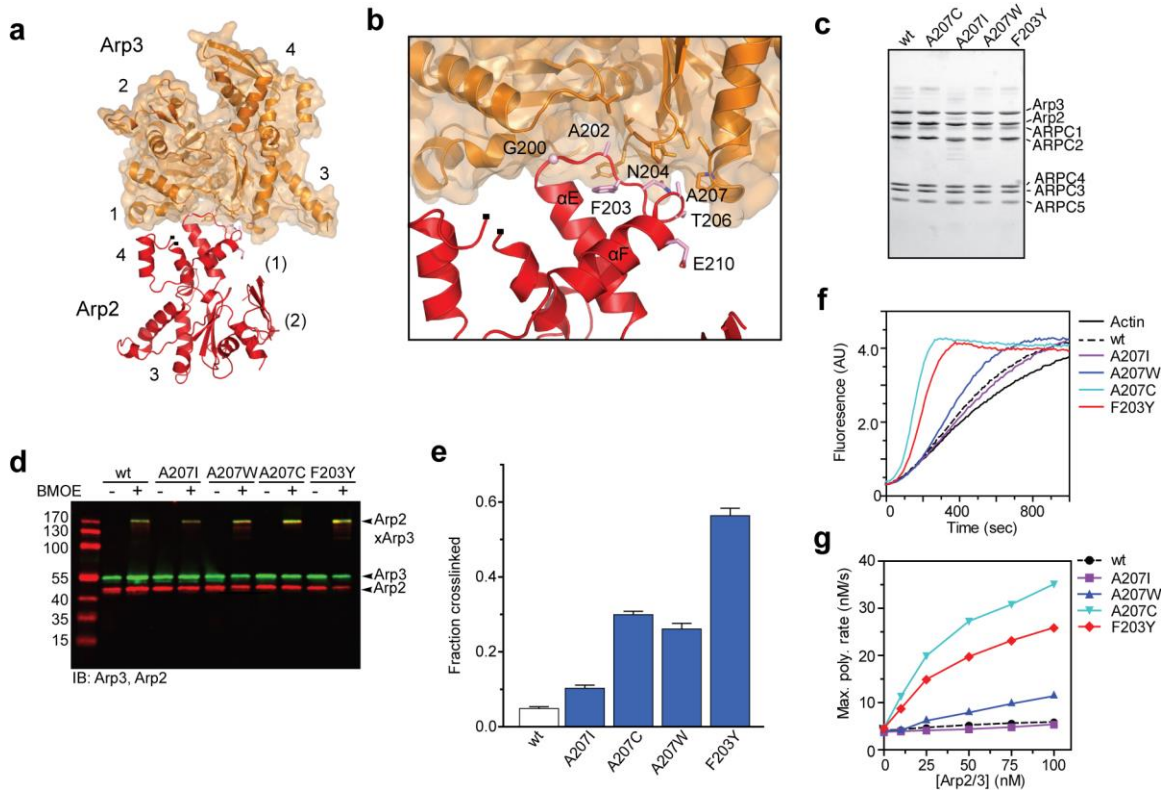


Figure 5 | Destabilization of the splayed Arp2-Arp3 interface stimulates the short pitch conformation and activates Arp2/3 complex.

(a) Ribbon diagram of Arp2 and Arp3 positioned in the splayed conformation (2P9K). Subdomains are numbered, with partially or fully disordered subdomains in Arp2 in parentheses. (b) Close up of the Arp2-Arp3 splayed interface, with key residues from Arp2 labeled based on *S. cerevisiae* sequence. (c) Coomassie stained gel of purified wild type and splayed interface mutants of ScArp2/3 complex. All budding yeast complexes in this panel and in subsequent figures harbor the engineered cysteine residues: (Arp2(R198C)/Arp3(L155C)). (d) Anti-Arp3 and anti-Arp2/anti-Arp3 western blots of 1 min crosslinking reactions with 1 μ M wild type or mutant ScArp2/3 complexes in 200 μ M ATP, 1 mM MgCl₂, 50 mM KCl, 20 mM Imidazole pH 7.0, and 1 mM EGTA. (e) Quantification of reaction described in panel D run in triplicate. Error bars show standard error for three reactions. (f) Time course of 3 μ M 15% pyrene actin polymerization with 25 nM wild type or splayed interface mutant Arp2/3 complexes as indicated. No NPF is present in these assays. (g) Maximum polymerization rate versus concentration of wild type or mutant ScArp2/3 complexes in pyrene actin polymerization assays as described in (e).

activity compared to the wild type complex, and the A207I mutant was nearly identical to wild type. Together, our data demonstrate that destabilization of the splayed interface not only potently stimulates formation of the short pitch conformation, but also increases the

NPF-independent nucleation activity of the complex. These data support a model in which the C-terminus prevents spurious activation of the complex by locking it into the splayed conformation.

ATP binding to both actin-related subunits is important for stimulation of the short pitch conformational change

The requirement for the Arp3 C-terminal tail in regulation of Arp2/3 complex *in vitro* and *in vivo*, together with evidence for structural plasticity of this feature, suggests factors that activate Arp2/3 complex could target the tail to decrease the stability of the splayed Arp2-Arp3 interface. Structural information addressing the influence of WASP family proteins on the complex is limited to low resolution EM reconstructions^{7,19,20}, small angle x-ray scattering models¹⁸, FRET^{19,48}, crosslinking⁴⁹⁻⁵³, photo-activatable label transfer-based constraints⁵⁴, and x-ray crystal structures showing electron densities that likely represent partial segments of bound WASP. In these structures, electron density at the interface of subdomain 3 and 4 in Arp3 is consistent with three residues of the A region of N-WASP^{55,56}. Further, tubes of electron density at the barbed ends of Arp2 and Arp3 in these structures could correspond to the predicted alpha helical segment in C⁵⁶. The lack of complete high-resolution structures for the bound activators makes it unclear how binding of WASP could switch Arp2/3 complex from the splayed to the short pitch state. ATP is also required for activation, and in contrast to other activators, several high-resolution structures of the complex in apo- versus ATP-bound states are available¹⁴⁻¹⁶. While these structures show that ATP binding closes the nucleotide binding cleft (NBC) of Arp3, Arp2 and Arp3 remain in a splayed conformation, so it is unclear how ATP

could contribute to activation. However, in these structures, NBC closure is correlated with widening of the barbed end groove and release of the tip of the Arp3 C-terminus³³ (Fig. 6a). These observations led us to propose a model in which ATP helps activate the complex by stimulating closure of the Arp3 nucleotide cleft, causing release of the autoinhibitory C-terminus from the barbed end groove and subsequent destabilization the splayed Arp2-Arp3 interface (Fig. 6a). As a first test of this model, we asked if binding of ATP to the complex stimulates population of the short pitch conformation. The crosslinking assays in Figures 4 and 5 of this study were run in buffers containing ATP to match conditions of polymerization assays, so we ran a set of experiments to directly compare short pitch crosslinking with and without ATP. These data demonstrate that ATP stimulates the short pitch conformation in the wild type complex. Even after five minutes of crosslinking, we did not detect any crosslinking in the absence of ATP, whereas 19 ± 2 % of the complex crosslinked in the presence of ATP (Fig. 6b,c). ATP binds to both Arp2 and Arp3, so binding to either Arp could be responsible for stimulating the splayed to short pitch conformational change^{6,30}. Therefore, we tested the ability of ATP to increase short pitch crosslinking using a previously described mutant complex defective in ATP binding to Arp3, Arp3(G358Y)⁷. Consistent with our model, the Arp3 nucleotide binding cleft mutant Arp3(G358Y) reduced the ability of the ATP to stimulate short pitch crosslinking, demonstrating that ATP binding to Arp3 is important for stimulating the short pitch dimer (Fig. 6d). To probe for a role for ATP binding to Arp2, we generated two mutations in the Arp2 NBC, D10A and G302Y. Both of these mutations decrease crosslinking of ATP to the Arp2 subunit and potently decrease Arp2/3 complex activity (Fig. S4)⁷. Unexpectedly, both mutations completely blocked ATP-

induced stimulation of short pitch conformation. Together, these data demonstrate that ATP binding to both Arp3 and Arp2 is important for stimulation of the short pitch conformation, but that ATP engagement at the Arp2 NBC plays a larger role.

To further investigate the link between nucleotide binding and the stability of the Arp2-Arp3 splayed interface, we tested how activating mutations in the C-terminus or in the Arp2 α E/ α F loop influenced the ability of ATP to stimulate the short pitch conformation. While the wild type complex showed no short pitch crosslinking in the absence of ATP, two of the mutants, including Arp2(A207C) and Arp2(F203Y), showed significant crosslinking in the absence of ATP (Fig. 6d). Importantly, ATP-bound mutant complexes showed 8-15 fold more potent crosslinking than ATP-bound wild type complex (Fig. 6e, Supplementary Table 3). These data indicate that the intrinsic stability of the splayed interface tunes the ability of ATP to shift the conformation toward the short pitch state. We note that the relatively weak ATP-induced stimulation of short pitch crosslinking in the wild type complex is consistent with the weak NPF-independent activity of the wild type *S. cerevisiae* complex in pyrene actin polymerization assays (Fig. 2c)^{20,57}.

Release of the tip of the Arp3 C-terminus from the barbed end groove stimulates formation of the short pitch conformation

Our data show that ATP binding to Arp3 stimulates adoption of the short pitch dimer, even though the nucleotide binding site is ~ 20 Å from the Arp2-Arp3 splayed interface. Therefore, we wondered if structural changes initiated at the Arp3 NBC could allosterically destabilize the splayed Arp2-Arp3 interface. As mentioned above, crystal

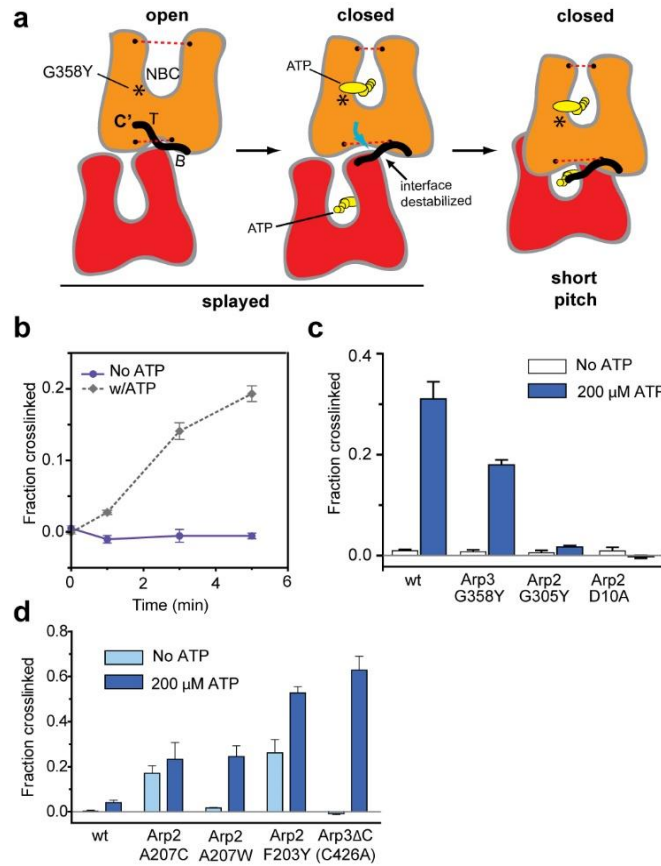


Figure 6 | The Arp3 C-terminus is an allosteric molecular switch that locks the complex in the inactive (splayed) conformation.

(a) Cartoon depicting proposed conformational link between the ATP binding cleft, the barbed end groove and the C-terminus of Arp3. Dotted red lines indicate widths of nucleotide binding cleft (NBC) and barbed end groove. The tip (T) and base (B) of the Arp3 C-terminus are indicated. (b) Time course of crosslinking assays containing 1 μM wild type ScArp2/3 complex with or without 100 μM Mg^{2+} -ATP. (c) Quantification of 5 min short pitch crosslinking for reactions containing 1 μM wild type or ATP-binding pocket mutation complexes with either 1 μM EDTA or 200 μM Mg^{2+} -ATP. (d) Quantification of 1 min short pitch crosslinking assays of wild-type or splayed interface mutations with or without 200 μM Mg^{2+} -ATP. Error bars in panels c and d show standard error for three reactions.

structures with ATP bound show the Arp3 cleft in a closed conformation, a state correlated with widening of the barbed end groove and disordering of the tip of the Arp3 C-terminus^{16,33,58} (Fig. 6a). In contrast, crystal structures of the complex with no nucleotide bound to Arp3 tend to show an open NBC, a closed barbed end groove, and

the Arp3 C-terminus engaged^{14,16}. These structural comparisons, along with molecular dynamics simulations, indicate that the NBC, the barbed end groove, and the Arp3 C-terminus are allosterically linked³³. The structural link between these regions is consistent with our measurements of etheno-ATP (ϵ -ATP) binding to the *S. pombe* complex, which specifically measures nucleotide binding to the Arp3 subunit (see methods). Specifically, we found that ϵ -ATP bound ~2.7 fold more tightly to the Arp3 Δ C mutant than the wild type SpArp2/3 complex (Fig. S5). Unexpectedly, the binding affinity of ϵ -ATP for the *S. cerevisiae* complex did not change when the Arp3 C-terminus was deleted (Fig. S5). This was surprising given that ATP binding and truncation of the Arp3 C-terminus stimulate the same conformational change in ScArp2/3 complex (Fig 4). While we cannot currently explain this result, one possibility is that ϵ -ATP engages the NBC differently than ATP so fails to form the same allosteric link to the Arp3 C-terminus.

The structural link between the nucleotide binding cleft, the barbed end groove, and the Arp3 C-terminus suggests that ATP binding could influence the stability of the splayed interface by controlling the engagement of the Arp3 C terminus with the barbed end groove. However, in the x-ray crystal structures, nucleotide-induced NBC closure generally results in disorder of the tip of the Arp3 C-terminal tail, while the base remains fully or partially ordered (Fig. 7a, Fig. S6). The Arp3 C-terminal truncations we describe above remove both the tip and base of the tail (Fig. 2b). Removal of base could directly destabilize the splayed conformation because it eliminates residues that participate in the splayed Arp3-Arp2 interface (Fig. 4a). Therefore, we wondered if disruption of the tip alone could allosterically destabilize the splayed interface. To test this, we mutated to aspartate the two conserved hydrophobic residues that pin the tip into the barbed end

groove (Fig. 7b). Like the complete C-terminal deletion, this mutation, Arp3(L445D/F446D), increased NPF-independent activity compared to the wild type complex (Fig. 7c,d). In addition, the Arp3(L445D/F446D) mutation stimulated formation of the short pitch conformation in the crosslinking assay, despite the fact that neither of the mutated residues directly contribute to the splayed interface (Fig. 4a, 7e). Similar to the C-terminal deletion mutant, the Arp3(L445D/F446D) mutant required ATP for potent stimulation of the short pitch conformation (Fig. 7e). Furthermore, like the Arp3 C-terminal truncation, the Arp3(L445D/F446D) mutant formed a secondary (non-short pitch) Arp3-Arp2 crosslinked band in the BMOE crosslinking assay (Fig. 7f). This secondary product forms due to a crosslink between an endogenous cysteine in Arp3, C426, and Arp2. C426 is at the barbed end of Arp3 adjacent to the C-terminal tail, and is reactive only when the C-terminal tail is deleted, but not in the wild type complex (Fig. 7b,d, Fig. S7). The C426 non-short pitch crosslink also occurs in the Arp3(L445D/F446D) mutant, suggesting that mutation of the tip of the tail increases the solvent exposure of Arp3 C426 similarly to the C-terminal truncation, providing additional evidence that the Arp3(L445D/F446D) mutation releases the tail from the barbed end groove. Together, these data strongly support a model in which release of the tip of the Arp3 C-terminus from the barbed end groove allosterically influences the conversion from the splayed to short pitch conformation, providing a molecular mechanism by which ATP helps relieve autoinhibition of Arp2/3 complex.

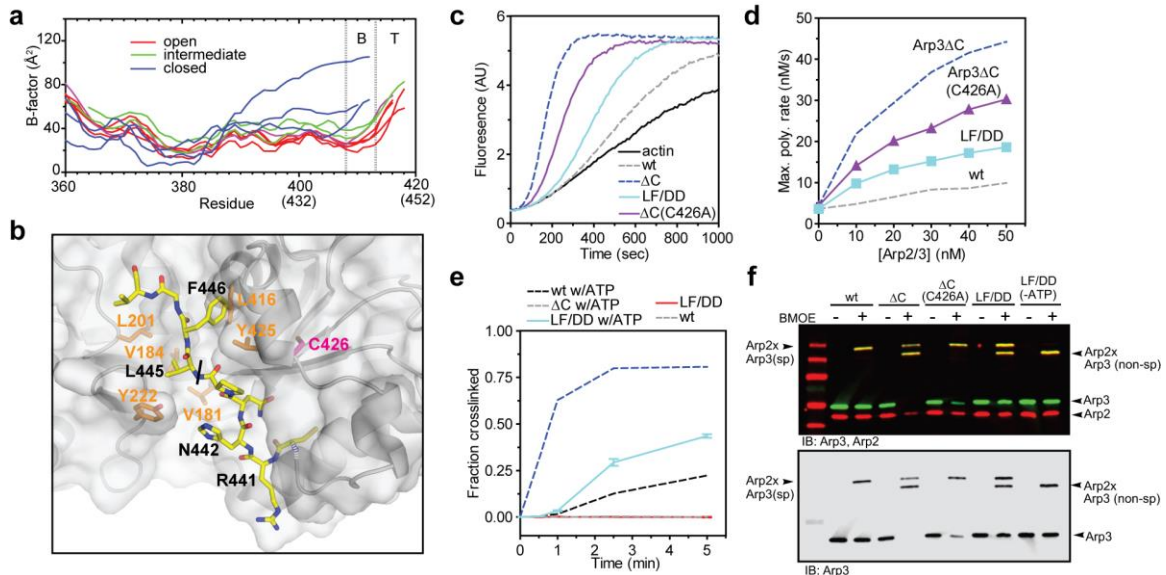


Figure 7 | Release of the tip of the Arp3 C-terminus from the barbed end groove stimulates formation of the short pitch conformation.

(a) Plot of average main chain B-factor versus residue number for the C-terminal residues in Arp3. Data taken from ten different *Bos taurus* Arp2/3 complex crystal structures in different nucleotide-bound states (1K8K, 2P9L, 1U2V, 2P9N, 2P9U, 2P9P, 1TYQ, 2P9I, 2P9K, 2P9S) (14-16). Nucleotide cleft widths are classified based on Nolen and Pollard¹⁶. B-factors were normalized so that each chain had the same average main chain B-factor. Residues missing in the electron density are omitted from the plot. Residue numbers in parenthesis are for ScArp2/3 complex. See Fig. S6 for more detailed B-factor analysis. (b) Surface representation of the barbed end groove with C-terminus of Arp3 bound (yellow stick representation, black labels) based off of structure 1K8K. Orange labels indicate key hydrophobic residues in the Arp3 barbed end groove. C426, a cysteine that becomes reactive upon deletion of the Arp3 C-terminal tail, is labeled in magenta. Residue labels are based on *S. cerevisiae* sequence. Black line indicates transition between the base and tip of the C-terminal tail. (c) Time courses of polymerization of 3 μM 15% pyrene actin in the presence of 10 nM wild type, Arp3ΔC, Arp3ΔC(C426A), or Arp3(L445D/F446D) ScArp2/3 complexes. The C426A mutation decreased activity slightly in the Arp3ΔC complex, but was still hyperactive compared to wild type. (d) Maximum polymerization rate versus complex concentrations for reactions described in C. (e) Time course of short pitch crosslinking for reactions containing 1 μM wild type, Arp3ΔC, or Arp3(L445D,F446D) ScArp2/3 complexes and 200 μM Mg²⁺-ATP. Error bars show standard error for at least three reactions. (f) Two color (anti-Arp2/anti-Arp3) western blot of crosslinking reactions containing 1 μM wild type or mutant ScArp2/3 complexes with or without 200 μM ATP as indicated. Reactions containing wild type and Arp3(L445D/F446D) complexes with or without ATP were run for 5 min. Reactions containing Arp3ΔC or Arp3ΔC(C426A) complexes were run for 1 min.

DISCUSSION

Our data indicate that Arp2/3 complex must be locked in the splayed conformation to prevent its spurious activation. Interactions that stabilize the splayed conformation can be described by two major sets of contacts¹⁴⁻¹⁶. First, Arp2 and Arp3 are held by a molecular clamp formed by ARPC1, ARPC2, ARPC4 and ARPC5 (Fig. S8). The clamp buries approximately 1500 Å² of surface area of Arp2 and 2100 Å² of Arp3. Second, Arp2 and Arp3 interact end-to-end in the splayed conformation within the clamp (Fig. S8). The contact area of the splayed Arp2-Arp3 interface is relatively small (~800 Å²), and based on computational predictions is not a relevant dimer interface in the absence of the clamp (data not shown)⁵⁹. However, we show that the Arp2-Arp3 splayed interface is critical for controlling the conformation of the complex. Furthermore, our data suggest that at least one activator, ATP, targets the splayed interface to activate the complex. In addition to Arp2/3 complex activators, we note that at least one inhibitor also targets the splayed Arp2-Arp3 interface. CK-666, a small molecule Arp2/3 complex inhibitor, binds in a pocket at the splayed interface, directly stabilizing the splayed arrangement to inactivate the complex²². Therefore, tuning the strength of the splayed Arp2-Arp3 interface may be a general mechanism by which regulators control branching nucleation by Arp2/3 complex.

Here we present a “tail release” model in which the Arp3 C-terminal tail serves as a molecular switch that controls the conformation and activity of the complex. In this model, when the tip of the tail is released from the barbed end groove, it destabilizes interactions between the base of the tail and Arp2, thereby stimulating the short pitch conformation (Fig. 6a). Existing biochemical and structural data support the tail release

model, but several lines of evidence indicate that activation involves additional structural mechanisms. For instance, ATP binding increased short pitch crosslinking in the Arp3 Δ C mutant, demonstrating that deletion of the Arp3 C-terminal tail is not sufficient to completely populate the short pitch state (Fig. 6e). In addition, our data show that ATP-induced activating structural changes are not exclusively propagated through the Arp3 subunit. While ATP binding to Arp3 contributed to stimulation of the short pitch conformation, mutations that blocked ATP binding to Arp2 completely abolished stimulation of the short pitch conformation. This indicates that ATP binding to Arp2 is actually more important than Arp3, and that nucleotide binding must also stimulate the short pitch conformation through mechanisms not directly involving the Arp3 C-terminus. We note that several other mutations in Arp2/3 complex are known to increase the NPF-independent nucleation activity of the complex. While the structural basis by which these mutations relieve autoinhibition is unknown, the location of the amino acid changes suggests they may not be directly linked to the tail release mechanism^{20,25}. Understanding how multiple structural features in the complex coordinately stimulate activation, and how Arp2/3 complex regulators target these features during activation remain important open questions. We anticipate that the short pitch crosslinking assay will provide an important tool in this regard.

ATP hydrolysis by Arp2/3 complex stimulates branch disassembly, so the requirement for ATP in activation creates a built in timing mechanism to control turnover of branched actin networks²⁸⁻³⁰. Mutational analysis shows that ATP binding to both Arp2 and Arp3 is important for branching nucleation^{7,21}, but how nucleotide binding to either Arp subunit could influence the activity of the complex was unknown. Here we

show that ATP stimulates formation of the short pitch conformation, explaining how it contributes to activation. By mutating the nucleotide binding cleft of Arp3, we showed that ATP binding to Arp3 is important for stimulation of the short pitch conformation, consistent with the tail release model. Previously published FRET experiments are consistent with our data, since mutations in the Arp3 NBC blocked an ATP-induced increase in FRET²¹. However, these data also showed that NBC mutations in Arp2 did not block the conformational change measured by FRET²¹, whereas the same mutations completely blocked short pitch crosslinking in our assays here, making it unclear if the FRET assay measures the short pitch conformational change. That ATP binding to Arp2 stimulates the short pitch conformation is also supported by a previously described NBC mutation in Arp2, Y309A. Arp2-Y309A increases the activity of the complex both in the presence and absence of NPF⁷. In EM reconstructions of negatively stained particles, the Y309A complex favors a conformation more closely resembling the wild type NPF-bound than free complex⁷. This suggests it may stimulate the short pitch conformation, and that like Arp3, the nucleotide cleft of Arp2 is allosterically linked to overall positions of Arp3 and Arp2 in the complex. Dissection of the structural basis for this allosteric link will be important for understanding how Arp2/3 complex is activated. In addition, we note that at cellular concentrations, ATP will bind rapidly to the nucleotide-free Arp subunits, so the apo-complex is likely more transient than the ADP-bound states. Therefore, determining precisely why ADP cannot activate Arp2/3 complex will also be important for understanding the nucleotide-controlled timing mechanism for branch dissociation.

Mutations that selectively uncouple the activity of Arp2/3 complex from each of its activating inputs (ATP, actin monomers, actin filaments, and NPFs) will be critical to understand how Arp2/3 complex integrates activating signals to control branching nucleation *in vivo*⁴⁻¹⁰. While substantial work remains to identify new mutants and characterize existing ones, important trends have already emerged. First, despite potent *in vitro* NPF-independent activation by some mutations, the phenotype of existing activating mutations is relatively mild. For instance, deletion of the Arp3 β 4/ β 5 insert increased activation of *S. pombe* Arp2/3 complex by WASP (Wsp1), but had no influence on endocytic actin patches²⁴. Similarly, the budding yeast Arp2(Y309A) mutant showed no obvious defects in endocytic actin patch localization or organization⁷. The *arp2-7* budding yeast strain, which harbors the Arp2(F203Y) mutation we characterize here (plus one additional mutation in Arp2), showed defects in patch dynamics^{13,23,46,47}, but like the *arp3 Δ C* strain, the patches remained cortical and resembled wild type actin patches. The failure of existing activating mutations to cause accumulation of ectopic actin structures suggests additional mechanisms regulate the activity of the mutant complexes *in vivo*. One possibility is that these mutations fail to uncouple the activity of the complex from the requirement to bind preformed filaments. Consistent with this hypothesis, several experiments suggest the *in vivo* activity of wild type Arp2/3 complex is limited by the availability of suitable preformed substrate filaments^{9,43,60}. Negative regulators of the complex or its activators (*e.g.*, Crn1, Syp1, Bbc1, Sla1, Lsb1) may also dampen the *in vivo* influence of the mutations, explaining the mild phenotypes^{13,51,61,62}. A second emerging trend is that while relatively mild, the phenotypes of each of the activating mutations are distinct. These differences cannot be explained by the relative *in vitro*

potency of the mutations. For instance, the *S. pombe* Arp3 Δ C mutation shows modest activity *in vitro* but has the most pronounced influence on actin dynamics *in vivo*. We speculate that the precise molecular mechanism by which these mutations uncouple activation from activating inputs influences their *in vivo* effect on actin dynamics. We note that the Arp3 Δ C mutant is particularly intriguing in that its influence on the dynamics of the actin patches (increased Fim1 lifetime and defective internalization) is similar to what has been observed for mutations that compromise the activity of the complex rather than activate it^{7,13}. We anticipate that further dissection of this and other key Arp2/3 complex mutants will provide important insight into the *in vivo* function of the complex.

MATERIALS AND METHODS

Construction of fission yeast strains

A fission yeast strain harboring the *arp3* Δ C(416-427) mutation was made by transforming the TP150 strain with a cassette harboring a premature stop codon and the KanMX6 marker as described³⁴. *FIMI* was tagged with GFP by homologous recombination strategy using a cassette generated from pFA6a-GFP-NatMX6⁶³. Both integrations were confirmed by amplifying and sequencing the entire regions. See Supplementary Table 4 for all fission yeast strains used in this study.

Construction of budding yeast strains

Splayed interface mutations in Arp2 were constructed by Quick Change PCR using as a template a previously constructed vector in which *arp2(R198C)* was subcloned into pRS317 with native promotor and terminator sequences²². Arp3(L445D/F446D), Arp3 Δ C⁴⁴⁰⁻⁴⁴⁹ and Arp3 Δ C⁴⁴⁰⁻⁴⁴⁹(C426A) expression plasmids were created by the same method, using a previously described template in which *arp3(L155C)* is flanked by native promoter and terminator sequences was cloned into pRS315. These plasmids were introduced into haploid strains with the corresponding Arp subunit knocked out and rescued on a *URA* plasmid. Haploid strains expressing Arp subunits off of the pRS plasmids were then mated, sporulated and selected through random spore analysis as previously described to generate the final yeast expression strains²². See Supplementary Table 5 and 6 for all budding yeast plasmids and strains used in this study.

Protein purification and labeling

Pyrene labeled rabbit skeletal muscle actin was purified and labeled as previously described^{22,24}. For expression of *S. pombe* Arp2/3 complex, *S. pombe* cells were grown in 200 mL of YES medium at 30 °C. After ~24 hours, 10 mL of this culture was used to inoculate 1 L cultures of YES, which were grown at 30 °C for 12-16 hours. An additional 35 g of YES was added to each 1 L culture, and cells were grown to an optical density at 600 nm of ~6.0 before harvesting. To produce *S. cerevisiae* cell pellets for protein purification, a starter culture grown in synthetic media lacking leu, lys, his, and trp was added to 1 L YPD medium and allowed to grow to OD₆₀₀ ~7-8. An additional 50g/L YPD powder was added and cells were harvested at OD₆₀₀ ~15-16. Before harvesting, 2 mM EDTA and 0.5mM PMSF was added to prevent proteolysis. Cells were pelleted in a F8B

rotor at 5K rpm for 5 minutes. Cells were resuspended in lysis buffer (20 mM Tris pH 8.0, 100 mM NaCl, 1 mM EDTA, 1 mM DTT), and stored at -80 degrees Celsius. *S. pombe* Arp2/3 complex was purified as previously described using an ammonium sulfate cut, a GST-N-WASP-VCA affinity column, a MonoQ anion ion exchange column (GE Healthcare), and a Superdex 200 gel filtration (GE Healthcare)²⁴. *S. cerevisiae* Arp2/3 complexes were purified using an ammonium sulfate cut, a GST-N-WASP-VCA affinity column, and a gel filtration step, as previously described²². Unlike the other complexes reported here, the Arp3 Δ C mutant complexes could not be eluted from a GST-N-WASP-VCA affinity column using high salt. These complexes were instead eluted with 50 mM reduced glutathione solution. The pooled fractions were then purified by monoQ and glutathione sepharose columns to remove any contaminating GST-N-WASP-VCA. Like the wild type complexes, the Arp3 Δ C complexes were gel filtered as a final purification step before flash freezing in liquid nitrogen. Anti-GST (Genescript A00865) western blots were used to demonstrate that there was no detectable GST-N-WASP-VCA in the complexes prepared with the modified purification method (Fig. S9).

Pyrene actin polymerization assays and kinetic data analysis

Pyrene actin polymerization assays were carried out as previously described²².

Fluorescence changes were monitored by exciting the sample at 365 nm and measuring the emission at 407 nm using a Tecan Safire 2 plate reader. The maximum rate of polymer formation was calculated as previously described²².

Microscopy

TIRF microscopy was carried out as previously described using a Nikon TE2000-U microscope outfitted with a 100 x TIRF objective lens, a 488 nm argon laser and a 561 nm diode laser²⁴. Confocal microscopy of *S. pombe* cells was carried out at 30 °C on the same microscope, using a Yokagawa CSU10 spinning-disc head. Cells were maintained in the exponential phase for 2 days before immobilization on a gelatin pad as described⁶⁴. Images were collected using Micromanager software and actin patches were tracked manually in Image J^{65,66}. For patch internalization measurements, patches were tracked from x separate cells in x different movies, using custom Matlab particle tracking scripts⁶⁷. Patches that moved 2 pixels (~0.2 μm) from their origin were classified as internalized, even if the patch movement was not perpendicular to the cell cortex. To quantify the intensity of patches over time, a circle with a diameter of seven pixels was drawn in ImageJ over isolated patches and the intensity was measured for each frame. The background was subtracted by measuring the intensity of a circle of the same size in the cytoplasm of the cells. Due to the frequent patch internalization failures in the Arp3ΔC strain, patches were aligned to the maximal intensity of Fim1-GFP, which typically reflects the time at which patch movement starts to occur^{41,68}. FM4-64 uptake assays were carried out as previously described⁶⁹.

ε-ATP binding assays

ε-ATP binding was measured by titration of a solution of 0.5 μM wild type or mutant fission yeast Arp2/3 complex in 10 mM Hepes pH 7.0, 50 mM KCl, 1 mM EGTA, 1 mM MgCl₂, 1 mM DTT, 1.4 % acrylamide with ε-ATP and measuring the fluorescence at 420 nm (excitation = 340 nm). The background fluorescence of unbound ε-ATP was

subtracted by assuming a linear relationship between the signal and ϵ -ATP at saturating concentrations. Data were fit as previously described²⁴. We note that while both actin-related subunits in the complex bind nucleotide, previous experiments showed that mutations in the Arp2 binding pocket that potently decreased crosslinking of ATP to Arp2 had no influence on the nucleotide affinity measured by this assay, indicating ϵ -ATP measures binding specifically to the Arp3 subunit⁷.

Short pitch crosslinking assays

All crosslinking assays were performed with budding yeast Arp2/3 complex containing the *arp2(R198C)* and *arp3(L155C)* mutations. Reaction mixes containing Arp2/3 complex with or without additional components (*e.g.* ATP or NPF) in KMEI were mixed with 4 μ L of 125 μ M BMOE for indicated times at 21 °C before adding SDS-PAGE loading buffer (1xSDS-PAGE buffer: 0.3 % SDS, 33 mM DTT, bromophenol blue) to stop the reaction. Reaction mixes were analyzed by SDS-PAGE and western blotting with goat anti-Arp3 (Santa Cruz, sc-11973, 1:1000 dilution), goat anti-Arp2 (Santa Cruz, sc-11969, 1:1000 dilution) or mouse anti-Arp3 (Santa Cruz, sc-376625, 1:1000 dilution) antibodies. Blots were imaged using a LICOR Odyssey Fc system.

Structural modeling

Models used for surface area and pKa calculations were constructed by first creating homology models of ScArp2 and ScArp3 with SWISS-Model (<http://swissmodel.expasy.org>) using 4JD2 as a template. Arp2 was then moved into the short pitch conformation using the Oda, *et. al.* filament model⁷⁰. Specifically, Arp3 was

superposed onto an actin subunit and Arp2 was then overlaid onto the subunit in the short pitch position relative to Arp3. The geometry of the structure was minimized using Phenix before running the calculations⁷¹

BRIDGE TO CHAPTER III

In this chapter, we investigated the structural features that hold Arp2/3 complex in its inactive conformation. We found that the splayed interface between Arp3 and subdomain 4 of Arp2 and the Arp3 C-terminus are key regions for holding the complex in its inactive state and disruption of these regions has dramatic effects both *in vitro* and *in vivo*. This work demonstrates that binding of ATP to both Arp subunits forms an allosteric link that is required for formation of the short pitch conformation and that one mechanism for this observed effect is due to displacement of the Arp3 C-terminus. In chapter III, we will investigate the role of a different activator of Arp2/3 complex, WASP, and biochemically dissect the requirements for stimulation of conformational changes by this NPF.

CHAPTER III

THE ROLE AND STRUCTURAL MECHANISM OF WASP-TRIGGERED CONFORMATIONAL CHANGES IN BRANCHED ACTIN FILAMENT NUCLEATION BY ARP2/3 COMPLEX

AUTHOR CONTRIBUTIONS

B.J.N. and M.R.-S. designed the experiments and interpreted the data. B.J.N. and M.R.-S. wrote the manuscript. B.J.N., M.R.-S., Q.L., and S.-L.L., generated reagents and carried out experiments.

INTRODUCTION

Proper regulation of the actin cytoskeleton is critical for cells to orchestrate processes like division, differentiation, motility and endocytosis. Assembly of new actin filaments is limited by a slow nucleation step, and cells rely on three classes of actin filament nucleators - tandem WH2 domain proteins, formins, and Arp2/3 complex - to control precisely when and where actin filament networks assemble (1, 2). Arp2/3 complex is unique among actin filament nucleators in that it typically nucleates branched (as opposed to linear) actin filaments (3-5). Branched actin filaments are important for assembling dendritic networks required for lamellipodial protrusion and endocytosis (6, 7).

Arp2/3 complex is tightly regulated, and multiple factors, including preformed actin filaments, actin monomers, ATP, and a class of proteins called nucleation

promoting factors (NPFs) are typically required for activation (5-7). In some species, phosphorylation of Arp2/3 complex is also required for activation (8). WASP (Wiskott-Aldrich Syndrome Protein) family proteins are the best understood NPFs, and share a conserved polypeptide sequence called VCA (Verprolin homology, Central, Acidic), which constitutes the minimal region sufficient for Arp2/3 complex activation. WASP proteins interact with actin monomers through their V and C regions, and bind Arp2/3 complex through C and A regions (9, 10). How WASP proteins activate Arp2/3 complex is unknown, but available data suggest they play multiple roles in the branching nucleation reaction. For instance, several lines of evidence indicate the CA segment of WASP proteins stimulates a conformational change in the complex important for activation (11-15). In addition, WASP-VCA recruits actin monomers to the complex through its V region. Kinetic simulations of the weak NPF-independent activity of Arp2/3 complex suggested actin monomers must bind the complex to form a nucleus, leading to the idea that WASP-recruited monomers could “jump start” nucleation (16, 17). The observation that the V region is required for WASP-mediated activation of the complex supported this idea, and indicated that direct monomer tethering might not only accelerate nucleation, but might be a general requirement for assembly of the nucleus (9, 10, 12). In addition to its activating influence, WASP-VCA can also have an inhibitory influence on the kinetics of branching nucleation. Specifically, recent single molecule TIRF experiments showed that VCA must be released from nascent branch junctions before nucleation, and that slow WASP-VCA release limits nucleation rates (18, 19). Efforts to understand the relative contributions of each of these roles of WASP on

activation have been hampered by a lack of methods that can disentangle these functions or directly probe the connection between conformation and activity.

Two of the seven protein subunits in Arp2/3 complex, Arp2 and Arp3, are homologous to actin. High-resolution crystal structures of inactive Arp2/3 complex show Arp2 and Arp3 interacting end-to-end in a “splayed” conformation (20-23). Upon activation, Arp2 is hypothesized to undergo a rigid body movement that moves it ~20 Å into position next to Arp3, forming an Arp2-Arp3 “short pitch” dimer that structurally mimics two consecutive actin subunits within a filament (20, 24). Low-resolution EM structures of Arp2/3 complex bound to the WASP proteins N-WASP or WAVE1 support this hypothesis, since they show Arp2 and Arp3 in a filament-like arrangement (15). In addition, recent experiments demonstrated that N-WASP stimulates site-specific crosslinking of engineered cysteines on Arp2 and Arp3 that react only when the complex adopts the short pitch conformation (11). These studies suggest a general function of WASP proteins may be to stimulate the short pitch conformation, providing an explanation for how they could activate the complex. However, whether this function is conserved among WASP proteins, and if adoption of the short pitch conformation is sufficient for activation is unknown. Importantly, because WASP must recruit actin monomers to the complex for potent activation (9, 12), it is possible that the short pitch Arp2-Arp3 dimer provides only the initial core of a nucleus, to which one or more WASP-tethered actin monomers must be added for nucleation (7). Therefore, whether stimulation of the short pitch conformation without direct monomer tethering could activate the complex is unknown.

Understanding WASP-mediated activation requires knowledge of both the role of the short pitch conformation and the mechanism by which WASP proteins could stimulate this conformational change. Despite numerous studies, how the WASP CA region binds Arp2/3 complex is still unclear. Biophysical and biochemical experiments, including analytical ultracentrifugation, isothermal titration calorimetry, and crosslinking indicate that Arp2/3 complex binds two WASP-CA molecules (25-27). Crosslinking and label transfer experiments suggest one CA binding site is on Arp3 and the second spans Arp2 and ARPC1 subunits (10, 25, 28-30). NMR line broadening experiments and mutational analyses suggest that the C region forms an amphipathic helix when it binds to the complex (31). Together with homology modeling and recent low resolution crystal structures, these data suggest that the C helix binds the barbed end groove of each Arp like the V region helix binds the barbed end groove of actin (25-27, 32) (Fig. 1A). Less is known about interactions with A, but a short segment of electron density between subdomains 3 and 4 in Arp3 in a co-crystal structure was interpreted as the conserved tryptophan from the A region of one bound WASP (27). The second A region is thought to bind the ARPC1 subunit, since this subunit in isolation can bind to VCA in a mode dependent on the conserved tryptophan (33). These data, together with distance measurements reported in a recent FRET study (26), have led to an approximate model for CA binding at each site (Fig 1A). This model is consistent with the majority but not all of the published data (15), and provides an important starting point for understanding the molecular basis for WASP-mediated conformational changes. Surprisingly, few studies have used mutational dissection of the complex to investigate WASP binding, and little high-resolution structural information is available (27, 34), so the model remains

tentative. Furthermore, the lack of biochemical dissection leaves open the important question of how engagement of WASP could stimulate the conformational rearrangement of the complex thought to be required for activation.

Here we use a newly developed engineered cysteine crosslinking assay to investigate the role of the short pitch conformation in Arp2/3 complex activation (11). Crosslinking the engineered cysteines to hold Arp3 and Arp2 in or near the short pitch conformation bypasses the need for WASP in activation. Remarkably, the complex shows NPF-independent hyperactivity when crosslinked in this conformation. This result indicates that the switch to the short pitch conformation is a critical activation step, and that direct actin monomer recruitment by WASP-VCA is not required for potent activity. Our crosslinking experiments indicate that stimulation of the short pitch conformation is a conserved feature of WASP proteins, and that the CA region is sufficient for this function. However, our data also suggest that the activating effect of the WASP-mediated conformational change may be masked by slow release of WASP from nascent branch junctions. Using structure-based mutational analysis and WASP-Arp fusion chimeras, we determined one mechanism by which WASP proteins can stimulate movement of the Arp2 and Arp3 subunits into the short pitch conformation. We show that WASP competes for binding to the barbed end groove of Arp3 with the Arp3 C-terminal tail, a structural element that forms an allosteric switch responsible for autoinhibition of the complex. These data support a model in which WASP binds the Arp3 barbed end groove, displacing the Arp3 C-terminal tail to relieve autoinhibition and stimulate the short pitch conformation.

Results

Stimulation of the short pitch conformation is a conserved feature of WASP family

NPFs

Several studies show that WASP family proteins cause conformational changes in Arp2/3 complex, and that these changes are likely important for activation. For example, binding of WASP-VCA to an Arp2/3 complex tagged with fluorescent proteins on ARPC1 and ARPC3 caused a conformational change detected by increased FRET (12). Mutations that blocked the conformational change decreased the activity of the complex (12). Similarly, EM reconstructions of negatively stained Arp2/3 complexes showed the WASP protein Las17 caused structural rearrangements interpreted as repositioning of Arp2 (13, 14). Electron densities from higher resolution EM reconstructions (~2.0 nm) of N-WASP and WAVE1-bound complexes showed a short pitch arrangement of Arp2 and Arp3 that could template nucleation (15). We reasoned that if stimulation of the short pitch conformation is important for activation, it should be a conserved function of WASP family proteins. To test this, we took advantage of a recently developed crosslinking assay in which engineered cysteines on budding yeast Arp2 and Arp3 crosslink only when the complex is in or very near the short pitch conformation (11) (Fig. 1B). Treatment of the dual cysteine engineered Arp2/3 complex with the 8 Å crosslinker BMOE produces a high molecular weight band cross reactive with both Arp2 and Arp3 antibodies (Fig. 2A). This band does not form in either of the single cysteine complexes (Fig. 2A). Furthermore, the engineered cysteines do not significantly influence the activity of the complex, demonstrating that the crosslinking assay can be used to probe for the conformational switch (11). We tested the influence of canonical WASP family

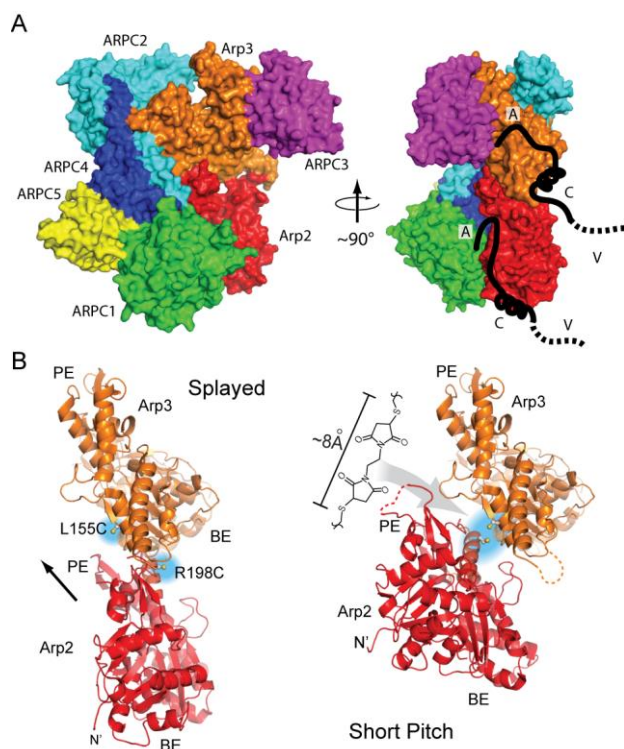


Figure 1: Hypothesized CA binding mode and schematic of short pitch crosslinking assay.

A. Hypothetical model showing proposed binding sites for WASP family CA region on Arp2/3 complex. Arp2/3 complex surface representation is based on the structure of GMF γ -bound Arp2/3 complex (4JD2) (23). **B.** Ribbon diagrams of Arp2 and Arp3 in the splayed and short pitch conformations showing design of engineered crosslinking assay. Structure 4JD2 was used to make both panels. In the right panel, the Oda, *et. al.* actin filament structure was used to move Arp2 into the short pitch conformation (67). Engineered cysteines (Arp3(L155C), Arp2(R198C)) are highlighted in cyan. Black arrow shows the direction of the ~20 Å movement required to position Arp2 into the short pitch conformation. The structure of the chemical crosslinker (BMOE) used in the short pitch crosslinking assay is indicated. The distance between engineered cysteines is 32.5 Å in the splayed conformation, and ranges from ~8-13 Å in different models of the short pitch conformation. (Also see SI Appendix, Fig. S1).

members from mammals and budding yeast on crosslinking of the dual cysteine engineered complex. Each NPF was added at multiple concentrations to reach saturation and remove the influence of binding site occupancy on the conformation. VCA segments from N-WASP, WAVE1, WASP, and Las17 each potently increased crosslinking (Fig. 2B,C, SI Appendix, Table S1). In one minute crosslinking reactions, near saturating

concentrations of each WASP family protein produced ~23-32% cross linked complex, a 7-10 fold increase over reactions without NPF. Multiple lines of evidence indicate the influence of these NPFs is not due to a change in the chemical reactivity of individual engineered cysteine residues, but instead due to increased population of the short pitch conformation. First, while WASP binding could influence the pKa of the cysteine thiol groups and formation of the thiolate, the high concentration of negative charges of the WASP A regions would be more likely to decrease than increase cysteine reactivity (35). Second, a chemically conservative point mutation in N-WASP potentially reduces stimulation of the short pitch crosslinking even at saturation (see below). This residue was previously determined by FRET to influence WASP-mediated conformational changes in the complex (12).

To better understand the structure of the BMOE crosslinked complex, we used morphing software to move Arp2 from its position in an inactive (splayed) crystal structure (4JD2) to its short pitch position in the low-resolution EM structure of Arp2/3 complex at a branch junction (24). At each point in the trajectory we calculated the solvent accessible surface crosslinking distance between the engineered cysteines (36). Given the crosslinker link of ~8 angstroms for BMOE, this analysis suggests that the crosslinked complex is either in or very near the short pitch conformation (SI Appendix, Fig. S1). Therefore, for simplicity, we will refer to the covalently trapped conformation as the short pitch conformation in the sections that follow. We discuss the possible limitations of this interpretation in the discussion section. Given these considerations, we conclude from the data above that diverse WASP proteins stimulate movement of Arp2 and Arp3 into the short pitch “filament-like” arrangement. Importantly, N-WASP-CA

alone stimulated this conformation as potently as N-WASP-VCA, consistent with binding assays showing that CA but not V interacts with Arp2/3 complex (Fig. 2B,C) (10).

CA binding to both Arp2 and Arp3 is important for stimulation of the short pitch conformation

Our data indicate that diverse WASP proteins stimulate the short pitch conformation, suggesting this structural state is important for activation. To better understand the role of the short pitch conformation and how it is promoted, we attempted to create a “locked” short pitch complex by fusing WASP-CA segments onto the C-terminus of either Arp2 or Arp3 in budding yeast Arp2/3 complex. We designed these fusions based on the binding mode previously proposed for WASP CA on each Arp (Fig. 1A)(25-27). Fusions were made in the context of the engineered cysteine mutations to allow us to test for formation of the short pitch conformation. We reasoned that this design could potentially create a constitutively activated complex, and provides a method to dissect the importance of CA engagement at each binding site. Furthermore, the fused WASP segments lack V regions, conferring two additional advantages. First, the fused CA cannot recruit monomers to the complex, potentially allowing us to isolate the role of CA-stimulated conformational changes in activation. Second, the V region is proposed to block elongation of nascent branch junctions, necessitating WASP release (32, 37). By not including the V region we aimed to eliminate the requirement for WASP release in the nucleation reaction. We show below that the fused CA segments properly engage the complex. Unexpectedly, we found that while CA fusion to either Arp2 or Arp3 stimulated the short pitch conformation, the effect was modest (Fig. 3A-C, SI Appendix,

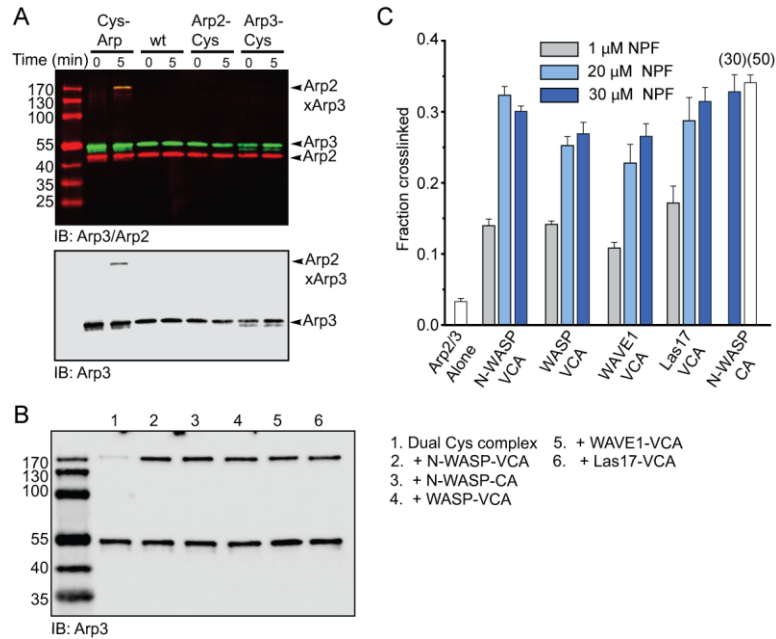


Figure 2: Stimulation of the short pitch conformation is a conserved feature of WASP family NPFs.

A. Single or two color western blots of short pitch crosslinking reactions containing 1 μ M wild type (wt), dual cysteine (Cys-Arp), or single cysteine (Arp2-Cys or Arp3-Cys) *S. cerevisiae* (Sc) Arp2/3 complexes and 25 μ M BMOE reacted for 0 or 5 min. **B.** Single color western blot of one minute crosslinking reactions containing 1 μ M dual cysteine (Cys-Arp), 25 μ M BMOE, and 30 μ M WASP family protein, as indicated. **C.** Quantification of reactions similar to those described in B, except multiple concentrations were tested. Parenthesis indicate concentrations of WASP-CA used (in μ M). Error bars show standard error from three reactions.

Table S2). Both CA-fusions failed to crosslink to the levels observed for wild type complex saturated with free N-WASP-CA. These observations suggest that binding of WASP-CA to both Arp2 and Arp3 is required to maximally stimulate the conformational switch. To challenge this hypothesis, we added free CA to each of the fusion complexes. Free WASP-CA added to the Arp3-CA fusion complex increased crosslinking to a level nearly identical to that observed with wild type complex with saturating CA ($23 \pm 2\%$ versus $26 \pm 2\%$), demonstrating that binding to both sites is required for potent short pitch stimulation (Fig. 3A-C). This result also shows that CA fused to Arp3 is nearly fully functional in its ability to stimulate the short pitch conformation, since addition of

free CA (to saturate the unoccupied Arp2 site) increases crosslinking efficiency to nearly the same level as CA-saturated wild type complex. Addition of CA to the Arp2-CA fusion complex yielded less short pitch crosslinking than CA-saturated wild type complex ($19 \pm 2\%$ versus $26 \pm 2\%$), suggesting that the Arp2-CA fusion is only partially functional in its stimulating the short pitch conformation, potentially due to a minor defect in the way the fused CA engages Arp2. We also attempted to create a dual CA-fusion complex, but sporulation of diploid yeast strains containing both Arp3-CA and Arp2-CA chimeras never yielded a haploid strain containing both chimeras in the absence of the wild type Arps, indicating that the dual CA fusion complex does not support viability.

CA release from Arp3 is likely important for nucleation

We next asked how fusion of CA to the complex influenced its nucleation activity. Specifically, we wondered if the modest increased population of the short pitch conformation in each CA fusion would result in increased nucleation activity of these complexes. As expected, the Arp2-CA fusion complex showed increased NPF-independent activity in pyrene actin polymerization assays compared to the wild type complex (Fig. 3D). In contrast, CA fused to Arp3 potently inhibited the complex, despite the fact that it stimulated the short pitch conformation (Fig. 3D). Previous experiments showed that WASP must be released from the nascent branch junction before nucleation (19), so we hypothesized that the decreased activity of the Arp3-CA fusion complex is due to slow (or no) CA release. To test this, we measured the influence of free CA on the activity of wild type and Arp2-CA fusion complexes. Addition of free CA blocked the

activity of both of these complexes in pyrene actin polymerization assays (Fig. 3E). Therefore, these data are consistent with a model in which slow CA release stalls branching nucleation. This result was unanticipated, because previous structural modeling predicted V (and not CA) sterically blocks actin monomers from associating with nascent branches to initiate elongation, necessitating WASP release (32, 37). Our data suggest that CA alone can block elongation. However, it is important to note that we cannot currently eliminate the possibility that fusion of CA to Arp3 may inhibit the complex for reasons unrelated to CA release. For instance, one study reported that CA binding to one of the two sites could inhibit the complex from binding to preformed filaments, so fused CA could block activation by inhibiting filament binding (27).

Locking Arp2/3 complex into the short pitch conformation causes potent NPF-independent activity

We created the CA fusion complexes to isolate the influence of the short pitch conformation on the branching nucleation reaction. However, the CA fusions had complicated effects on the reaction, both stimulating the short pitch conformation and presumably decreasing nucleation by preventing CA release. Therefore, we sought a new strategy to probe the role of the short pitch conformation. Our crosslinking experiments showed that even without WASP, a small fraction of the complex adopts the short pitch conformation (Fig. 2A,C), consistent with the weak NPF-independent activity of the budding yeast complex (13, 38). Therefore, we reasoned that crosslinking could be used to trap a fraction of the complex in the short pitch conformation to directly test its influence on nucleation activity. We crosslinked the dual cysteine complex with BMOE,

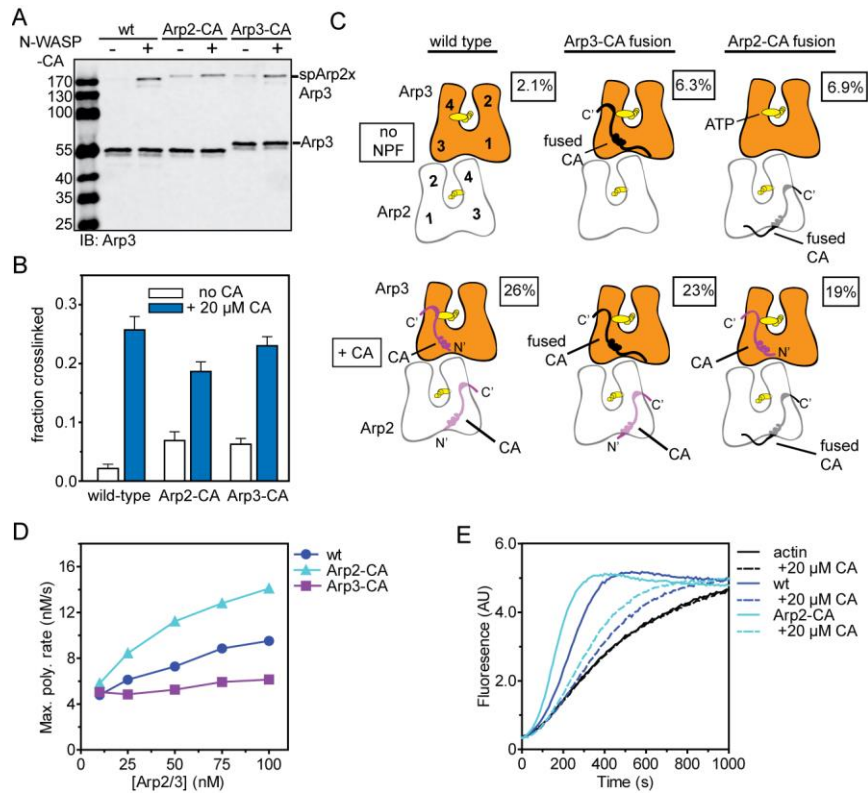


Figure 3: CA binding to both Arp2 and Arp3 is important for stimulating the short pitch conformation change.

A. Anti-Arp3 western blots of short pitch crosslinking assays containing 1 μM wild type or CA-fusion ScArp2/3 complexes (with dual cysteine mutations) and 25 μM BMOE reacted for 1 min in the presence or absence of 20 μM N-WASP-CA. **B.** Quantification of three reactions run under conditions described in A. Error bars show standard error of three reactions. **C.** Cartoon summarizing the short pitch crosslinking results for wild type and CA fusion complexes with or without N-WASP-CA. The average percentage of short pitch crosslinked product formed under each condition is indicated. **D.** Maximum polymerization rate vs. concentration of wild type or Arp-CA fusion complexes in 3 μM 15% pyrene actin polymerization assays. **E.** Time courses of 3 μM 15% pyrene actin polymerization assays containing 100 nM wild type or Arp2-CA fusion complex with and without 20 μM N-WASP-CA.

quenched the reaction at various time points with DTT, and tested the product in pyrene actin polymerization assays without NPFs (Fig. 4). Remarkably, crosslinking potently activated the NPF-independent activity of the complex, demonstrating that adoption of the short pitch conformation is a critical activation step (Fig. 4). These results were unexpected because, as noted above, direct recruitment of actin monomers by WASP is

required for WASP-mediated activation of Arp2/3 complex (9). Our data demonstrate that even in the absence of VCA-mediated monomer tethering, the complex is activated once locked in the short pitch conformation.

The complex locked into the short pitch conformation is hyperactivated

Our data suggest the dominant activating influence of WASP on the kinetics of branching nucleation stems from its influence on the conformation of Arp2/3 complex. However, WASP-mediated activation of Arp2/3 complex involves additional steps that could also influence branching rates, including direct monomer recruitment and WASP release from the branch junctions. To better understand the relative contribution of each of these steps to the reaction kinetics, we directly compared the NPF-independent activity of the crosslinked complex to WASP-activated uncrosslinked complex. To accomplish this, we first separated the crosslinked complex from uncrosslinked complex using an affinity column charged with GST-tagged Dip1, a recently described Arp2/3 complex activator which binds preferentially to the crosslinked complex (5)(SI Appendix, Fig. S2). This protocol yielded 98% pure crosslinked complex (Fig. 5A). In pyrene actin polymerization assays, 10 nM purified crosslinked complex produced a maximum polymerization rate of 40.6 ± 2.2 nM/s with a time to half maximal polymerization of 33.3 ± 5.8 s (Fig. 5B-D). By comparison, activation of the uncrosslinked complex by the optimal concentration of N-WASP-VCA produced a slower maximum polymerization rate (28.5 ± 1.0 nM/s) and an increased $t_{1/2}$ (93.3 ± 5.8 s) (Fig. 5B-D). These observations lead to the surprising conclusion that the crosslinked complex is more active than N-WASP-activated uncrosslinked complex. In some contexts, dimerizing WASP increases

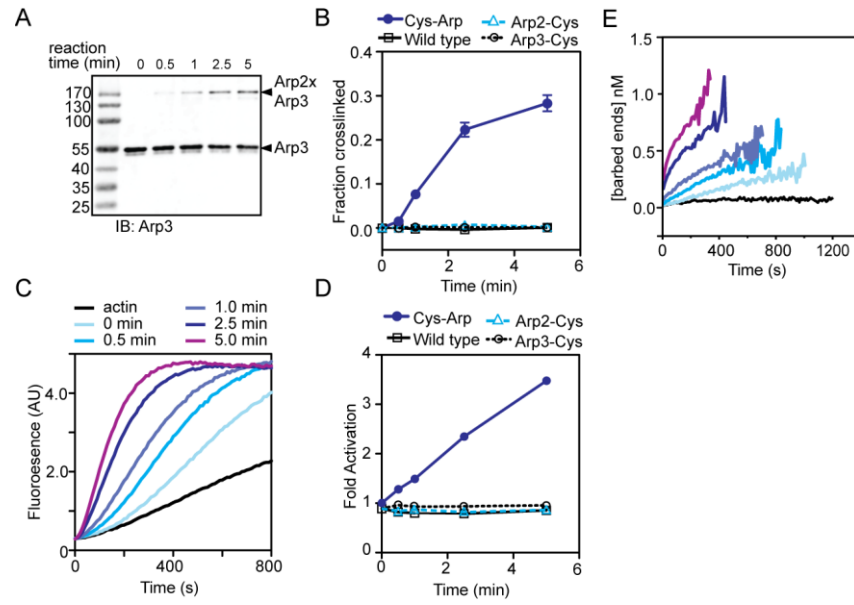


Figure 4: Locking Arp2/3 complex into the short pitch conformation bypasses the requirement for NPFs in activation.

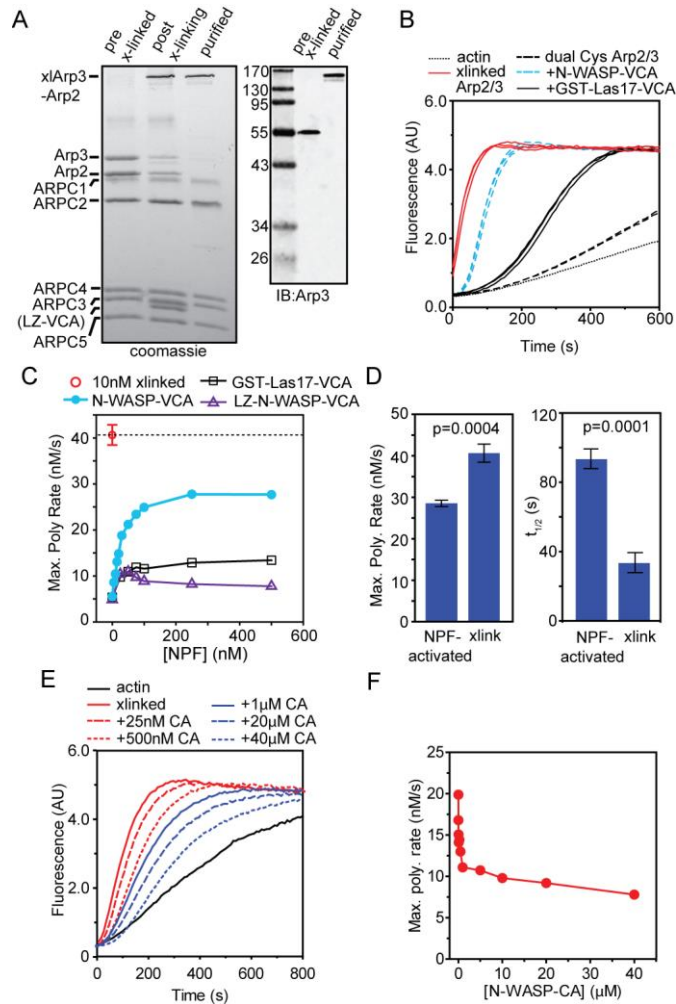
A. Western blot of SDS-PAGE gel of crosslinking reactions containing 1 μM dual cysteine ScArp2/3 complex (Cys-Arp) and 25 μM BMOE. Reactions were quenched with 1 mM DTT at the times indicated. **B.** Quantification of data in A. Error bars show standard errors from three separate reactions. **C.** Time course of pyrene actin polymerization for assays containing 3 μM 15% pyrene-labeled actin and 10 nM dual cysteine complex crosslinked for the times indicated. AU, arbitrary units. **D.** Fold activation of dual cysteine complex calculated by dividing the maximum polymerization rate at a given crosslinking time by the maximum polymerization rate of the uncrosslinked complex. Data taken from panel C. **E.** Plot of number of barbed ends created versus time for reactions in C.

NPF activity (25, 37, 39), so we also compared optimal activation of the uncrosslinked complex by GST-Las17-VCA and leucine-zipper dimerized N-WASP-VCA to the activity of the crosslinked complex. Neither of these NPFs activated the uncrosslinked complex as potently as crosslinking (Fig. 5B,C). The maximum polymerization rate in reactions containing Arp2/3 complex with either GST-Las17-VCA or LZ-N-WASP-VCA was ~ 4 fold less than reactions with the same concentration of short pitch crosslinked complex. These data demonstrate that the crosslinked complex is hyperactivated compared to WASP-activated Arp2/3 complex. One explanation for this phenomenon is

the slow WASP release step is bypassed in the WASP-independent activity of the short pitch crosslinked Arp2/3 complex. To challenge this model, we tested the influence of free WASP-CA on the activity of the crosslinked complex. As predicted, CA inhibited nucleation, supporting a model in which locking the complex into the short pitch conformation hyper-activates it by allowing it to bypass the slow WASP release step (Fig 5E,F). We note that other attributes of the crosslinked complex may also contribute to its hyperactivity. For instance, WASP-bound Arp2/3 complex may not fully populate the short pitch state, leading to decreased nucleation rates compared to the crosslinked complex. In addition, if the crosslinked complex requires preformed filaments for nucleation, CA could inhibit by decreasing actin filament binding (27). However, CA did not block the crosslinked complex from binding filaments in copelleting assays, arguing against this mechanism (SI Appendix, Fig. S3). Finally, inhibition of spontaneous

Figure 5 (next page): The short pitch crosslinked complex is more active than WASP-activated uncrosslinked complex.

A. (Left panel) Coomassie stained SDS-PAGE gel showing the pre-crosslinked dual cysteine complex, the post crosslinking reaction, and the purified crosslinked complex after passing through a MonoQ column and a GST-Dip1 affinity column. (Right panel) Anti-Arp3 western blot of purified crosslinked and uncrosslinked samples. **B.** Time courses of 3 μM 15% pyrene actin polymerization for reactions containing 10 nM dual crosslinked cysteine ScArp2/3 complex (“xlinked Arp2/3”) or 10 nM uncrosslinked complex with either no NPF (“dual Cys Arp2/3”), 250 nM N-WASP-VCA or 50 nM GST-Las17-VCA, as indicated. Multiple reaction time courses are shown for the fastest reactions. **C.** Maximum polymerization rate versus NPF concentration for reactions containing 10 nM uncrosslinked complex with N-WASP-VCA, GST-Las17-VCA, or leucine-zipper dimerized N-WASP-VCA in conditions identical to panel B. The average maximum polymerization rate for purified crosslinked complex without NPFs is shown as a red circle. Error bar indicates the standard deviation (n=3). **D.** Comparison of maximum polymerization and time to one half maximal polymerization for 10 nM crosslinked complex versus 10 nM uncrosslinked complex with 250 nM N-WASP-VCA. Error bars indicate the standard deviation (n=3). **E.** Time course of polymerization of a reaction containing 3 μM 15 % pyrene labeled actin, 2.5 nM purified crosslinked complex, and 0-40 μM N-WASP-CA, as indicated. **F.** Plot of the maximum polymerization rate versus N-WASP-CA concentration for reactions in E.



nucleation by WASP may also decrease the maximal polymerization rate even at optimal WASP concentrations, leading to greater activity of the short pitch crosslinked complex (16).

Residues in the C region influence the ability of WASP to stimulate the short pitch conformational change

How CA binding stimulates movement of Arp2 into the short pitch position is unknown. As a first step in dissecting the mechanism, we used the crosslinking assay to test the role of specific WASP-CA residues in stimulating the conformational change.

The C consensus sequence is characterized by several conserved hydrophobic residues

(Fig. 6A)(31). NMR line broadening experiments and mutational analysis suggest these hydrophobic residues occupy one face of an amphipathic helix that forms when WASP binds Arp2/3 complex (31). Immediately C-terminal to the proposed amphipathic helix is a conserved arginine, R477 in WASP. The R477K (R478K in N-WASP) mutation is found in Wiskott-Aldrich syndrome patients and reduces WASP-mediated activation of Arp2/3 complex (Fig. 6B) (9, 40). This mutation decreased crosslinking ~2.5-fold at saturation compared to wild type N-WASP, demonstrating the importance of this residue in stimulating the short pitch switch (Fig. 6C, SI Appendix, Fig. S4, SI Appendix, Table S3). Previous data showed that another mutation within the C region, WASP L470A (L471A in N-WASP), decreased activity in polymerization assays and blocked a conformational change measured by FRET, suggesting this residue may be also important for stimulating the short pitch conformation (12, 31). Consistent with this hypothesis, the L471A mutation decreased short pitch crosslinking by ~3-fold compared to wild type N-WASP-VCA (Fig. 6C). These observations support a model in which contacts with the C region are critical for stimulating the short pitch conformation, and identify two key residues for stimulating this switch.

The A region of WASP family proteins is characterized by a conserved tryptophan surrounded by several acidic residues (Fig. 6A). The A region confers most of the Arp2/3 complex binding affinity to WASP proteins (9). The acidic residues in A play an important role in branching nucleation kinetics. Specifically, deletion of acidic residues in N-WASP-VCA increases the affinity of N-WASP for the complex and decreases branching nucleation rates (19), whereas addition of acidic residues to WAVE1 increases nucleation rates (30). To test the influence of the acidic residues in stimulating

the short pitch switch, we created a (monomeric) N-WASP construct with five acidic residues deleted from A. This construct stimulated crosslinking to the same extent as the wild type N-WASP-VCA (Fig. 6C, S3, SI Appendix, Table S3). Therefore, decreased activation of the complex by the N-WASP(Δ DEDED) mutant cannot be explained by a failure to induce the short pitch conformation, and instead is likely due to slow release of the N-WASP(Δ DEDED) from branch junctions (19).

CA-fusion complexes suggest the N-WASP C region binds to the barbed end grooves of Arp2 and Arp3

Our data demonstrate that CA regions from diverse WASP proteins stimulate the short pitch conformation, and that residues in the C region are critical for stimulating the switch. However, understanding how C stimulates this conformation requires knowledge of how C interacts with the complex. Based on biochemical and biophysical studies described above, WASP C has been proposed to interact with the barbed end grooves of Arp2 and Arp3 (25-27, 32, 34). The C-termini of Arp2 and Arp3 terminate between subdomains 1 and 3, filling the back portion of the barbed end grooves in a position that either overlaps or sits immediately adjacent to the predicted binding sites for C (20) (Fig. 7). This arrangement provides a fortuitous opportunity to test the proposed binding mode. As described above, we created chimeric subunits in which the CA region of N-WASP is fused to the C-terminus of either Arp2 or Arp3 (Fig. 7A-C). Based on the proposed binding mode, the tip of the Arp3 C-terminus sterically overlaps the WASP C helix, so we truncated Arp3 by 7 residues, removing the tip of the C-terminal tail and connecting

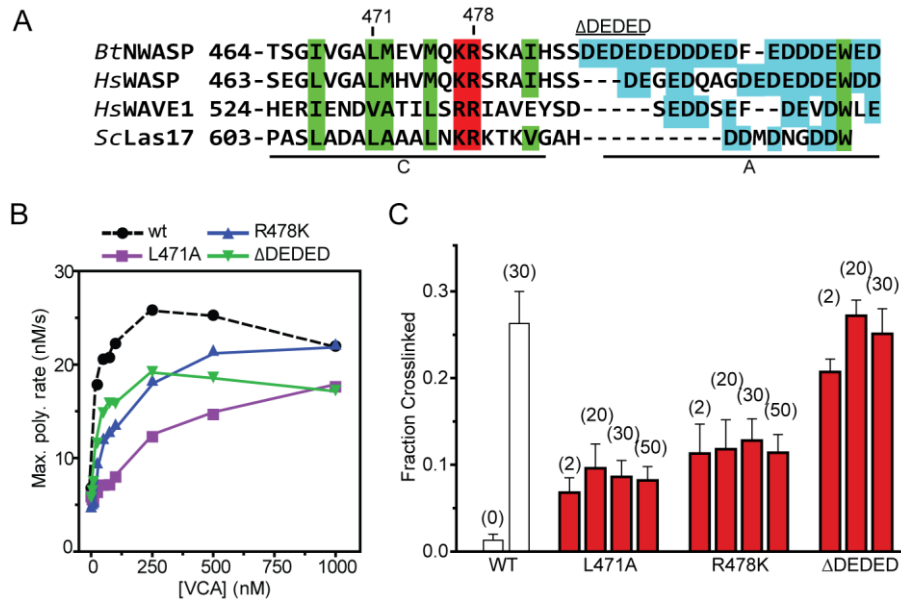


Figure 6: Residues in the C region tune are important for stimulating the short pitch conformational change.

A. Sequence alignment of WASP family CA regions. Conserved hydrophobic (green boxes) and basic (red boxes) residues are indicated, and acidic residues in the A region are boxed in cyan. N-WASP point mutations and deletion construct investigated in this study are indicated. *Bt*, *Bos taurus*; *Hs* *Homo sapiens*; *Sc*, *Saccharomyces cerevisiae*. **B.** Maximum polymerization rate versus NPF concentration for polymerization reactions containing 3 μ M 15% pyrene actin, 10 nM dual cysteine Arp2/3 complex, and the indicated concentration of each NPF. **C.** Results of 1 min short pitch crosslinking reactions containing 1 μ M dual cysteine Arp2/3 complex, 25 μ M BMOE and the indicated concentrations (in μ M) of mutant or wild type N-WASP-VCA. Error bars show standard error from three reactions.

the base of the tail to the N-terminus of the N-WASP CA region with a short linker (GSG). We reasoned that fused CA would properly engage Arp3 only if the front of the barbed end groove is the correct binding site for C, as predicted by the model. A similar strategy was used for Arp2, except that the Arp2 C-terminus is shorter, so the binding model predicted that truncation of only three residues from the C-terminus would allow the C helix to fold into its predicted position in the groove (Fig. 7C).

To determine if fused CA segments are properly engaged, we asked if they could compete with VCA for binding to the complex. To accomplish this, we first reacted the

bi-functional crosslinker benzophenone-4-maleimide (B4M) with N-WASP-VCA at an engineered cysteine residue (T464C) immediately N-terminal to the C region (Fig. 7D). We used UV radiation to crosslink this adduct, N-WASP-VCA-T464C-B4M, to the wild type complex, producing VCA crosslinked adducts of both Arp2 and Arp3, as expected based on previously published crosslinking studies (Fig. 7E,F) (28). Unlabeled VCA competes with N-WASP-VCA-T464C-B4M for crosslinking to the wild type complex at the Arp2 and Arp3 sites, demonstrating the reaction is specific. Importantly, the Arp3-CA fusion completely blocked N-WASP-VCA-T464C-B4M from crosslinking to Arp3 (Fig. 7E-G). This result suggests that CA properly engages its site on Arp3 in the fusion chimera, providing support for a model in which the C-region binds the Arp3 barbed end groove. Fusion of CA to Arp3 did not influence N-WASP-VCA-T464C-B4M crosslinking to Arp2, indicating that the Arp3-CA fusion specifically blocks binding of CA to the Arp3 site. We repeated the B4M crosslinking experiments to test whether the Arp2-CA fusion engages the Arp2 CA binding site. Under our reaction conditions, 67% of Arp2 from wild type complex crosslinked to N-WASP-VCA-T464C-B4M, whereas only 4.3% of the Arp2 was crosslinked in the Arp2-CA chimera (Fig. 7E-G). This potent reduction in crosslinking demonstrates that CA fused to the C-terminus of Arp2 blocks the Arp2 CA binding site. Together these experiments support the proposed binding modes, in which the C region of WASP binds the barbed end groove of either Arp2 or Arp3. The proposed binding modes are also consistent with recent low-resolution x-ray crystal structures of Arp2/3 complex crystals grown in the presence of WASP-CA, which show putative electron density for WASP C bound to the barbed ends of Arp2 and Arp3 (34).

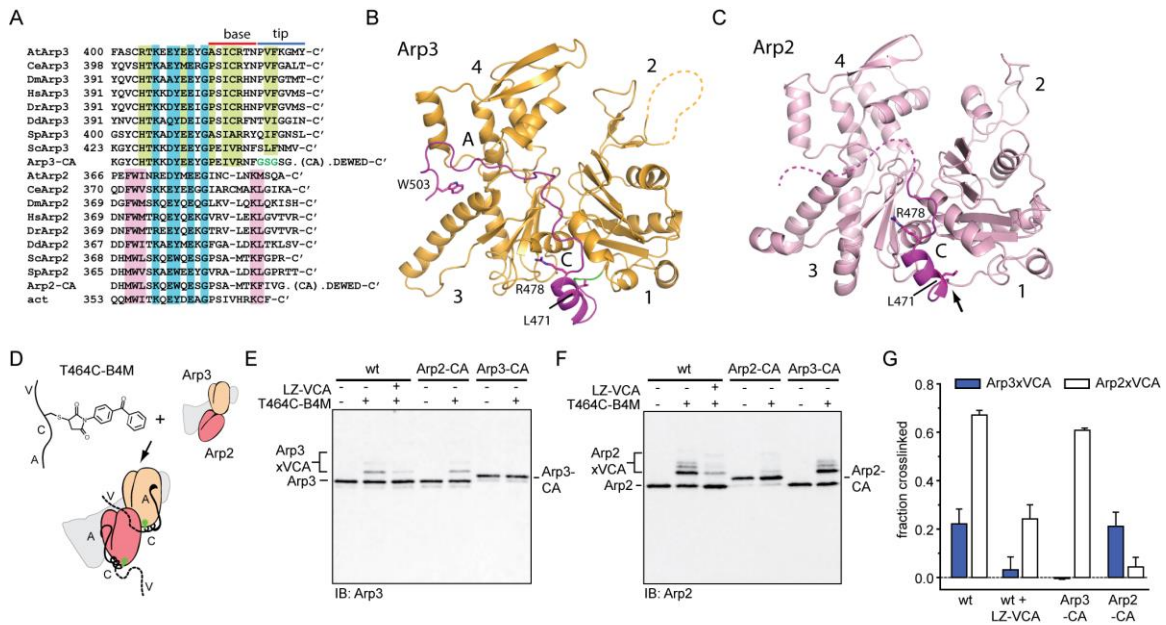


Figure 7: WASP-CA fused to the C-terminus of Arp2 or Arp3 blocks binding of soluble WASP-VCA to the CA-fusion subunit

A. Sequence alignment of the C-terminus of Arp2, Arp3 and actin, showing design of Arp CA-fusion constructs. Residues conserved in Arp2 and Arp3 (cyan boxes), Arp2 only (pink boxes), or Arp3 only (green boxes) are indicated. Residues in Arp3 that mark the tip (blue line) and base (red line) of the Arp3 C-terminal tail are indicated. The majority of residues from the fused CA segments were omitted from the alignment, indicated by “(CA)”. **B.** Hypothetical model of Arp3-CA fusion structure. The fused CA sequence is shown in magenta, and the linker is in green. The model was constructed from the crystal structure of Arp2/3 complex with bound ATP (2P9K) (22), with the WASP C region modeled into position based on a WASP-V bound actin structure (2A3Z) (32). The A region was placed between subdomains 3 and 4 based on the structure 3TSE (27). **C.** Hypothetical model of Arp2-CA fusion structure. The model was constructed from the crystal structure of GMF-bound Arp2/3 complex (4J2D) (23), with WASP C modeled into position as described above. **D.** Schematic of benzophenone-4-maleimide (B4M) crosslinking assay to probe WASP-CA binding at each site on the complex. **E.** Anti-Arp3 western blot of B4M UV crosslinking reactions containing 1.5 μ M dual cysteine (“wt”), Arp2-CA fusion, or Arp3-CA fusions complexes with 200 μ M ATP and either no NPF, 4 μ M N-WASP-VCA(T464C)-B4M or 100 μ M leucine zipper dimerized VCA (LZ-VCA), as indicated. All three complexes harbor the dual cysteine engineered mutations. **F.** Reactions from E run analyzed by western blotting with anti-Arp2 antibody. **G.** Quantification of B4M crosslinking reactions as described in E and F. Error bars are standard errors from three reactions.

WASP C likely displaces the C-terminus from the barbed end groove of Arp3 to relieve autoinhibition and stimulate the short pitch conformation

How could WASP-CA stimulate the short pitch conformation? We analyzed crystal structures of inactive Arp2/3 complex in the context of the CA binding model to identify interactions that could potentially destabilize inter-subunit contacts important for holding the complex in the splayed conformation. We also analyzed low resolution EM models of Arp2/3 complex at a branch junction to identify WASP-CA interactions that could stabilize the short pitch conformation (24). These analyses, in conjunction with results from a recently submitted study, led us to hypothesize that interactions of WASP-C with the Arp3 barbed end groove are critical for stimulating the short pitch conformation. We recently found that the Arp3 C-terminus is an autoregulatory switch important for holding the complex inactive in the absence of NPFs (manuscript submitted). The Arp3 C-terminal tail engages the Arp3 barbed end groove and occupies a critical position at the splayed Arp2-Arp3 interface (Fig. 8A,B). The base of the Arp3 C-terminal tail directly contacts Arp2 to stabilize the splayed conformation, whereas the most C-terminal residues in the Arp3 tail (the “tip”) do not directly contact Arp2, but instead fill the front portion of the barbed end groove (20-22). Deletion of the entire Arp3 C-terminal tail in either budding or fission yeast Arp2/3 complexes stimulates the short pitch conformation and increases NPF-independent activity (submitted). Furthermore, mutations that disrupt interactions of the tip of the tail with the barbed end groove also stimulate the short pitch conformation (submitted), supporting a model in which release of the tip from the barbed end groove allosterically relieves autoinhibition by destabilizing the splayed Arp2-Arp3 interface (Fig. 8A). Importantly, our CA-fusion data,

along with recently published low resolution crystal structures (34), suggest WASP-C engages the barbed end groove of Arp3, where it would overlap with the tip of the C terminal tail (Fig. 7, 8A,B). Therefore, we hypothesized that WASP could activate the complex by displacing the Arp3 C-terminal tail from the Arp3 barbed end groove. To test this, we first asked if the C-terminus and WASP-CA compete for binding to the complex. We used fluorescence anisotropy to measure the affinity of rhodamine-labeled WASP proteins for the budding yeast and fission yeast Arp3 Δ C complexes. Using a single-site binding model (see materials and methods and (27)), we found the affinity of rhodamine-labeled WASP proteins increased four to six fold for the Arp3 Δ C mutants compared to wild type complexes (Fig. 8C, SI Appendix, Fig. S5). To eliminate the influence of the rhodamine label, we ran competition assays to measure binding of unlabeled WASP proteins. These experiments showed that the Arp3 Δ C complexes bind to WASP proteins 4 to 13-fold more tightly than wild type complex (Fig. 8C). While the fluorescence anisotropy assay does not allow us to distinguish between binding to Arp2 or Arp3, we took advantage of the observation that truncation of the Arp3 C-terminus causes a previously unreactive endogenous cysteine in Arp3, C426, to react in the BMOE crosslinking assay (Fig. 8D). Arp3 C426 lines the barbed end groove (Fig. 8B), and deletion of the C-terminus allows this residue to crosslink with Arp2 to form a non-short pitch crosslink that migrates below the short pitch crosslinked Arp3-Arp2 adduct (Fig 8D, SI Appendix, Fig. S6). We reasoned that if CA binds to the barbed end groove of Arp3, it could directly block the reactivity of C426. Consistent with this prediction, addition of CA to the Arp3 Δ C complex decreased crosslinking between Arp2 and Arp3 C426 (Fig. 8D). To provide additional evidence that WASP-C binds the barbed end of

Arp3, we asked if WASP-C could be directly crosslinked to C426 in Arp3. To this end, we designed a VCA construct (N-WASP-VCA(V468C)) with a cysteine residue immediately N-terminal to C (SI Appendix, Fig. S7). N-WASP-VCA(V468C) formed a disulfide crosslink with C426 in the Arp3 Δ C complex in the presence of CuSO₄ (Fig. 8E). The crosslinking was abolished by addition of cysteine-free N-WASP-CA, indicating that the crosslinking occurs between bound N-WASP-VCA(V468C) and Arp3. These data support a model in which WASP C directly competes with the Arp3 C-terminus to displace it from the barbed end groove, revealing a structural mechanism by which WASP binding can stimulate the short pitch conformation. However, we note that in the absence of high-resolution structures of Arp3 with bound WASP-CA, we cannot eliminate the possibility that competition is not direct, but instead involves an allosteric link between the WASP-CA binding site and the Arp3 C-terminus.

Discussion

Stimulating the short pitch conformation is a critical NPF function

Previous models for activation of Arp2/3 complex ascribed two major functions for WASP: 1.) stimulation of an activating conformational change in the complex (11-13, 15) and 2.) direct recruitment of actin monomers to assemble a nucleus consisting of Arp2, Arp3 and one or more actin monomers (9, 41). The relative contribution of each of these functions was unknown. Here we show that locking Arp2/3 complex into the short pitch conformation potently activates it without NPFs, demonstrating that direct

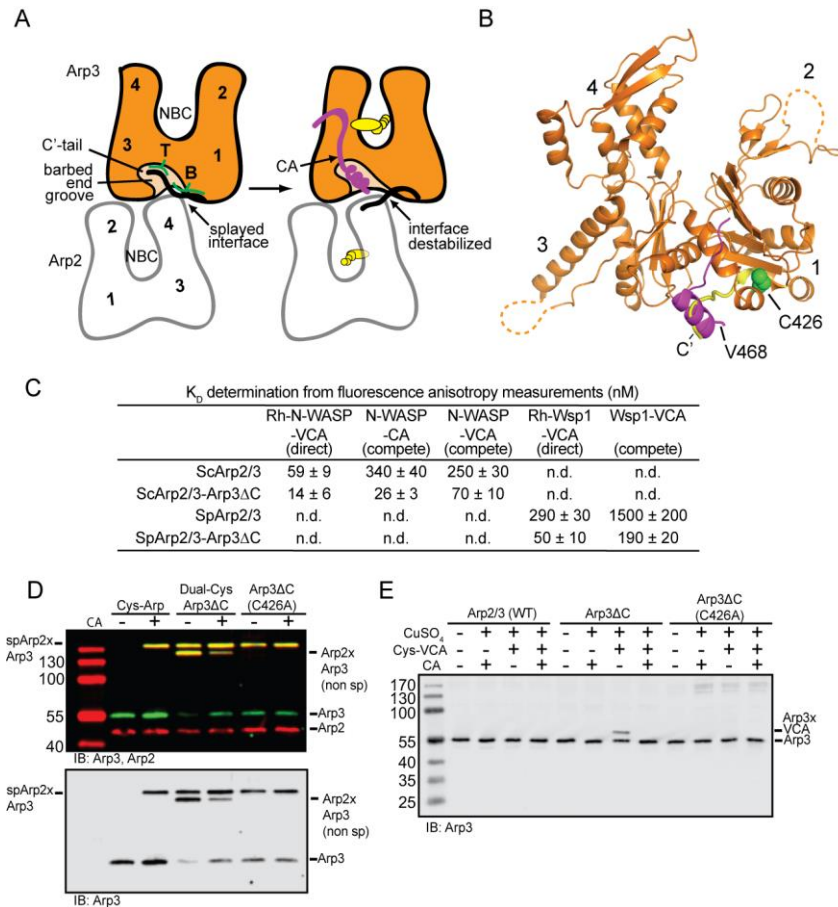


Figure 8: WASP competes with the Arp3 C-terminus for binding the barbed end groove of Arp3

A. Model for relief of autoinhibition of Arp2/3 complex by WASP-CA binding. NBC, nucleotide binding cleft; T, tip of the Arp3 C-terminal tail; B, base of the Arp3 C-terminal tail. Subdomains of Arp3 and Arp3 are numbered 1-4. **B.** Hypothetical model of WASP-CA (magenta) bound to Arp3 showing clash between WASP-C and the tip of the Arp3 C-terminal tail (yellow). Cysteine 426, a residue that becomes reactive when the C-terminus is deleted, is shown in green spheres. Arp3 ribbon diagram is based on 1K8K, and WASP-C is modeled into barbed end groove of Arp3 based on WASP-V bound actin structure (2A3Z) (32). **C.** Tabulated results from fluorescence anisotropy binding assays. **D.** Two color (anti-Arp3/anti-Arp2, top) or one color (anti-Arp3, bottom) western blots of crosslinking reactions containing 1.0 μM wild type, Arp3ΔC or Arp3ΔC(C426A) fusions complexes (each with dual cysteine mutations) with or without 20 μM N-WASP-CA showing short pitch (sp) or non short pitch (non sp) products **E.** Anti-Arp3 western blot of VCA crosslinking reactions containing 0.5 μM wild type, Arp3ΔC, or Arp3ΔC(C426C) *S. cerevisiae* Arp2/3 complex, 2 μM N-WASP-VCA(V468C), 50 μM CuSO₄, 10 mM Imidazole pH 7.0, 50 mM KCl, 50 μM EGTA, 1 mM MgCl₂ and 200 μM ATP with or without 50 μM N-WASP-CA. Note that the Arp2/3 complexes in this assay lack the engineered cysteines for short pitch crosslinking.

monomer tethering is not required to assemble the nucleus, as previously anticipated. Therefore, whether or not direct actin monomer tethering is required for potent activation by any NPF likely depends on the identity and mechanism of the NPF, and is not a fundamental requirement of the branching nucleation reaction. Consistent with this hypothesis, WISH/DIP/SPIN90 (WDS) family proteins can potently activate Arp2/3 complex but lack known actin monomer binding domains (5). While little is known about this class of NPFs, we previously used the crosslinking assay to show that WDS protein Dip1 stimulates formation of the short pitch conformation, and our data here suggest this is sufficient for Dip1-mediated activation of the complex (5). Like WDS family proteins, type II NPFs like cortactin and fission yeast myosin I interact with Arp2/3 complex and actin filaments but not actin monomers (37, 42-44). Unlike WDS proteins, type II NPFs are generally weak activators on their own (7). Recent experiments indicate that at least in the case of cortactin, this weak activity is due to an inability to directly deliver monomers to Arp2/3 complex (42). Type II NPFs typically interact with actin monomer binding proteins that allow them to indirectly deliver monomers to the complex and potently increase their ability to activate (7, 45, 46). Therefore, as with WASP, a requirement for actin monomer recruitment may be programmed into the activation mechanism of type II NPFs. An important future direction will be to determine why actin monomer recruitment is required for potent activation by some NPFs but not others, and how this requirement is structurally encoded into the activation mechanism.

Here we propose a model in which WASP CA stimulates the short pitch conformation by displacing the Arp3 C-terminal tail from the barbed end groove, thereby triggering destabilization of the splayed conformation. Our data indicate this mechanism

must work coordinately with other activation triggers. For example, in a recent study, we provide evidence that ATP bound to the Arp3 nucleotide cleft allosterically disrupts interactions between the Arp3 tail and the barbed end groove, providing another mechanism to destabilize the splayed conformation (manuscript submitted). Structural features other than the Arp3 C-terminal tail must also be involved in triggering activation. For example, here we showed that CA engagement with Arp2 is also important for stimulation of the short pitch conformation. In addition, phosphorylation of Arp2 near its interface with ARPC4/ARPC2 is required for activation of the complex in some species, and is thought to destabilize the splayed conformation (8, 47). Understanding how Arp2/3 complex structurally integrates each of these activating responses remains an important open question in the field.

The role of WASP, actin monomers and actin filaments in activation

Because actin monomers, WASP and actin filaments are required to activate the complex in most contexts (4, 5, 9, 10), it has generally been assumed that cooperation between each of these factors is required to shift the conformation into the short pitch conformation, thereby stimulating activation. Our data lead us to re-evaluate the relationship between activity and conformation. Specifically, the observation that WASP-VCA (or CA) alone can stimulate crosslinking between short pitch engineered cysteines makes it unclear why WASP-recruited monomers and actin filaments are also required for activation. Because the crosslinking assay conformationally traps the complex, one possibility is that WASP-bound Arp2/3 complex may not significantly populate the short pitch state, but by crosslinking we amplify a functionally insignificant effect of WASP on

the concentration of short pitch complex. Previous experiments indeed demonstrate that WASP binding is not sufficient to fully populate the short pitch conformation, since WASP-recruited actin monomers potentially increase the amount of short pitch crosslinking over reactions with WASP alone (11). However, comparisons of the relative amount of complex crosslinked under different conditions, while yielding no information about absolute equilibrium populations, indicate the bias toward the short pitch conformation in the presence of WASP alone should be functionally significant. Without WASP, only ~3% of the Arp2/3 complex was crosslinked after one minute of crosslinking, suggesting the complex only weakly adopts the short pitch conformation in the absence of NPF. However, this amount is functionally significant, since ScArp2/3 complex shows NPF-independent activity in pyrene actin polymerization assays. Therefore, the ~7-10 fold increase in crosslinking stimulated by WASP-CA (or VCA) proteins without actin probably reports on functionally significant increases in the short pitch conformation. Several previously published biochemical and biophysical experiments agree with this interpretation, since they indicate that WASP alone causes a significant shift in the conformational equilibrium of the complex, presumably toward an activated state (12-15).

A second explanation for the insufficiency of WASP-CA in activation (despite its influence on the conformation of the complex) is that WASP-CA binding stimulates an intermediate conformation close to but distinct from the short pitch arrangement. Our data cannot not eliminate this possibility, since BMOE crosslinking may not necessarily strictly constrain the complex to the short pitch state, as noted above. From an intermediate WASP-CA stimulated conformation, WASP-recruited actin monomers and

filaments could trigger population of the “fully” short pitch state. However, recent EM reconstructions of negatively stained NPF-bound Arp2/3 complexes argue against intermediate WASP-bound conformations, since the particles segregated into only two different conformational classes (15). One class corresponded to the inactive “splayed” conformation seen in crystal structures, and the second (NPF-bound) class produced three-dimensional density consistent with a filament-like (short-pitch) arrangement of Arp2 and Arp3. This study is in contrast with slightly lower resolution reconstructions of NPF-bound Arp2/3 complexes that indicated a third conformational class corresponding to an intermediate state (13). Thus, the precise structures of WASP bound complexes and their role in activation remain an important open question.

Finally, another possibility is that actin filaments (and potentially WASP-recruited monomers) could stimulate activating steps distinct from the adoption of short pitch conformation. In addition to movement of Arp2 and Arp3 into the filament-like arrangement, the EM branch junction model describes intramolecular rearrangements within the Arp subunits that may be important for activation, and could be stimulated by actin filaments or monomers. This hypothesis is attractive given recent experiments suggesting that WASP must be released from nascent branch junctions for nucleation to occur (19, 37). Conformational changes initiated by filaments but distinct from the short pitch switch could help accelerate WASP release, potentially explaining the requirement for filaments in activation. We anticipate that in addition to the engineered “short pitch” dual cysteine Arp2/3 complex, additional biophysical tools and high resolution structures will be required to dissect the conformational pathway to activation, including the molecular basis for WASP release. We note that our data provide two new observations

that may be important for understanding the release mechanism. First, while previous studies used single molecule TIRF to show WASP release triggers nucleation, these studies used only dimeric WASP proteins (19). Experiments here indicate slow detachment of monomeric WASP proteins might also limit branching rates. Second, previous structural models suggested that the WASP V region blocks monomers from associating with nascent branch junctions (32, 37), explaining the requirement for WASP release. Here we show that CA alone stalls nucleation, demonstrating that the structural features that program WASP release into the nucleation mechanism are more complicated than previously anticipated.

Role of WASP engagement at each binding site

We show that engagement of WASP-CA with Arp3 is critical for stimulating the short pitch conformation. However, experiments with the CA fusion complexes revealed that engagement of WASP-CA at the Arp2-ARPC1 site is also important for this conformational change. WASP engaged at this site likely uses a mechanism other than C-terminal tail displacement, because unlike Arp3, the Arp2 C-terminus does not make contacts that stabilize the splayed (inactive) conformation (20-23). ITC binding measurements show a ten fold difference in the binding affinity at each of the two WASP-CA binding sites (26, 27), and it will be important to determine how the asymmetry in binding affinities influences the reaction kinetics. We note that our studies indicate that Arp3 harbors the high affinity site, because the fluorescence anisotropy binding assay measures binding to the high affinity site (27), and affinities measured by this method increased when competition with the Arp3 C-terminal tail was eliminated.

This conclusion is in agreement with other studies that indicate the high affinity site is on Arp3 (48). However, some experiments point to the Arp2-ARPC1 site as the high affinity site (26, 27, 33). For instance, a recent ITC study directly demonstrated that WASP delivers actin monomers to the Arp2 site first, suggesting that at least in the presence of monomers, the Arp2 site is the higher affinity site (49). While the complexity of this issue has precluded a clear consensus on the issue, we speculate that the preferred binding site may depend on whether or not WASP is bound to actin monomers.

BRIDGE TO CHAPTER IV

In this chapter, we demonstrated that diverse type I NPFs are capable of stimulation of the short pitch conformation and that binding of these NPFs to either the Arp2 or Arp3 site is important for activation of the complex, and determined which residues in N-WASP are important for this conformational change. We showed that WASP likely binds to the barbed end grooves of each Arp and that displacement of the Arp3 C-terminus by WASP is a mechanism for how this protein activates Arp2/3 complex. Remarkably, we showed that Arp2/3 complex locked into the short pitch conformation is hyperactive compared to NPF-activated complex, which is likely due to release of WASP from the complex stalling nucleation rates. In the next chapter, I summarize the results from the entirety of my dissertation, and discuss some future directions from this work.

CHAPTER IV

SUMMARY AND CONCLUDING REMARKS

Coordinate regulation of branched actin networks has been an exciting field of research for over a decade. Many roles for Arp2/3 complex and its regulators have been identified throughout the years, but biochemically dissecting how NPFs activate the complex still requires more research. At the beginning of this project, we were motivated to contribute to the research on branched actin networks by understanding how Arp2/3 complex is locked in its inactive state in the absence of NPFs, and how NPFs promote an activating conformational change where Arp2/3 complex mimics a stable actin dimer that templates growth of a new branched actin filament.

In chapter II, we dissected the contacts in Arp2/3 complex that hold it in its inactive conformation and how ATP destabilizes some of these contacts to promote activation of the complex. We hypothesized that the Arp3 C-terminus is an important regulatory element that holds the complex in its inactive state, where the “base” of the C-terminus stabilizes the splayed conformation by contacting subdomain 4 of Arp2 and the “tip” of the C-terminus is wedged in the barbed end groove of Arp3, forming an allosteric link that promotes opening of the nucleotide cleft. To test this hypothesis, we truncated the C-terminus in *S. pombe* and *S. cerevisiae* Arp2/3 complexes and biochemically characterized them. We found that the Arp3 Δ C complexes displayed NPF-independent activity with the *S. cerevisiae* complex showing a profound increase in bulk actin polymerization assays. We showed that this effect is due to favoring the short pitch conformation using a crosslinking assay that only form when Arp2/3 complex is in this

conformation. To see if removal of the C-terminus had an effect *in vivo*, we monitored endocytic patches in wild type and Arp3 Δ C *S. pombe* cells. Patches in Arp3 Δ C cells displayed longer lifetimes with decreased assembly and disassembly rates. This caused a functional defect in endocytosis, as shown by the relative lack up uptake of the dye FM4-64. This data shows that deletion of the Arp3 C-terminus has functional consequences *in vitro* and *in vivo*. The Arp2 α E/ α F loop in subdomain 4 forms contacts with Arp3 in the inactive structure, yet we did not predict that it forms significant contacts in the short pitch conformation, so we posited that this region is important for holding Arp2/3 complex in the splayed conformation. To test this hypothesis, we made point mutations in positions F203 and A207 and found that destabilizing this region caused activation of the complex, as measured by both polymerization and short pitch crosslinking assays.

Since ATP binding promoted closing of nucleotide cleft and release of the tip of the C-terminus in crystal structures, we hypothesized that ATP is required for stimulation of the short pitch conformation. In the absence of ATP, we detected no short pitch crosslinking, indicating that ATP is required for the short pitch conformation. We tested point mutants in either Arp2 or Arp3 nucleotide binding cleft and showed that mutants defective in binding ATP at either the Arp2 or Arp3 site formed significantly less short pitch crosslinking, with mutations at the Arp2 site forming no detectable crosslinks, indicating that binding of ATP to the Arp2 site plays a larger role in short pitch stimulation. When we tested the requirement of ATP with the Arp2 α E/ α F and Arp3 Δ C mutants, we found that each mutant still required ATP for short pitch crosslinking, with only two mutants (F203Y and A207C) forming any detectable crosslinks in the absence of ATP. To test if removal of the C-terminus promoted closing of the nucleotide cleft, we

performed binding assays with the ATP analog, etheno-ATP (ϵ -ATP). We found that the *S. pombe* Arp3 Δ C complex had a ~ 2.7 -fold increase in affinity for ϵ -ATP, however this effect was not seen in the *S. cerevisiae* complex, although this could be due to ϵ -ATP failing to form the same allosteric link as ATP. This data indicates that ATP binding causes allosteric changes that causes destabilization of the splayed conformation, favoring the short pitch conformation.

We showed that deletion of the C-terminus causes pronounced effects on the conformation and activity of Arp2/3 complex, and that binding of ATP to the Arp3 nucleotide binding pocket causes closing of the nucleotide cleft and release of the tip of the C-terminus from the Arp3 barbed end groove. To isolate the effects of binding of the tip of the C-terminus to the Arp3 nucleotide cleft, we used a more conservative approach where we mutated two conserved hydrophobic residues that form the most significant contacts between these two regions. Mutation of L445 and F446 to glutamic acid moderately increased activity of Arp2/3 complex in polymerization and crosslinking assays, indicating that release of the tip of the C-terminus alone causes the complex to favor the short pitch state. Interestingly, we observed in our crosslinking assays that deletion of the C-terminus exposes an endogenous cysteine, Arp3 C426, causes a non-short pitch crosslink that also appears in the LF/DD mutant, providing further evidence the a model where release of the Arp3 C-terminus stimulates the short pitch conformation, providing a mechanism as to how ATP relieves autoinhibition of Arp2/3 complex.

In chapter III, we shifted our focus to the mechanisms of WASP-mediated activation of Arp2/3 complex. Since there are many WASP-related NPFs, we first

demonstrated that the conserved VCA regions from these proteins all were capable of potently stimulating the short pitch conformation. To biochemically characterize Arp2/3 complex in the short pitch conformation, we designed WASP-Arp chimeras where the CA region of N-WASP was fused the C-terminus of either Arp2 or Arp3 to isolate Arp2/3 complex that constitutively favors the short pitch conformation. Unexpectedly, the Arp-CA chimeras only slightly increased short pitch crosslinking in the absence of exogenous CA. One chimera, Arp2-CA, had a very modest increase in activity over wild type complex, while Arp3-CA showed decreased nucleation rates. When CA was added to these complex, we observed a similar degree of crosslinking to wild type complex with added CA, indicating that CA binding to both sites is important for full stimulation of the short pitch conformation. Interestingly, addition of CA to wild type and Arp-CA complexes inhibited nucleation in polymerization assays, demonstrating for the first time that CA alone stalls nucleation rates due to lack of release by CA, despite structural modeling suggesting that the V region blocks association of new actin monomers, necessitating release of VCA.

Due to the complicated effects of the Arp-CA chimeras, we sought to use the short pitch crosslinked complex to understand the role of the short pitch conformation. We found that crosslinking caused potent activity, even in the absence of WASP, demonstrating that once locked into the short pitch conformation, Arp2/3 complex no longer needs WASP for activation. Since WASP also recruits actin monomers, presumably to stabilize the nascent nucleus, we sought to compare the activity of the crosslinked complex versus WASP-activated complex. This required pure crosslinked complex, which we successfully purified using an affinity column charged with GST-

Dip1, which binds the crosslinked complex with higher affinity. Comparison of purified crosslinked complex versus WASP-activated complex showed that the crosslinked complex had much higher nucleation rates versus uncrosslinked, WASP-activated complex. This surprising result suggested that monomer recruitment is not required for stabilization of the nucleus and that WASP release stalls nucleation. Consistent with this model, WASP-CA decreased nucleation rates of the crosslinked complex.

To biochemically dissect the mechanism for WASP-mediated stimulation of the short pitch conformation, we first investigated the residues important for full stimulation of the short pitch conformation. While mutations of residues in the C region and removal of acidic residues in the A region both decreased nucleation rates compared to wild type N-WASP-VCA, only the mutations in the C region caused a decrease in short pitch crosslinking, indicating that the C region is important for stimulation of the short pitch conformation, while activity caused by residues in the A region is due to a different mechanism, such as release from the complex. Since residues in the C region are important for stimulation of the short pitch conformation, we wished to characterize how the C region contacts the Arp subunits. The C region is predicted to form an amphipathic helix similar to how the V region engages the barbed end groove of actin, so we predicted the C region binds in a similar fashion to the Arp subunits. Using the Arp-CA chimeras, we demonstrated that the fused CA at each subunit blocks association with exogenous CA, allowing us to isolate CA binding to each site. Using VCA with the C region labeled with B4M, we demonstrated that binding of VCA to each site caused crosslinking to their respective Arp subunits, supporting the hypothesis that the C region engages the barbed end grooves of Arp2 and Arp3.

The model where the C regions bind the barbed end grooves of Arp2 and Arp3 suggests that CA competes with the C-terminus of Arp3 for binding in this region. Consistent with this hypothesis, WASP had a 4 to 6-fold increase in affinity to Arp3 Δ C complexes compared to wild type. Consistent with the previous experiments, addition of CA prevented crosslinks to C426, the endogenous cysteine that lines the barbed end groove of Arp3. We provided additional evidence that the C region engages the barbed end groove by directly crosslinking Arp3 C426 with CuSO₄ to a VCA construct with a cysteine introduced in the N-terminal portion of the C region. This data strongly suggests that WASP CA competes for the Arp3 C-terminus at the barbed end groove to promote activation of the complex.

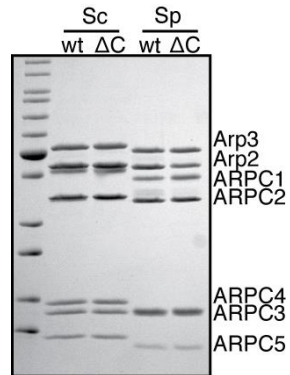
In this dissertation, we provided evidence that the splayed interface contacts are important for hold Arp2/3 complex in its inactive state, and that ATP and WASP promote relief of the autoinhibition of the complex by displacing the Arp3 C-terminus from the barbed end groove of Arp3. Future direction will be focused on determining the effects of actin monomer recruitment by WASP and the role of actin filaments in the branched actin nucleation pathway. Since we showed that actin monomer recruitment was not required once Arp2/3 complex was locked in the short pitch conformation, further work still needs to be done on why monomer recruitment is important for short pitch stimulation, and therefore activation. In addition, our data is consistent with previous data suggesting that while WASP, ATP and actin monomers potently stimulate the short pitch conformation, actin filaments are still required for branch formation, indicating that filaments are likely involved in a sequential process. Biochemically determining the requirement for actin

filaments will help explain why Arp2/3 complex is exclusively a branched actin nucleator.

APPENDIX A

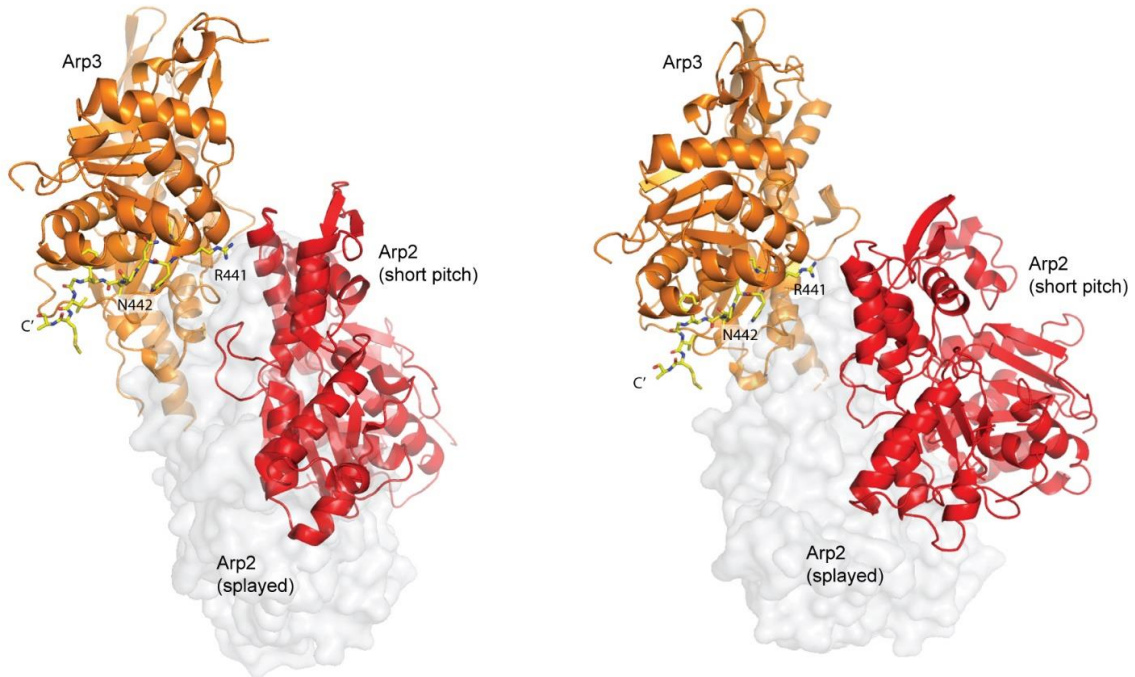
SUPPLEMENTARY MATERIAL FOR CHAPTER II

Supplementary Figure 1 | Coomassie-stained gel of purified wild type and Arp3 Δ C complexes from budding and fission yeast.



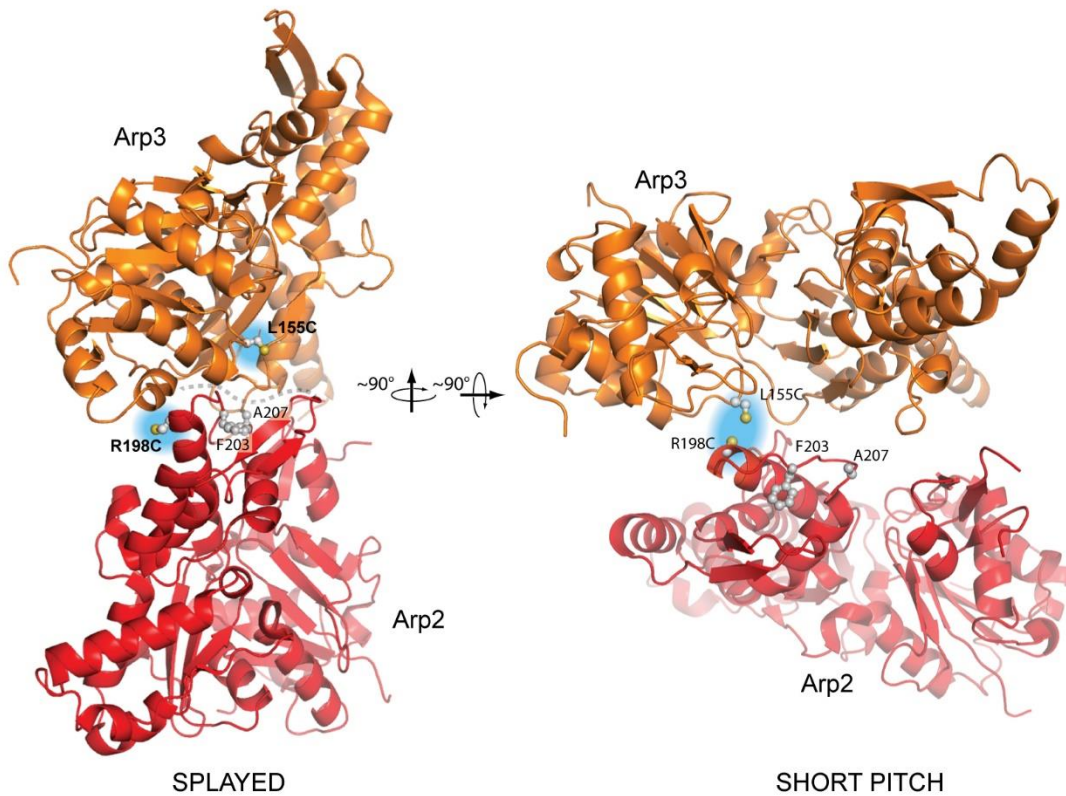
Supplementary Figure 2 | Analysis of potential contacts of Arp3 C-terminus with Arp2/3 complex in the short pitch conformation at a branch.

(Left panel) Model of Arp3 and Arp3 in the short pitch and splayed conformations. The hypothetical short pitch model was created by superposing the actin filament model of Oda, et al (2ZWH) (1) onto the Arp3 subunit of 1K8K. The splayed model shows Arp2 from 4JD2 overlaid onto Arp2 from 1K8K. The Arp3 C-terminus is shown in yellow stick representation. R441 and N442 (ScArp3 residue IDs are used in this figure) are key residues from the base of the Arp3 C-terminal tail that contact Arp2 in the splayed conformation. (Right panel) Same analysis as in left panel, except that all subunits are taken from the electron tomography model of Arp2/3 complex at a branch junction (2). Arp2 is further from Arp3 in this model.



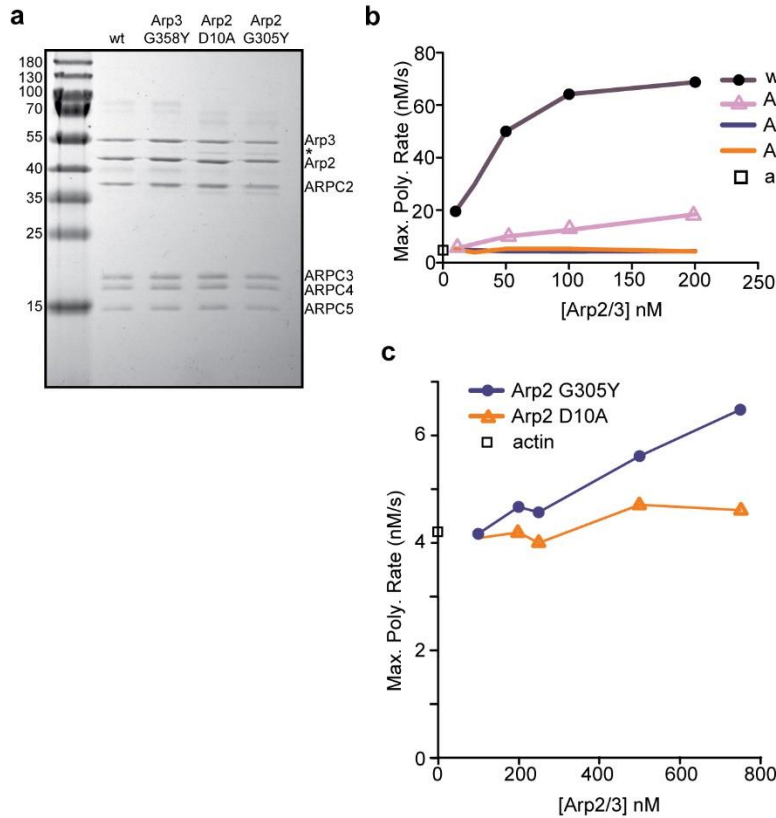
Supplementary Figure 3 | Ribbon diagram showing positions of engineered cysteine residues and splayed interface mutations in splayed or short pitch conformations.

(Left panel) Arp2/3 complex in the splayed conformation from the structure of Arp2/3 complex bound to GMF (4JD2) (3). Splayed interface mutations and engineered cysteine residues are shown in ball-and-stick representation. Engineered cysteine residues (highlighted in cyan clouds) are on opposite sides of the complex in the splayed conformation and the solvent accessible crosslinking distance is 32.5 Å (C β -C β)(4). Dashed line shows the approximate location of the splayed Arp2-Arp3 interface. (Right panel) Hypothetical model of Arp2/3 complex in the short pitch conformation. Model was constructed by overlaying actin filament from Oda, et al, (1ZWH) (1) onto Arp3 from 1K8K and moving Arp2 from 4JD2 into the short pitch position. The solvent accessible crosslinking distance between the engineered cysteine residues is 8 Å in this model (C β -C β). The electron tomography structure of Arp2/3 complex at a branch junction shows similar overall positioning of Arp2 and Arp3 but using that model the solvent accessible crosslinking distance between the engineered cysteines is 11.3 Å (2)



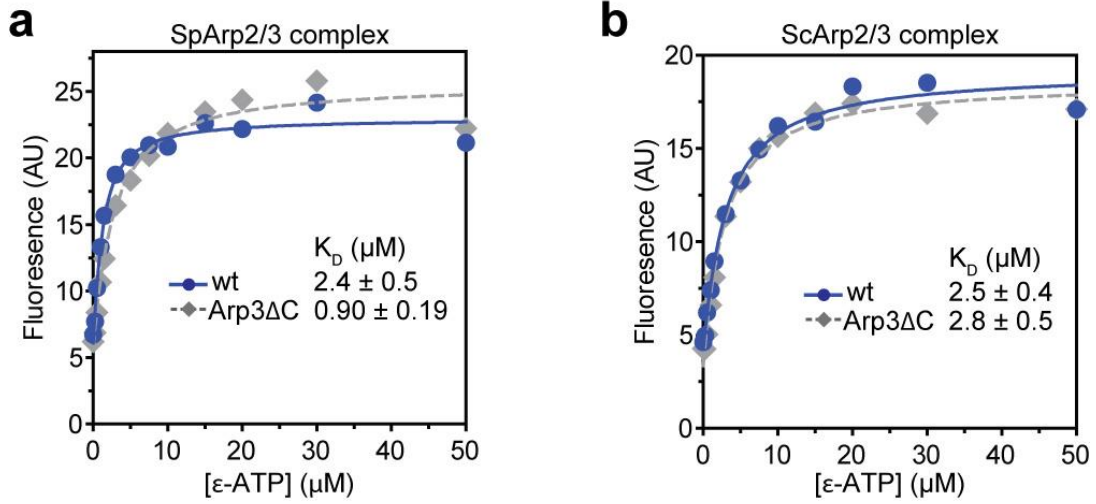
Supplementary Figure 4 | Purification and activity of Arp2 and Arp3 nucleotide binding cleft (NBC) mutant Arp2/3 complexes.

(a) Coomassie stained gel of purified wild type and NBC *S. cerevisiae* mutant Arp2/3 complexes. Asterisks indicates possible Arp3 degradation as previously reported (6). **(b)** Maximum polymerization rates calculated from time courses of pyrene actin polymerization for reactions containing 3 μ M 15% pyrene actin, 250 nM N-WASP-VCA, 500 μ M ATP and the indicated concentrations of ScArp2/3 complex. Note that all complexes harbor the dual cysteine residues for short pitch crosslinking. **(c)** Maximum polymerization rates versus Arp2/3 complex concentration for reactions identical to b, except higher concentrations of Arp2/3 complex were used.



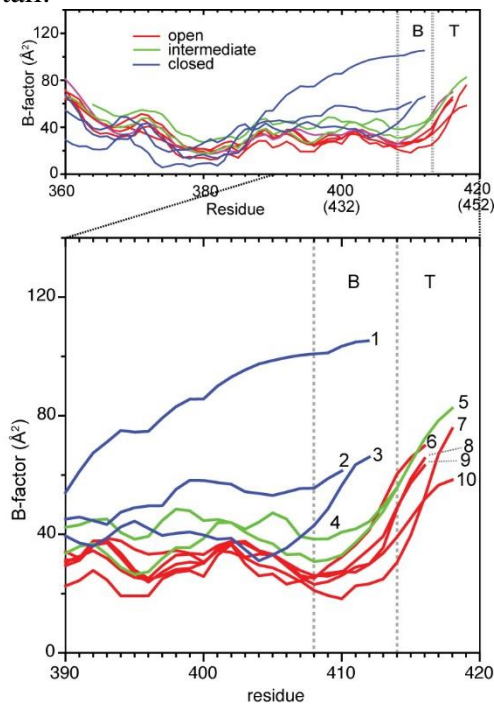
Supplementary Figure 5 | ϵ -ATP binding assays.

Plot of background subtracted fluorescence versus ϵ -ATP concentration for reactions containing 0.5 μM *S. pombe* (a) or *S. cerevisiae* Arp2/3 complex. Data were fit assuming one binding site as described in the methods.



Supplementary Figure 6 | The width of the nucleotide binding cleft is correlated to the release of the C-terminal tail in Arp2/3 complex crystal structures.

(related to Fig 7a in the main text) Left panels show a plot of average main chain B-factor versus residue number for the C-terminal residues in Arp3. Table on right indicates distances across the cleft, ligand bound, and classification of cleft closure. Data are taken from ten different *Bos taurus* (Bt) Arp2/3 complex crystal structures in different nucleotide-bound states (1K8K, 2P9L, 1U2V, 2P9N, 2P9U, 2P9P, 1TYQ, 2P9I, 2P9K, 2P9S) (14-16). Nucleotide cleft widths are classified based on Nolen and Pollard (16). B-factors were normalized so that each chain had the same average main chain B-factor. Residues missing in the electron density are omitted from the plot. Residue numbers in parenthesis are for ScArp2/3 complex. B – base of Arp3 C-terminal tail, T- tip of C-terminal tail.



code	ligand	G15-Ca/ D172-Ca distance(Å)	category	
1	2P9I	ADP/Ca	5.5	closed
2	2P9K	ATP/Ca	5.7	closed
3	2P9S	ATP/Mg	5.6	closed
4	2P9P	ADP/Ca	6.2	intermediate
5	1TYQ	ATP/Ca	6.2	intermediate
6	2P9U	ANP/Ca	7.0	open
7	1U2V	ADP/Ca	8.0	open
8	2P9N	ADP/Ca	7.6	open
9	2P9L	APO	7.1	open
10	1K8K	APO	7.7	open

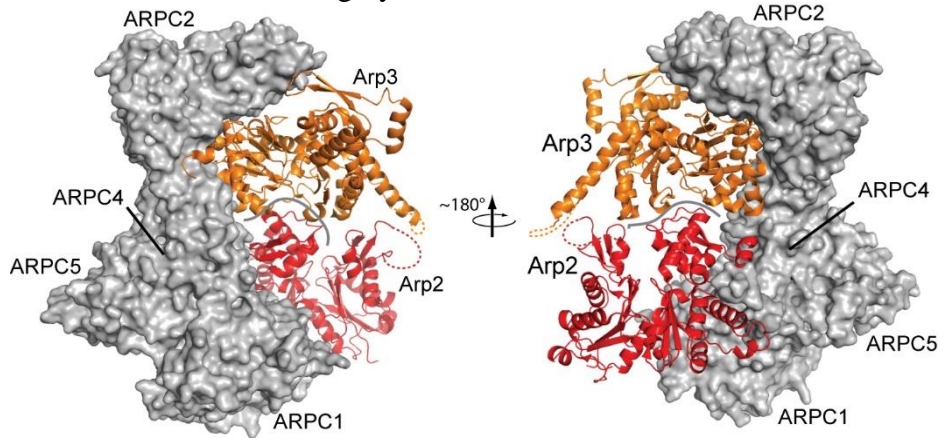
Supplementary Figure 7 | An endogenous cysteine in Arp3, C426, becomes exposed and reactive upon deletion or mutation of the Arp3 C-terminal tail.

Structure of Arp3 from BtArp2/3 complex crystal structure (4JD2) showing the C-terminal tail (yellow), the two conserved hydrophobic residues in the tail (L445/F446 in *S. cerevisiae* Arp3, yellow sticks) and C426 (ball and stick).



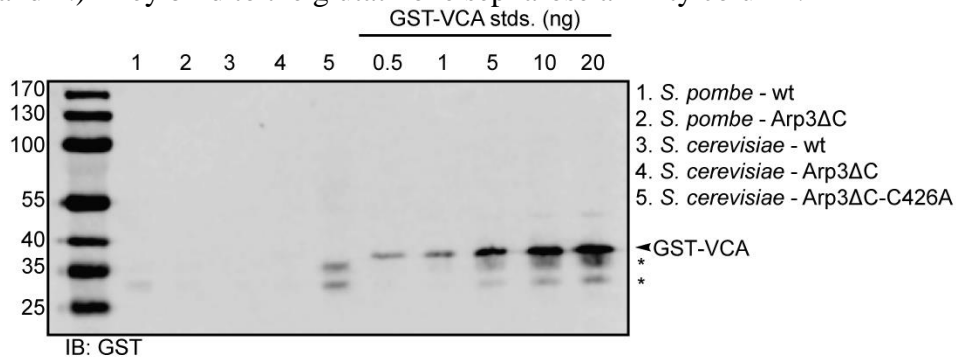
Supplementary Figure 8 | Structural visualization of contacts that hold Arp2/3 complex in the splayed conformation in the absence of activators.

Structure of Arp3 and Arp3 in the short pitch conformation from the x-ray crystal structure of GMF-bound BtArp2/3 complex (4JD2) (3). ARPC1, ARPC2, ARPC4 and ARPC5 form a clamp (grey surface representation) that contacts Arp2 and Arp3 in the splayed conformation. The approximate location of the splayed interface between Arp2 and Arp3 is indicated with a solid grey line.



Supplementary Figure 9 | Validation of purification procedure for Arp3ΔC complexes.

Anti-GST Western blot of Arp3ΔC *S. pombe* (Sp) and *S. cerevisiae* (Sc) Arp2/3 complexes versus GST-VCA standard. No GST-VCA is detectable in any of the purified complexes. Under the conditions of the loading, GST-VCA band in any of the purified samples (1-5) with the same intensity as the 0.5 ng GST-VCA standard would correspond to ~0.7 nM dimeric GST-VCA in a 1 μM solution of the purified complex. Sample 5 was not re-purified through the glutathione sepharose affinity column because no full length GST-VCA contaminant was present. We conclude that the lower molecular weight bands (asterisks) are C-terminal truncations of GST-VCA because 1.) They elute from the monoQ much earlier than full length GST-VCA, consistent with truncation of the acidic region and 2.) They bind to the glutathione sepharose affinity column.



Supplementary Movie 1: Spinning disk confocal fluorescence microscopy movie of fission yeast expressing Fim1p-GFP and wild type Arp2/3 complex. Frames are taken at 0.5 sec intervals and length of entire movie is 120 seconds.

Supplementary Movie 2: Spinning disk confocal fluorescence microscopy movie of fission yeast expressing Fim1p-GFP and Arp3ΔC Arp2/3 complex. Frames are taken at 0.5 sec intervals and length of entire movie is 120 seconds.

Supplementary Table 1 | Calculated pKa and solvent accessible surface areas for engineered cysteine residues in the context of the short pitch conformation of Arp2/3 complex.

	predicted pKa	SASA (Å) ²
WT		
Arp3-L155C	> 12.0	98.7
Arp2-R198C	> 12.0	53.4
F203Y		
Arp3-L155C	> 12.0	98.7
Arp2-R198C	> 12.0	53.4
A207C		
Arp3-L155C	> 12.0	98.7
Arp2-R198C	> 12.0	53.4
A207W		
Arp3-L155C	> 12.0	98.7
Arp2-R198C	> 12.0	53.4
Arp3ΔC		
Arp3-L155C	> 12.0	98.7
Arp2-R198C	> 12.0	53.4

SASA = solvent exposed surface area. pKa calculations were carried out using H++ and SASA calculations were made with POPS (7, 8)

Supplementary Table 2 | Table of p-values for Figure 5E.

	WT	A207C	A207W	A207I	F203Y
WT		p < 0.001	p < 0.001	0.049	p < 0.001
A207C			n.s.	p < 0.001	p < 0.001
A207W				p < 0.001	p < 0.001
A207I					p < 0.001
F203Y					

n.s. = non-significant. p-values calculated as two-tailed t-test comparing means of at least three experiments.

Supplementary Table 3 | Table of p-values for Figure 6C.

		WT		Arp3 (G358Y)		Arp2 (G305Y)		Arp2 (D10A)	
		No ATP	With ATP	No ATP	With ATP	No ATP	With ATP	No ATP	With ATP
WT	No ATP		p < 0.001	n.s.	p < 0.001	n.s.	n.s.	n.s.	n.s.
	With ATP			p < 0.001	0.02	p < 0.001	0.001	0.001	p < 0.001
Arp3 (G358Y)	No ATP				p < 0.001	n.s.	n.s.	n.s.	n.s.
	With ATP					p < 0.001	p < 0.001	p < 0.001	p < 0.001
Arp2 (G305Y)	No ATP						n.s.	n.s.	n.s.
	With ATP							n.s.	n.s.
Arp2 (D10A)	No ATP								n.s.
	With ATP								

Supplementary Table 4 | Table of p-values for Figure 6D.

		WT		A207C		A207W		F203Y		Arp3ΔC (C426A)	
		No ATP	With ATP	No ATP	With ATP	No ATP	With ATP	No ATP	With ATP	No ATP	With ATP
WT	No ATP		0.036	0.009	0.037	0.040	0.007	0.013	p < 0.001	0.024	0.004
	With ATP			0.062	0.023	n.s.	0.014	0.022	p < 0.001	n.s.	0.006
A207C	No ATP				n.s.	0.012	n.s.	n.s.	0.0014	0.035	n.s.
	With ATP					0.044	n.s.	n.s.	0.021	n.s.	n.s.
A207W	No ATP						0.009	0.015	p < 0.001	n.s.	0.004
	With ATP							n.s.	0.007	0.018	n.s.
F203Y	No ATP								0.016	0.028	n.s.
	With ATP									p < 0.001	0.033
Arp3ΔC (C426A)	No ATP										0.009
	With ATP										

n.s. = non-significant. p-values calculated as two-tailed t-test comparing means of at least three experiments.

Supplementary Table 5 | List of fission yeast strains used.

Strain	Genotype	Source
BN024	<i>leu1-32 sm902 arp3Δ416-427::kanMX6</i>	This study
BN052	<i>leu1-32 sm902 arp3Δ416-427::kanMX6 mEGFP-fim1::natMX6</i>	This study
TP150	<i>h⁻ leu1-32 sm902</i>	M. Yanagida
TP194	<i>h⁻ ade6-M216 leu1-32 his3-D1 ura4-D18 Δwsp1::kanMX6</i>	V. Sirotkin

Supplementary Table 6 | List of budding yeast expression plasmids used.

Name	Gene	Vector
pDW6	<i>ARP2</i>	pRS316
pDW20	<i>ARP3-MYC-HISx6</i>	pRS316
pCE04	<i>ARP2</i>	pRS305
pCE05	<i>ARP3</i>	pRS305
pBN01	<i>ARP2</i>	pRS317
pBN02	<i>ARP3</i>	pRS315
pBN03	<i>arp2 R198C</i>	pRS317
pBN09	<i>arp3 L155C</i>	pRS315
pMR01	<i>arp2 R198C, A207C</i>	pRS317
pMR02	<i>arp2 R198C, A207I</i>	pRS317
pMR03	<i>arp2 R198C, A207W</i>	pRS317
pMR04	<i>arp2 R198C, F203Y</i>	pRS317
pMR09	<i>arp3ΔCterm440-449, L155C</i>	pRS315
pMR14	<i>arp3ΔCterm440-449, L155C, C426A</i>	pRS315
pMR17	<i>arp3 L155C, L445D, F446D</i>	pRS315
pMR18	<i>arp2 D10A, R198C</i>	pRS317
pMR20	<i>arp2 R198C, G305Y</i>	pRS317
pMR22	<i>arp3 L155C, G358Y</i>	pRS315

Supplementary Table 7 | List of budding yeast strains used.

Strain	Genotype	Source
KEBY88	<i>MATa, ura3-52, his3-Δ200, leu2-3, lys2-801, trp1-901, suc2-Δ9, pep4-3</i>	T. Stevens
RLY188	<i>MATa, ura3-52, his3-Δ200, leu2-3, lys2-801, Δarp3::HIS3, pDW20::URA3</i>	R. Li
BN002	<i>MATa, ura3-52, his3-Δ200, leu2-3, lys2-801, trp1-901, Δarp2::TRP1 pDW6::URA3</i>	(9)
BN021	<i>MATa, ura3-52, his3-Δ200, leu2-3, lys2-801, trp1-901, Δarp2::TRP1 Δarp3::HIS3 pBN09::LEU2, pBN03::LYS2</i>	(9)
MR001	<i>MATa, ura3-52, his3-Δ200, leu2-3, lys2-801, trp1-901, Δarp3::HIS3, pDW20::URA3</i>	This study
MR002	<i>MATa, ura3-52, his3-Δ200, leu2-3, lys2-801, trp1-901, Δarp2::TRP1, pMR01::LYS2</i>	This study
MR003	<i>MATa, ura3-52, his3-Δ200, leu2-3, lys2-801, trp1-901, Δarp2::TRP1, pMR02::LYS2</i>	This study
MR004	<i>MATa, ura3-52, his3-Δ200, leu2-3, lys2-801, trp1-901, Δarp2::TRP1, pMR03::LYS2</i>	This study
MR005	<i>MATa, ura3-52, his3-Δ200, leu2-3, lys2-801, trp1-901, Δarp2::TRP1, pMR04::LYS2</i>	This study
MR010	<i>MATa, ura3-52, his3-Δ200, leu2-3, lys2-801, trp1-901, Δarp3::HIS3, pBN09::LEU2</i>	This study
MR012	<i>MATa, ura3-52, his3-Δ200, leu2-3, lys2-801, trp1-901, Δarp3::HIS3, pMR09::LEU2</i>	This study
MR016	<i>MATa, ura3-52, his3-Δ200, leu2-3, lys2-801, trp1-901, Δarp2::TRP1, pBN03::LYS2</i>	This study
MR017	<i>MATa, ura3-52, his3-Δ200, leu2-3, lys2-801, trp1-901, Δarp2::TRP1, Δarp3::HIS3, pBN09::LEU2, pMR01::LYS2</i>	This study
MR018	<i>MATa, ura3-52, his3-Δ200, leu2-3, lys2-801, trp1-901, Δarp2::TRP1, Δarp3::HIS3, pBN09::LEU2, pMR02::LYS2</i>	This study
MR019	<i>MATa, ura3-52, his3-Δ200, leu2-3, lys2-801, trp1-901, Δarp2::TRP1, Δarp3::HIS3, pBN09::LEU2 pMR03::LYS2</i>	This study
MR020	<i>MATa, ura3-52, his3-Δ200, leu2-3, lys2-801, trp1-901, Δarp2::TRP1, Δarp3::HIS3, pBN09::LEU2 pMR04::LYS2</i>	This study
MR022	<i>MATa, ura3-52, his3-Δ200, leu2-3, lys2-801, trp1-901, Δarp2::TRP1, Δarp3::HIS3, pBN03::LYS2 pMR09::LEU2</i>	This study
MR030	<i>MATa, ura3-52, his3-Δ200, leu2-3, lys2-801, trp1-901, Δarp3::HIS3, pMR14::LEU2</i>	This study
MR032	<i>MATa, ura3-52, his3-Δ200, leu2-3, lys2-801, trp1-901, Δarp2::TRP1, Δarp3::HIS3, pBN03::LYS2, pMR14::LEU2</i>	This study
MR034	<i>MATa, ura3-52, his3-Δ200, leu2-3, lys2-801, trp1-901, Δarp2::TRP1, pMR18::LYS2</i>	This study
MR035	<i>MATa, ura3-52, his3-Δ200, leu2-3, lys2-801, trp1-901, Δarp2::TRP1, pMR20::LYS2</i>	This study
MR037	<i>MATa, ura3-52, his3-Δ200, leu2-3, lys2-801, trp1-901, Δarp3::HIS3, pMR22::LEU2</i>	This study
MR040	<i>MATa, ura3-52, his3-Δ200, leu2-3, lys2-801, trp1-901, Δarp2::TRP1, Δarp3::HIS3, pBN003::LYS2, pMR17::LEU2</i>	This study
MR041	<i>MATa, ura3-52, his3-Δ200, leu2-3, lys2-801, trp1-901, Δarp2::TRP1, Δarp3::HIS3, pBN003::LYS2, pMR18::LEU2</i>	This study
MR042	<i>MATa, ura3-52, his3-Δ200, leu2-3, lys2-801, trp1-901, Δarp2::TRP1, Δarp3::HIS3, pBN003::LYS2, pMR20::LEU2</i>	This study
MR044	<i>MATa, ura3-52, his3-Δ200, leu2-3, lys2-801, trp1-901, Δarp2::TRP1, Δarp3::HIS3, pBN003::LYS2, pMR22::LEU2</i>	This study

APPENDIX B

SUPPLEMENTARY MATERIAL FOR CHAPTER III

Fig. S1: Analysis of crosslinking distances between the engineered cysteines along the trajectory from the splayed to the short pitch conformation.

A. Ribbon diagram showing the relative position of Arp3 (orange) and Arp2 (splayed, semi-transparent red; short-pitch, semi-transparent grey) in the trajectory from the splayed to short pitch conformation. The engineered cysteine residues are shown in ball-and-stick representation and highlighted in cyan. Blue spheres represent the center of mass of Arp2 throughout the trajectory. Sphere numbers represent the relative Arp2 position within the trajectory (1-fully splayed, 30 – fully short pitch). **B.** Plot of the solvent accessible surface distance between the engineered cysteine residues for each structure along the trajectory. Trajectories (morphs) were generated using the short pitch conformation observed in the low resolution branch junction model (EM-model) (1), or derived from a model in which an actin filament structure was used to align the Arps in the short pitch conformation (“actin” model) (2).

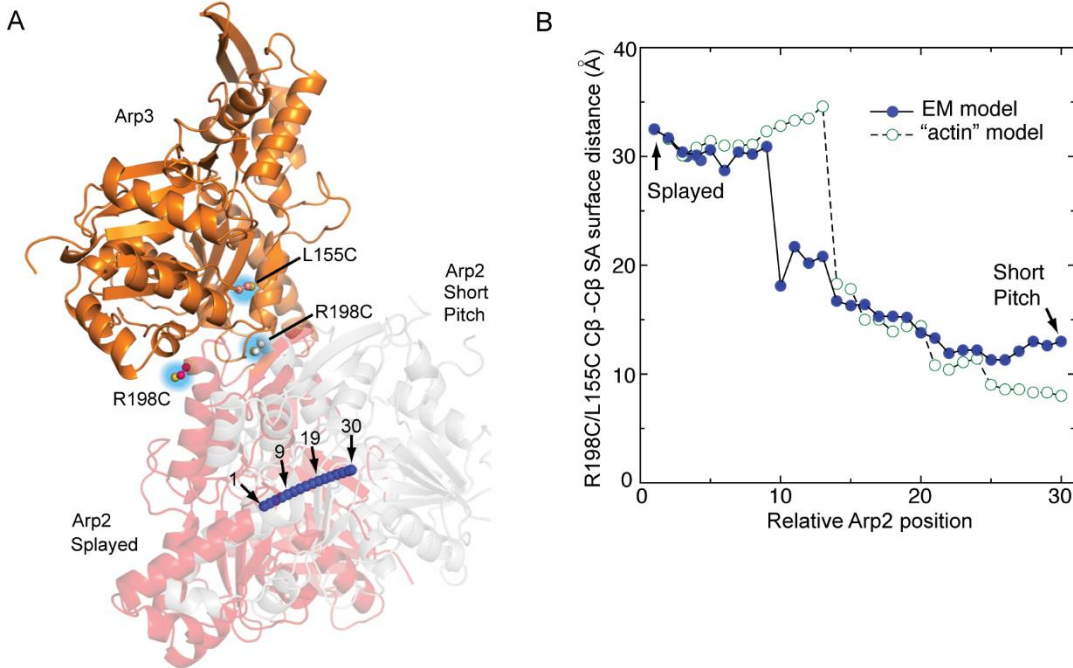


Fig. S2: Separation of crosslinked and uncrosslinked complex by binding to GST-Dip1 coated beads.

Dual cysteine Arp2/3 complex (1 μ M) was reacted with 25 μ M BMOE for 30 min and incubated with GST-Dip1 coated glutathione sepharose beads at the indicated KCl concentration before pelleting and analysis by SDS-PAGE and western blotting with an Arp3 antibody. S-soluble, P-pellet.

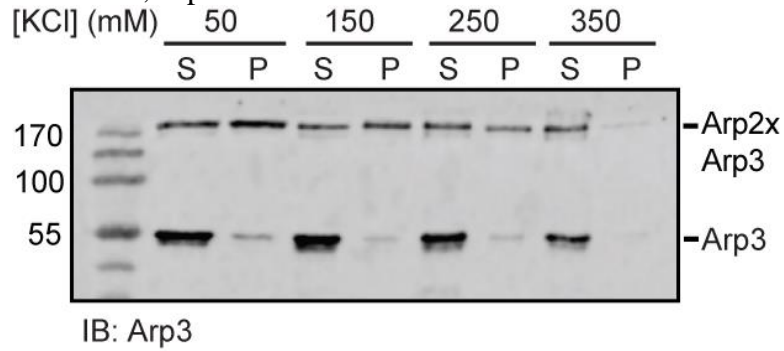


Fig. S3: Actin filament copelleting assay showing that N-WASP CA does not block crosslinked Arp2/3 complex from binding actin filaments.

A. Anti-Arp3 western blot showing copelleting of 0.1 μ M purified crosslinked complex with 5 μ M actin filaments and 20 μ M N-WASP-CA where indicated. S-soluble, P-pellet.

B. Fraction of Arp2/3 complex in actin pellet from data in A. Error bars show standard errors from three separate reactions. ***, $p < 0.0005$.

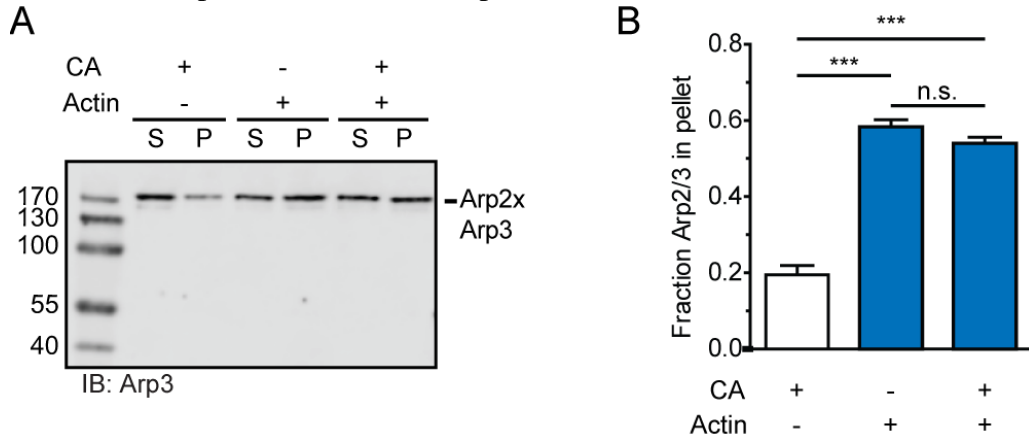


Fig. S4: Time course of short pitch crosslinking assays comparing wild type versus mutant N-WASP proteins.

Reactions contained 1 μM dual cysteine Arp2/3 complex, 25 μM BMOE, and 50 μM wild type or mutant N-WASP-VCA proteins. Reactions were quenched at the times indicated with 1 mM DTT and analyzed by SDS-PAGE and western blotting with an anti-Arp3 antibody. Asterisk indicates time point used for experiments shown in Fig. 6C in the main text.

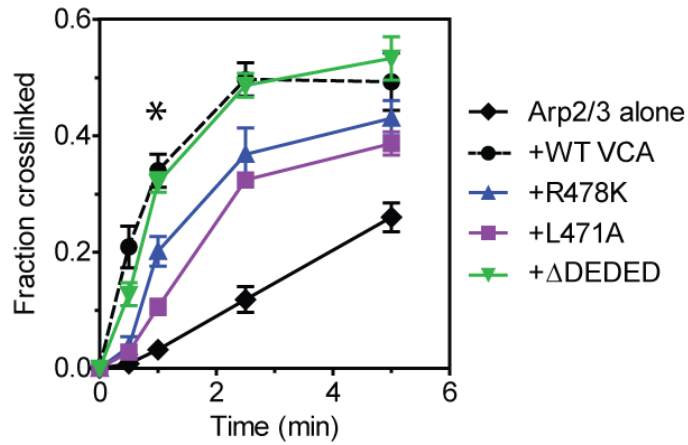


Fig. S5: Fluorescence anisotropy binding assays to investigate interaction of WASP proteins with wt and Arp3 Δ C Arp2/3 complexes.

A. Binding isotherms from fluorescence anisotropy binding assays. Main panel shows measured anisotropy values for titration of 0.5 μ M wild type *S. pombe* Arp2/3 complex and 75 nM Wsp1-Rh-VCA with unlabeled Wsp1-VCA. Inset shows anisotropy values for titration of 75 nM Wsp1-Rh-VCA with *S. pombe* Arp2/3 complex. **B.** Binding isotherms for reactions identical to C, except 0.3 μ M *S. pombe* Arp3 Δ C complex was used. **C.** Main panel shows measured anisotropy values for titration of 0.2 μ M wild type *S. cerevisiae* Arp2/3 complex and 30 nM N-WASP-Rh-VCA with unlabeled N-WASP-VCA or N-WASP-CA. Inset shows anisotropy values for titration of 30 nM Wsp1-Rh-VCA with *S. cerevisiae* Arp2/3 complex. **D.** Binding isotherms for reactions identical to C, except 0.1 μ M *S. cerevisiae* Arp3 Δ C complex was used.

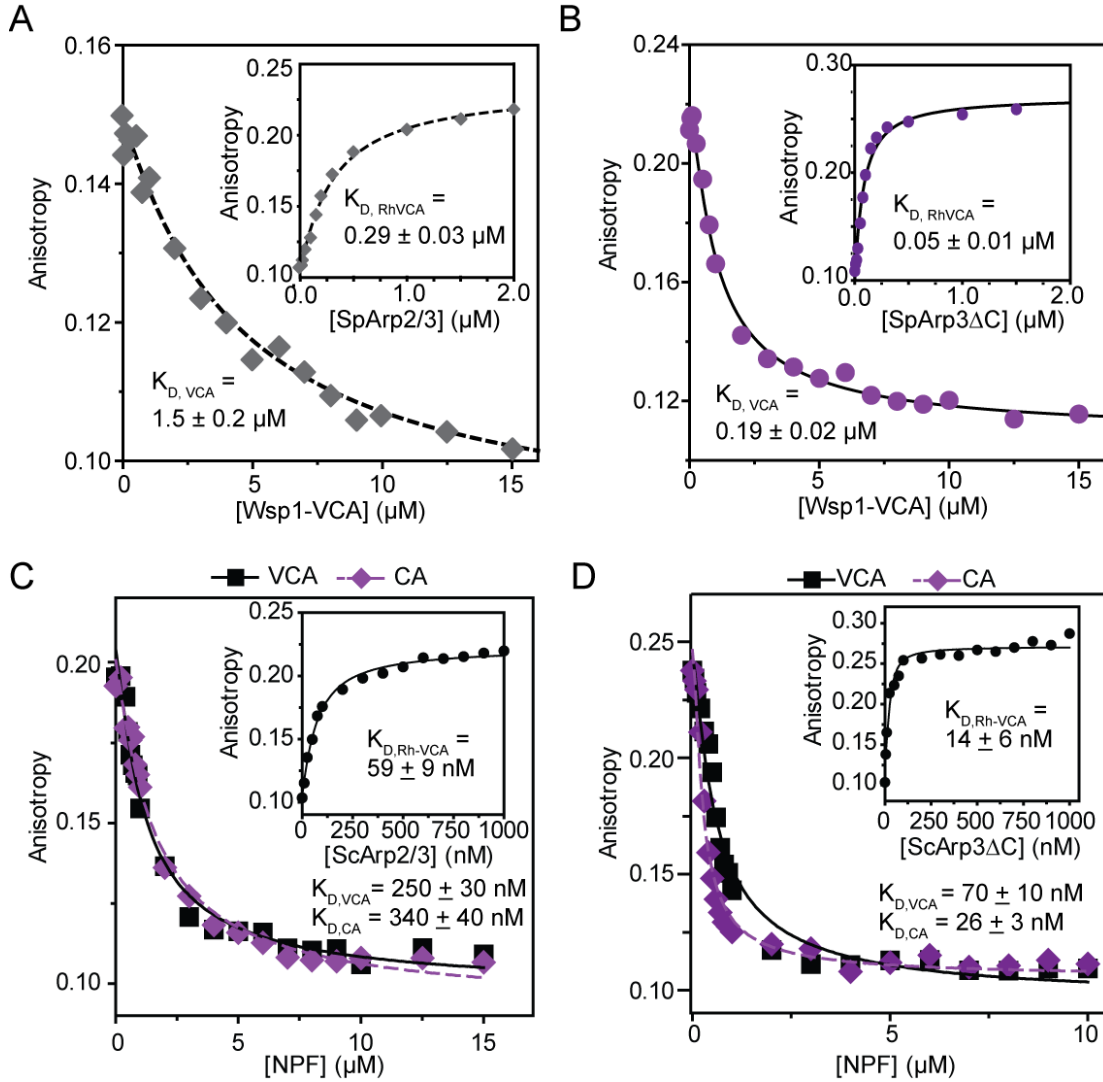


Fig. S6 (next page): Hypothetical molecular models showing engineered and endogenous cysteine residues in Arp2 and Arp3.

Stereo ribbon diagrams of Arp3 (orange) and Arp2 (red) showing the positions and C α Euclidian distances between engineered Arp2 cysteine R198C and Arp3 engineered and endogenous cysteine residues L155C and C426. Endogenous cysteine residues (green carbon atoms and yellow sulfur) are buried and inaccessible. Top pair shows Arp2 and Arp3 in the splayed conformation (based on structures 1K8K and 4JD2) and bottom pair shows the proposed short pitch arrangement. The solvent accessible crosslinking distances between Arp3 C426 and Arp2 R198C are 28.6 Å in the splayed conformation and 45.4 Å in the short pitch conformation (3). This analysis indicates that the crosslink between Arp2 and Arp3 C426 (Fig. 8) is a non-short pitch crosslink and likely involves R198C in Arp2.

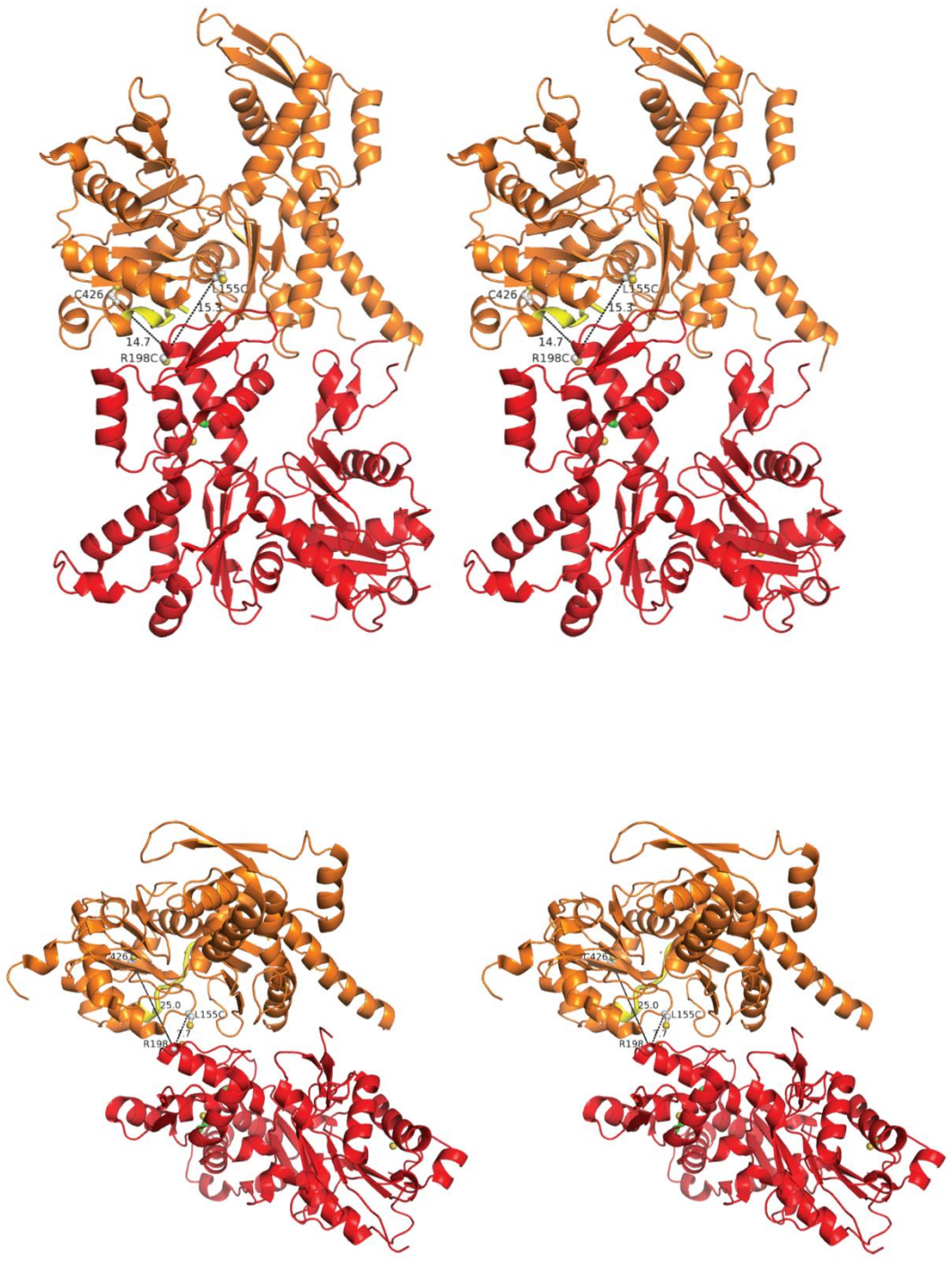
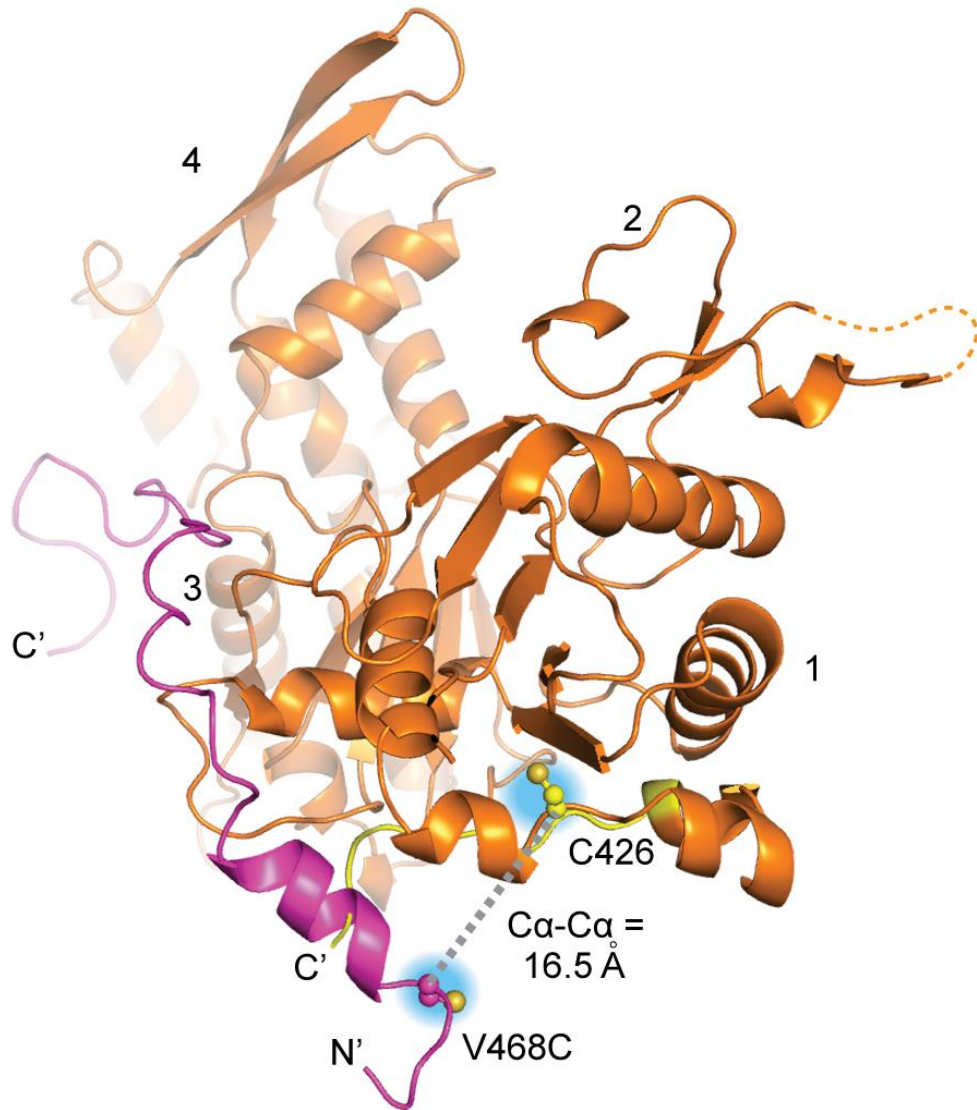


Fig. S7: Hypothetical molecular model showing the relative positions of V468C in N-WASP-VCA relative to the reactive cysteine (C426) in the Arp3 Δ C Arp2/3 complex. Ribbon diagram of Arp3 (orange) based on crystal structure 1K8K, with CA (magenta) modeled into the proposed binding site as described in Fig. 8 in the main text. Cysteine residues that crosslink in the CuSO₄ crosslinking assay are shown in ball-and-stick representation. Subdomains of Arp3 are numbered. Segment of Arp3 C-terminus that is deleted in the Arp3 Δ C Arp2/3 complex is yellow.



Supplemental Materials and Methods:

Construction of budding yeast plasmids for Arp2/3 complex expression

S. cerevisiae *ARP2* and *ARP3* including ~200-250 (203 for Arp2 / 252 for Arp3) upstream and ~150 (179 for Arp2 / 147 for Arp3) nucleotides downstream were subcloned from pCE04 and pCE05 (gift from Rong Li) into pRS317 and pRS315, respectively, to make vectors pBN01 and pBN02 (Table S5). Arp2(R198C) and Arp3(L155C) were introduced into pBN01 and pBN02 by the Quick Change PCR protocol and subcloned into pRS317 and pRS315, respectively. Arp3 Δ C⁴⁴⁰⁻⁴⁴⁹ and Arp3 Δ C⁴⁴⁰⁻⁴⁴⁹(C426A) were created using the same method in the context of either wild type or dual-cysteine mutations. CA-fusion constructs were generated by overlap extension PCR. A bovine N-WASP-CA⁴⁶⁷⁻⁵⁰⁵ fragment was amplified using primers containing linker sequences along with sequences that overlapped the regions in the *arp2(R198C)* and *arp3(L155C)* genes targeted for insertion. Mutant plasmids were confirmed by sequencing.

Construction of budding yeast strains

Strain RLY188 (a gift from Rong Li, Stowers Institute) was crossed with strain KEBY88 and sporulated to create ScMR001, a strain with the *trp1-901* mutation and *ARP3* knocked out with the *HIS3* marker and rescued with a *ARP3::URA* plasmid (pDW20) (See Tables S4 and S5). Arp2 or Arp3 expression plasmids were transformed into strains ScBN002 and ScMR001, respectively, and plated on the appropriate selective media (Leu- or Lys-) to select for the expression plasmid. *URA* plasmids containing wild type *ARP2* or *ARP3* were subsequently kicked out by plating on 5-Fluoroorotic acid. Resulting

single cysteine haploids expressing mutant but not wild type Arp2 or Arp3 were mated and diploids plated on synthetic medium lacking leucine, tryptophan, lysine and histidine. Sporulated diploids were analyzed by random spore analysis to select for the *LEU*, *LYS*, *HIS* and *TRP* markers. Final strains were confirmed as haploids by mating with tester strains and the expression plasmids were isolated and resequenced.

Protein purification and labeling

Most yeast Arp2/3 complexes were purified using an ammonium sulfate cut, a GST-N-WASP-VCA affinity column, and a gel filtration step, as previously described (4, 5). The Arp3 Δ C complexes were an exception, since they could not be eluted from a GST-N-WASP-VCA affinity column using high salt, as in the standard procedure. Therefore, we eluted Arp3 Δ C complexes with a 50 mM reduced glutathione solution, then ran the complex through a MonoQ (GE Healthcare) column and a glutathione sepharose column to remove the GST-N-WASP-VCA. Pooled fractions were concentrated and loaded on a Superdex 200 (GE Healthcare) gel filtration column as the final polishing step. The CA-fusion complexes also required modifications of the purification protocol. Specifically, wild type complexes were loaded onto the affinity column in PKME buffer (25 mM PIPES pH 7.0, 50 mM KCl, 3 mM MgCl₂, 1 mM EGTA, 100 μ M ATP, 1 mM DTT), washed with PKME followed by 275 mM KCl PKME, and eluted with either a gradient of 275 mM KCl PKME to QB buffer (20 mM Tris pH 8.0, 1 M NaCl, 3 mM MgCl₂, 1 mM EGTA, 100 μ M ATP, 1 mM DTT) or a step elution of high magnesium buffer (25 mM PIPES pH 7.0, 25 mM KCl, 200 mM MgCl₂, 1 mM EGTA, 100 μ M ATP, 1 mM DTT). In contrast, CA-fusion complexes were loaded

in 25 mM KCl PKME and the high salt PKME wash was omitted. Elution was accomplished with a gradient of PKME containing 25 mM to 500 mM KCl. The affinity column elutions for CA-fusion preparations were passed through MonoQ and gel filtration columns. For all complexes used in crosslinking assays, the gel filtration and final storage buffer lacked reducing agent. Complexes were concentrated to ~5-25 μ M in Vivaspin Turbo 15 centrifugal concentrators (50K MWCO, Sartorius Stedim Biotech) and flash frozen within hours of the final gel filtration step. Flash freezing did not influence the activity of any of the purified complexes in pyrene actin polymerization assays.

To purify crosslinked complex, the dual cysteine complex was isolated using the standard (wild type) protocol and gel filtered in KMEI buffer + ATP (10 mM Imidazole pH 7.0, 50 mM KCl, 1 mM MgCl₂, 1 mM EGTA, 200 μ M ATP). Pooled fractions were diluted to 1 μ M. 5 μ M LZ-N-WASP-VCA was added to the mixture and crosslinking was initiated by adding 10 μ M BMOE and reacting for 1 hour at room temperature. The reaction was quenched with 1 mM DTT and the reaction mix was passed over a MonoQ column (20 mM PIPES pH 7.0, 50-500 mM NaCl, 1 mM DTT) to separate LZ-N-WASP-VCA. Fractions containing Arp2/3 complex were pooled and dialyzed into GST-Dip1 binding buffer (25 mM Tris pH 8.0, 50 mM KCl, 1mM MgCl₂, 100 μ M ATP, 1 mM DTT). A Dip1 affinity column was prepared by passing ~10 mg of previously frozen GST-Dip1 on a 5 mL GSTrap FF column (GE life sciences) equilibrated with GST-binding buffer (20 mM Tris pH 8.0, 140 mM NaCl, 1 mM EDTA) and then washed with GST-Dip1 binding buffer. The crosslinking reaction mixture was loaded on the column at a flow rate of 0.25 mL/min, washed with 10 column volumes GST-Dip1 binding buffer

and eluted with the same buffer containing 500 mM KCl. Eluted fractions containing pure crosslinked Arp2/3 complex were pooled and dialyzed into storage buffer (20 mM Tris pH 8.0, 50 mM NaCl, 1 mM DTT) before concentrating and flash freezing. Please see supplemental material for description of purification of actin and NPF proteins, as well as protocols for biochemical assays.

Construction of fission yeast strains

A fission yeast strain harboring the *arp3ΔC*(416-427) mutation was made by transforming the TP150 strain with a cassette harboring a premature stop codon and the KanMX6 marker as described (6). The integrated mutant gene was confirmed by amplifying and sequencing the region. See Table S6 for list of fission yeast strains used in this study.

Construction of bacterial expression plasmids

Bos taurus N-WASP-VCA(C431A)⁽⁴²⁸⁻⁵⁰⁵⁾, LZ-N-WASP-VCA(C431A)⁽⁴²⁸⁻⁵⁰⁵⁾, and N-WASP-CA⁽⁴⁶⁷⁻⁵⁰⁵⁾, human WASP-VCA⁽⁴²⁹⁻⁵⁰²⁾ and WAVE1-VCA⁽⁴⁸⁵⁻⁵⁵⁹⁾ and budding yeast Las17-VCA⁽⁵²⁹⁻⁶³³⁾ were each subcloned into the vector pGV67 as GST-TEV-fusion constructs. The L471A, R478K, V468C, T464C and ΔDEDED mutations were introduced into *Bos taurus* N-WASP-VCA(C431A) by the Quick Change PCR protocol.

Protein purification and labeling

Pyrene labeled rabbit skeletal muscle actin, N-WASP-VCA(C431A)⁽⁴²⁸⁻⁵⁰⁵⁾, LZ-N-WASP-VCA(C431)⁽⁴²⁸⁻⁵⁰⁵⁾, N-WASP-CA⁽⁴⁶⁷⁻⁵⁰⁵⁾, WASP-VCA⁽⁴²⁹⁻⁵⁰²⁾, WAVE1-

VCA⁽⁴⁸⁵⁻⁵⁵⁹⁾, Las17-VCA⁽⁵²⁹⁻⁶³³⁾, Wsp1-VCA⁽⁴⁹⁷⁻⁵⁷⁴⁾ and GST-Dip1 were purified as previously described (4, 7-9). Briefly, constructs were expressed as GST-TEV-fusion constructs in BL21(DE3) *E.coli* cells and isolated using GS4B resin (GE Healthcare) following lysis. Constructs were eluted from the column using 50 mM reduced glutathione, and the GST tag was cleaved with TEV protease overnight. Cleaved constructs were isolated by passing through a Source30Q column followed by gel filtration on a Superdex 75 column (GE Healthcare). All constructs used in crosslinking assays were either stored in buffer lacking DTT or dialyzed prior to crosslinking reactions to remove DTT. N-WASP-VCA(C431A, T464C) was labeled with benzophenone-4-maleimide (B4M) and SpWsp1-VCA was labeled with rhodamine as previously described (7).

Pyrene actin polymerization assays and kinetic data analysis

Pyrene actin polymerization assays were carried out by adding 1 μ L of 100X antifoam (100X: 0.005% Antifoam-204, Sigma) and 2 μ L of 10X ME buffer (10X: 5 mM MgCl₂, 20 mM EGTA) to 20 μ L of a 5X actin stock and incubated for 2 minutes to exchange calcium from G-buffer to magnesium. To initiate polymerization, 77 μ L of buffer, salts, Arp2/3 complex and NPFs were added to bring the final concentrations to 10 mM Imidazole pH 7.0, 50 mM KCl, 1 mM EGTA, 1 mM MgCl₂, 200 μ M ATP and 1 mM DTT. Polymerization was monitored by exciting the sample at 365 nm and monitoring the emission at 407 nm using a Tecan Safire 2 plate reader. The maximum rate of polymer formation was calculated by determining the maximum slope from each curve and converting RFU/s to nM/s by using the equation below, where the concentration of

polymer is the equilibrium concentration, equal to the total concentration of actin minus 0.1 μM :

$$\text{Polymerization rate} \left(\frac{\text{nM}}{\text{s}} \right) = \frac{\text{Maximum slope} * [\text{polymer}]}{\text{maxRFU} - \text{minRFU}}$$

The concentration of barbed ends was calculated by the following equation:

$$[\text{barbed ends}](\text{nM}) = \frac{\text{Polymerization rate}}{11600 \text{ nM}^{-1}\text{s}^{-1}[\text{monomer}]}$$

Where $11600 \text{ nM}^{-1}\text{s}^{-1}$ is the previously determined barbed end assembly rate (10). Time to half-maximal polymerization was calculated by determining the time point where the fluorescence equaled the average of the maximum and minimum fluorescence units for every curve.

Short pitch crosslinking assays

In a typical short pitch crosslinking assay, 16 μL of a solution containing Arp2/3 complex with or without additional components (*e.g.* ATP or NPF) in KMEI was mixed with 4 μL of 125 μM BMOE in water for one minute before adding 80 μL 1.25x SDS-PAGE loading buffer (1x SDS-PAGE buffer: 0.3 % SDS, 33 mM DTT, bromophenol blue). For experiments in figure 3, wild type complex was dialyzed into KMEI buffer without DTT prior to crosslinking and reactions were quenched with 1 mM DTT before running polymerization assays. All replicates for comparison of different conditions within a given panel in the manuscript were run in a single set of reactions on the same day to

reduce variability. Reactions were run on SDS-PAGE and transferred to nitrocellulose membranes. For single color western blots, membranes were treated with goat anti-Arp3 (Santa Cruz, sc-11973, 1:1000 dilution) followed by donkey anti-goat IRDye 680RD (LICOR, 1:10000 dilution). For two color blots, goat anti-Arp2 (Santa Cruz, sc-11969, 1:1000 dilution) and mouse anti-Arp3 (Santa Cruz, sc-376625, 1:1000 dilution) were simultaneously incubated followed by donkey anti-goat IRDye 680RD and donkey anti-mouse IRDye 800CW (LICOR, 1:10000 dilution). Blots were scanned and quantified using a LICOR Odyssey Fc imaging system. Truncation of the Arp3 C-terminus exposed at least one endogenous cysteine on Arp3 (Cys 426), resulting in formation of an additional crosslinking product that complicated our analysis (Fig. 8D). To reduce crosslinking with endogenous cysteines, we created an Arp3 Δ C(C426A) mutant in the context of the engineered dual cysteines.

B4M crosslinking reactions

B4M crosslinking reactions were carried out by mixing 1.5 μ M Arp2/3 complex with 4 μ M N-WASP-VCA(T464C-B4M) in KMEH buffer (10 mM HEPES pH 7.0, 50 mM KCl, 1 mM MgCl₂, 1 mM EGTA, 200 μ M ATP) with and without 100 μ M LZ-VCA. Reactions were illuminated with a UV transilluminator equipped with 350nm bulbs for 10 minutes at 4 °C. Reaction products were separated by SDS-PAGE, transferred to nitrocellulose membranes and blotted with either goat anti-Arp2 (Santa Cruz, sc-11969, 1:1000 dilution) or goat anti-Arp3 (Santa Cruz, sc-11973, 1:1000 dilution) followed by donkey anti-goat IRDye 680RD (LICOR, 1:10000 dilution).

Analysis of crosslinking distances

To investigate the crosslinking distance between the engineered cysteines in the trajectory from the splayed to the short pitch conformation, we first generated structural morphs from the splayed to short pitch state using Pymol. For the splayed conformation we used the crystal structure of *Bos taurus* Arp2/3 complex with bound GMF (GMF was not included in the morph) (11), as this is the only high resolution Arp2/3 complex crystal structure in which nearly all of Arp2 is ordered. For the short pitch conformation we used either the branch junction EM model, or a model constructed using the cryoEM structure of an actin filament (3G37) as a short pitch template. An actin subunit from 3G37 was overlaid onto subdomains 1 and 2 of Arp3 in 4JD2, then Arp2 from 4JD2 was superposed onto the actin in the short pitch position. Modeled structures along each of the two trajectory were input into Xwalk, a program that calculates the solvent accessible surface distance between crosslinkable residues (3). In contrast to the Euclidian distance, this calculation accounts for the fact that crosslinkers cannot pass through sterically occluded space.

CuSO₄ crosslinking assays

Copper sulfate crosslinking assays were carried out by mixing 0.5 μM wild type, Arp3 ΔC , or Arp3 ΔC (C426A) *S. cerevisiae* Arp2/3 complex with 2 μM N-WASP-VCA(V468C) in buffer containing 50 μM CuSO₄, 10 mM Imidazole pH 7.0, 50 mM KCl, 50 μM EGTA, 1 mM MgCl₂ and 200 μM ATP. Some reactions also contained 50 μM N-WASP-CA. After incubation for 1 hr at room temperature, samples were mixed with SDS-PAGE loading buffer containing 2 mM N-Ethylmaleimide and no reducing agent

before separation by SDS-PAGE. The Arp2/3 complexes used in these crosslinking assays did not contain the engineered short pitch crosslinking cysteines.

Actin filament copelleting assays

100 nM short pitch crosslinked Arp2/3 complex with or without 20 μ M N-WASP-CA were incubated for 20 minutes with 5 μ M pre-formed actin filaments in a final volume of 50 μ L. Reactions were spun in a TLA100 rotor (Beckman Coulter) at 85K rpm for 15 minutes. Supernatant was removed and transferred to a fresh tube and 10 μ L of 6x SDS-loading buffer was added to bring the final volume to 60 μ L. Pellets were dissolved with 60 μ L of pre-warmed 1x SDS-loading buffer and then samples were resolved by SDS-PAGE followed by western blot analysis using goat anti-Arp3 (Santa Cruz, sc-11973, 1:1000 dilution) and donkey anti-goat IRDye 680RD (LICOR, 1:10000 dilution).

Fluorescence anisotropy binding assays

The fluorescence anisotropy of a mixture of 75nM Rhodamine-labeled SpWsp1-VCA, 2 μ M wild type or 1.5 μ M Arp3 Δ C *S. pombe* Arp2/3 complex in KMEI (10 mM Imidazole pH 7.0, 50 mM KCl, 1 mM EGTA, 1 mM MgCl₂, 200 μ M ATP, 1 mM DTT) was measured using an ISS PC1 fluorometer. The excitation wavelength was 557 nm and emission wavelength was 574 nm. Arp2/3 complex was sequentially diluted by removing a portion of the reaction and then diluting it with the same volume of an identical solution lacking Arp2/3 complex. The fluorescence anisotropy was measured for a range of Arp2/3 complex concentrations. Because the two WASP-CA sites show an approximate

ten-fold difference in binding affinity in other Arp2/3 complexes tested, we assumed that under the conditions of the assay, only binding to the high affinity site contributes significantly to the anisotropy change (12, 13). The data were fit to the single-site binding equation below:

$$\text{Anisotropy} = L_F + (L_B - L_F) \frac{(L_T + K_D + [\text{Arp2/3}]) - \sqrt{(-L_T - K_D - [\text{Arp2/3}])^2 - 4(L_T * [\text{Arp2/3}])}}{2L_T}$$

Where L_B and L_F are the anisotropy values of fully bound and free Rho-Wsp1-VCA, respectively, and L_T is the total Rho-Wsp1-VCA concentration. Competition binding assays with unlabeled Wsp1-VCA were performed by measuring the anisotropy of 15 μM Wsp1-VCA with 75 nM Rho-Wsp1-VCA and 500 nM wild type or 300 nM Arp3 ΔC Arp2/3 complex. Wsp1-VCA was diluted using an identical buffer lacking Wsp1-VCA. Competition binding data sets were fit as described by Wang (14).

Table S1: Table of p values for Figure 2C.

n.s. = non-significant. p-values calculated as two-tailed t-test comparing means of at least three experiments.

		N-WASP-VCA			WASP-VCA			WAVE1-VCA			Las17-VCA			N-WASP-CA		
		1 μM	20 μM	30 μM	1 μM	20 μM	30 μM	1 μM	20 μM	30 μM	1 μM	20 μM	30 μM	30 μM	50 μM	
Arp2/3 alone		0.0005 0	p<0.000 1	p<0.000 1	p<0.000 1	p<0.000 1	0.0001 3	0.0011	0.001 9	0.0002 2	0.004 4	0.001 5	0.0001 4	p<0.000 1	p<0.000 1	
N-WASP-VCA	1 μM															
	20 μM		0.0003	0.00019	n.s.	0.0019	0.0022	n.s.	0.034	0.0033	n.s.	0.012	0.0013	0.0018	p<0.000 1	
	30 μM			n.s.	0.00017 p<0.000 1	0.016	n.s.	0.00013 p<0.000 1	0.031	n.s.	0.004 8	n.s.	n.s.	n.s.	n.s.	
WASP-VCA	1 μM														0.016 p<0.000 1	
	20 μM					0.0011	0.0015	0.022	0.032	0.0025	n.s.	0.012	0.0010	0.0015	0.014	
	30 μM						n.s.	0.00061	n.s.	n.s.	0.039	n.s.	n.s.	0.047	0.0068	
WAVE1-VCA	1 μM														p<0.000 1	
	20 μM								0.012	0.0013	n.s.	0.006	1	0.00090	1	
	30 μM										0.034	n.s.	n.s.	n.s.	0.0078	
Las17-VCA	1 μM												0.046	0.0096	0.0094	0.00056
	20 μM													n.s.	n.s.	
	30 μM													n.s.	n.s.	
N-WASP-CA	30 μM														n.s.	
	50 μM														n.s.	

Table S2: Table of p values for Figure 3B.

n.s. = non-significant. p-values calculated as two-tailed t-test comparing means of at least three experiments.

	WT	WT + CA	Arp2-CA	Arp2-CA + CA	Arp3-CA	Arp3-CA + CA
WT		p<0.0001	0.0035	p<0.0001	0.0018	p<0.0001
WT + CA			0.0048	0.046	0.00023	n.s.
Arp2-CA				0.0019	n.s.	0.00031
Arp2-CA + CA					0.00064	n.s.
Arp3-CA						p<0.0001
Arp3-CA + CA						

Table S3: Table of p values for Figure 6C.

n.s. = non-significant. p-values calculated as two-tailed t-test comparing means of at least three experiments.

	NWASP (30μM)	L471A (50μM)	R478K (50μM)	ΔDEDED (30μM)
Arp2/3 + ATP	0.00057	0.0065	0.0012	0.00021
+N-WASP (30μM)		0.0042	0.0053	n.s.
+L471A (50μM)			n.s.	0.0022
+R478K (50μM)				0.0033
+ΔDEDED (30μM)				

Table S4: List of budding yeast expression plasmids used.

Name	Gene	Vector	Source
pDW6	<i>ARP2</i>	pRS316	R. Li
pDW20	<i>ARP3-MYC-HISx6</i>	pRS316	R. Li
pCE04	<i>ARP2</i>	pRS305	R. Li
pCE05	<i>ARP3</i>	pRS305	R. Li
pBN01	<i>ARP2</i>	pRS317	(4)
pBN02	<i>ARP3</i>	pRS315	(4)
pBN03	<i>arp2 R198C</i>	pRS317	(4)
pBN09	<i>arp3 L155C</i>	pRS315	(4)
pMR06	<i>arp2-CA, R198C</i>	pRS317	This study
pMR09	<i>arp3ΔCterm440-449, L155C</i>	pRS315	This study
pMR11	<i>arp3-CA, L155C</i>	pRS315	This study
pMR14	<i>arp3ΔCterm440-449, L155C, C426A</i>	pRS315	This study
pMR28	<i>arp3ΔCterm440-449</i>	pRS315	This study
pMR29	<i>arp3ΔCterm440-449, C426A</i>	pRS315	This study

Table S5: List of budding yeast strains used.

Strain	Genotype	Source
KEBY88	<i>MATa, ura3-52, his3-Δ200, leu2-3, lys2-801, trp1-901, suc2-Δ9, pep4-3</i>	T. Stevens
RLY188	<i>MATa, ura3-52, his3-Δ200, leu2-3, lys2-801, Δarp3::HIS3, pDW20::URA3</i>	R. Li
“wild type”	<i>pep4-3::KAN</i>	T. Stevens
BN002	<i>MATa, ura3-52, his3-Δ200, leu2-3, lys2-801, trp1-901, Δarp2::TRP1 pDW6::URA3</i>	(4)
BN021	<i>MATa, ura3-52, his3-Δ200, leu2-3, lys2-801, trp1-901, Δarp2::TRP1 Δarp3::HIS3 pBN09::LEU2 pBN03::LYS2</i>	(4)
MR001	<i>MATa, ura3-52, his3-Δ200, leu2-3, lys2-801, trp1-901, Δarp3::HIS3, pDW20::URA3</i>	This study
MR008	<i>MATa, ura3-52, his3-Δ200, leu2-3, lys2-801, trp1-901, Δarp2::trp1-901, pMR06::LYS2</i>	This study
MR010	<i>MATa, ura3-52, his3-Δ200, leu2-3, lys2-801, trp1-901, Δarp3::HIS3, pBN09::LEU2</i>	This study
MR012	<i>MATa, ura3-52, his3-Δ200, leu2-3, lys2-801, trp1-901, Δarp3::HIS3, pMR09::LEU2</i>	This study
MR014	<i>MATa, ura3-52, his3-Δ200, leu2-3, lys2-801, trp1-901, Δarp3::HIS3, pMR11::LEU2</i>	This study
MR016	<i>MATa, ura3-52, his3-Δ200, leu2-3, lys2-801, trp1-901, Δarp2::TRP1, pBN03::LYS2</i>	This study
MR017	<i>MATa, ura3-52, his3-Δ200, leu2-3, lys2-801, trp1-901, Δarp2::TRP1, Δarp3::HIS3 pBN09::LEU2 pMR01::LYS2</i>	This study
MR019	<i>MATa, ura3-52, his3-Δ200, leu2-3, lys2-801, trp1-901, Δarp2::TRP1 Δarp3::HIS3 pBN09::LEU2 pMR03::LYS2</i>	This study
MR020	<i>MATa, ura3-52, his3-Δ200, leu2-3, lys2-801, trp1-901, Δarp2::TRP1 Δarp3::HIS3 pBN09::LEU2 pMR04::LYS2</i>	This study
MR022	<i>MATa, ura3-52, his3-Δ200, leu2-3, lys2-801, trp1-901, Δarp2::TRP1 Δarp3::HIS3 pBN03::LYS2 pMR09::LEU2</i>	This study
MR025	<i>MATa, ura3-52, his3-Δ200, leu2-3, lys2-801, trp1-901, Δarp2::trp1-901 Δarp3::HIS3 pBN09::LEU2 pMR06::LYS2</i>	This study
MR027	<i>MATa, ura3-52, his3-Δ200, leu2-3, lys2-801, trp1-901, Δarp2::trp1-901 Δarp3::HIS3 pBN03::LYS2 pMR11::LEU2</i>	This study
MR030	<i>MATa, ura3-52, his3-Δ200, leu2-3, lys2-801, trp1-901, Δarp3::HIS3 pMR14::LEU2</i>	This study
MR032	<i>MATa, ura3-52, his3-Δ200, leu2-3, lys2-801, trp1-901, Δarp2::TRP1 Δarp3::HIS3 pBN03::LYS2, pMR14::LEU2</i>	This study
MR050	<i>MATa, ura3-52, his3-Δ200, leu2-3, lys2-801, trp1-901, Δarp3::HIS3, pMR28::LEU2</i>	This study
MR051	<i>MATa, ura3-52, his3-Δ200, leu2-3, lys2-801, trp1-901, Δarp3::HIS3, pMR29::LEU2</i>	This study

Table S6: List of fission yeast strains used.

Strain	Genotype	Source
BN024	<i>leu1-32 sm902 arp3Δ416-427::kanMX6</i>	(Submitted)
TP150	<i>h⁻ leu1-32 sm902</i>	M. Yanagida

REFERENCES CITED

CHAPTER I

- Amann, K. J., & Pollard, T. D. (2001a). Direct real-time observation of actin filament branching mediated by Arp2/3 complex using total internal reflection fluorescence microscopy. *Proceedings of the National Academy of Sciences of the United States of America*, 98(26), 15009–13. doi:10.1073/pnas.211556398
- Amann, K. J., & Pollard, T. D. (2001b). The Arp2/3 complex nucleates actin filament branches from the sides of pre-existing filaments. *Nature Cell Biology*, 3(3), 306–310. doi:10.1038/35060104
- Ayala, I., Baldassarre, M., Giacchetti, G., Caldieri, G., Tetè, S., Luini, A., & Buccione, R. (2008). Multiple regulatory inputs converge on cortactin to control invadopodia biogenesis and extracellular matrix degradation. *Journal of Cell Science*, 121(Pt 3), 369–378. doi:10.1242/jcs.008037
- Blanchoin, L., Amann, K., Higgs, H., Marchand, J. B., Kaiser, D., & Pollard, T. (2000). Direct observation of dendritic actin complex and WASP / Scar proteins. *Nature*, 404(1994), 1007–1011. doi:10.1038/35010008
- Blanchoin, L., Pollard, T. D., & Mullins, R. D. R. D. (2000). Interactions of ADF/cofilin, Arp2/3 complex, capping protein and profilin in remodeling of branched actin filament networks. *Current Biology*, 10(20), 1273–1282. doi:10.1016/S0960-9822(00)00749-1
- Boczkowska, M., Rebowski, G., Kast, D. J., & Dominguez, R. (2014). Structural analysis of the transitional state of Arp2/3 complex activation by two actin-bound WCAs. *Nature Communications*, 5, 3308. doi:10.1038/ncomms4308
- Boczkowska, M., Rebowski, G., Petoukhov, M. V., Hayes, D. B., Svergun, D. I., & Dominguez, R. (2008). X-ray scattering study of activated Arp2/3 complex with bound actin-WCA. *Structure (London, England : 1993)*, 16(5), 695–704. doi:10.1016/j.str.2008.02.013
- Breitsprecher, D., Jaiswal, R., Bombardier, J. P., Gould, C. J., Gelles, J., & Goode, B. L. (2012). Rocket launcher mechanism of collaborative actin assembly defined by single-molecule imaging. *Science (New York, N.Y.)*, 336(6085), 1164–8. doi:10.1126/science.1218062
- Campellone, K. G., & Welch, M. D. (2010). A nucleator arms race: cellular control of actin assembly. *Nature Reviews. Molecular Cell Biology*, 11(4), 237–51. doi:10.1038/nrm2867
- Carrier, A. M., Laurent, V., Santolini, J., Melki, R., Xia, G., Hong, Y., ... Didry, D. (2012). Actin Depolymerizing Factor (ADF/Cofilin) Enhances the Rate of Actin Depolymerizing Filament Turnover : Motility Implication in Actin-based. *The Journal of Cell Biology*, 136(6), 1307–1322.

- Chang, F., Drubin, D., & Nurse, P. (1997). Cdc12P, a Protein Required for Cytokinesis in Fission Yeast, Is a Component of the Cell Division Ring and Interacts With Profilin. *Journal of Cell Biology*, *137*(1), 169–182. doi:10.1083/jcb.137.1.169
- Chereau, D., Kerff, F., Graceffa, P., Grabarek, Z., Langsetmo, K., & Dominguez, R. (2005). Actin-bound structures of Wiskott-Aldrich syndrome protein (WASP)-homology domain 2 and the implications for filament assembly. *Proceedings of the National Academy of Sciences of the United States of America*, *102*(46), 16644–16649. doi:10.1073/pnas.0507021102
- D'Agostino, J. L., & Goode, B. L. (2005). Dissection of Arp2/3 complex actin nucleation mechanism and distinct roles for its nucleation-promoting factors in *Saccharomyces cerevisiae*. *Genetics*, *171*(1), 35–47. doi:10.1534/genetics.105.040634
- Dalhaimer, P., Pollard, T. D., & Nolen, B. J. (2008). Nucleotide-Mediated Conformational Changes of Monomeric Actin and Arp3 Studied by Molecular Dynamics Simulations. *Journal of Molecular Biology*, *376*(1), 166–183. doi:10.1016/j.jmb.2007.11.068
- Dayel, M. J., Holleran, E. a., & Mullins, R. D. (2001). Arp2/3 complex requires hydrolyzable ATP for nucleation of new actin filaments. *Proceedings of the National Academy of Sciences of the United States of America*, *98*(26), 14871–6. doi:10.1073/pnas.261419298
- Dayel, M. J., & Mullins, R. D. (2004). Activation of Arp2/3 complex: addition of the first subunit of the new filament by a WASP protein triggers rapid ATP hydrolysis on Arp2. *PLoS Biology*, *2*(4), E91. doi:10.1371/journal.pbio.0020091
- Derry, J. M. j., Kerns, J. A., Weinberg, K. I., Ochs, H. D., Volpini, V., Estivill, X., ... Francke, U. (1995). Wasp gene-mutations in wiskott-aldrich syndrome and x-linked thrombocytopenia. *Human Molecular Genetics*, *4*(7), 1127–1135. doi:10.1093/hmg/4.7.1127
- Dominguez, R. (2009). Actin filament nucleation and elongation factors--structure-function relationships. *Critical Reviews in Biochemistry and Molecular Biology*, *44*(6), 351–66. doi:10.3109/10409230903277340
- Dominguez, R., & Holmes, K. C. (2011). Actin structure and function. *Annual Review of Biophysics*, *40*, 169–86. doi:10.1146/annurev-biophys-042910-155359
- Edwards, M., Zwolak, A., Schafer, D. A., Sept, D., Dominguez, R., & Cooper, J. A. (2014). Capping protein regulators fine-tune actin assembly dynamics. *Nature Reviews. Molecular Cell Biology*, *15*(10), 677–89. doi:10.1038/nrm3869
- Egile, C., Rouiller, I., Xu, X. P., Volkmann, N., Li, R., & Hanein, D. (2005). Mechanism of filament nucleation and branch stability revealed by the structure of the Arp2/3 complex at actin branch junctions. *PLoS Biology*, *3*(11), 1902–1909. doi:10.1371/journal.pbio.0030383
- Evangelista, M., Klebl, B. M., Tong, A. H. Y., Webb, B. A., Leeuw, T., Leberer, E., ... Boone, C. (2000). A role for myosin-I in actin assembly through interactions with Vrp1p, Bee1p, and the Arp2/3 complex. *Journal of Cell Biology*, *148*(2), 353–362.

doi:10.1083/jcb.148.2.353

- Fujiwara, I., Vavylonis, D., & Pollard, T. D. (2007). Polymerization kinetics of ADP- and ADP-Pi-actin determined by fluorescence microscopy. *Proceedings of the National Academy of Sciences*, *104*(21), 8827–8832. doi:10.1073/pnas.0702510104
- Gandhi, M., Smith, B. a, Bovellan, M., Paavilainen, V., Daugherty-Clarke, K., Gelles, J., Goode, B. L. (2010). GMF is a cofilin homolog that binds Arp2/3 complex to stimulate filament debranching and inhibit actin nucleation. *Current Biology : CB*, *20*(9), 861–7. doi:10.1016/j.cub.2010.03.026
- Geeves, M. A., & Holmes, K. C. (1999). Structural Mechanism of Muscle Contraction. *Annual Review of Biochemistry*, *68*(1), 687–728. doi:10.1146/annurev.biochem.68.1.687
- Gimona, M., Djinovic-Carugo, K., Kranewitter, W. J., & Winder, S. J. (2002). Functional plasticity of CH domains. *FEBS Letters*, *513*(1), 98–106. doi:10.1016/S0014-5793(01)03240-9
- Gohl, C., Banovic, D., Grevelhörster, A., & Bogdan, S. (2010). WAVE forms hetero- and homo-oligomeric complexes at integrin junctions in Drosophila visualized by bimolecular fluorescence complementation. *Journal of Biological Chemistry*, *285*(51), 40171–40179. doi:10.1074/jbc.M110.139337
- Goley, E. D., Rammohan, A., Znameroski, E. a, Firat-Karalar, E. N., Sept, D., & Welch, M. D. (2010). An actin-filament-binding interface on the Arp2/3 complex is critical for nucleation and branch stability. *Proceedings of the National Academy of Sciences of the United States of America*, *107*(18), 8159–64. doi:10.1073/pnas.0911668107
- Goley, E. D., Rodenbusch, S. E., Martin, A. C., & Welch, M. D. (2004). Critical Conformational Changes in the Arp2 / 3 Complex Are Induced by Nucleotide and Nucleation Promoting Factor, *16*, 269–279.
- Goley, E. D., & Welch, M. D. (2006). The ARP2/3 complex: an actin nucleator comes of age. *Nature Reviews. Molecular Cell Biology*, *7*(10), 713–26. doi:10.1038/nrm2026
- Goode, B. L., Rodal, a a, Barnes, G., & Drubin, D. G. (2001). Activation of the Arp2/3 complex by the actin filament binding protein Abp1p. *The Journal of Cell Biology*, *153*(3), 627–34. Retrieved from <http://www.pubmedcentral.nih.gov/articlerender.fcgi?artid=2190564&tool=pmcentrez&rendertype=abstract>
- Helgeson, L. a, & Nolen, B. J. (2013). Mechanism of synergistic activation of Arp2/3 complex by cortactin and N-WASP. *eLife*, *2*, e00884. doi:10.7554/eLife.00884
- Helgeson, L. a, Prendergast, J. G., Wagner, A. R., Rodnick-Smith, M., & Nolen, B. J. (2014). Interactions with actin monomers, actin filaments, and Arp2/3 complex define the roles of WASP family proteins and cortactin in coordinately regulating branched actin networks. *The Journal of Biological Chemistry*, *289*(42), 28856–69. doi:10.1074/jbc.M114.587527
- Hetrick, B., Han, M. S., Helgeson, L. A., & Nolen, B. J. (2013). Small Molecules CK-

666 and CK-869 Inhibit Actin-Related Protein 2/3 Complex by Blocking an Activating Conformational Change. *Chemistry & Biology*, 1–12. doi:10.1016/j.chembiol.2013.03.019

- Higgs, H. N., Blanchoin, L., & Pollard, T. D. (1999). Influence of the C terminus of Wiskott-Aldrich syndrome protein (WASp) and the Arp2/3 complex on actin polymerization. *Biochemistry*, 38(46), 15212–15222. doi:10.1021/bi991843+
- Humphries, C. L., Balcer, H. I., D'Agostino, J. L., Winsor, B., Drubin, D. G., Barnes, G., Goode, B. L. (2002). Direct regulation of Arp2/3 complex activity and function by the actin binding protein coronin. *Journal of Cell Biology*, 159(6), 993–1004. doi:10.1083/jcb.200206113
- Ingerman, E., Hsiao, J. Y., & Mullins, R. D. (2013). Arp2/3 complex ATP hydrolysis promotes lamellipodial actin network disassembly but is dispensable for assembly. *Journal of Cell Biology*, 200(5), 619–633. doi:10.1083/jcb.201211069
- Jurgenson, C. T., & Pollard, T. D. (2015). Crystals of the Arp2/3 complex in two new space groups with structural information about actin-related protein 2 and potential WASP binding sites. *Acta Crystallographica Section F Structural Biology Communications*, 71(9), 1161–1168. doi:10.1107/S2053230X15013515
- Kabsch, W., Mannherz, H. G., Suck, D., Pai, E. F., & Holmes, K. C. (1990). Atomic structure of the actin: DNase I complex. *Nature*, 347(6288), 37–44. Retrieved from <http://dx.doi.org/10.1038/347037a0>
- Kelly, A. E., Kranitz, H., Dötsch, V., & Mullins, R. D. (2006). Actin binding to the central domain of WASP/Scar proteins plays a critical role in the activation of the Arp2/3 complex. *The Journal of Biological Chemistry*, 281(15), 10589–97. doi:10.1074/jbc.M507470200
- Kreishman-Deitrick, M., Goley, E. D., Burdine, L., Denison, C., Egile, C., Li, R., ... Rosen, M. K. (2005). NMR analyses of the activation of the Arp2/3 complex by neuronal Wiskott-Aldrich syndrome protein. *Biochemistry*, 44(46), 15247–15256. doi:10.1021/bi051065n
- Le Clainche, C., Pantaloni, D., & Carlier, M.-F. (2003). ATP hydrolysis on Arp2/3 complex causes debranching of actin arrays. *P.N.a.S.*, 100(11), 6337–6342.
- Li, R., & Gundersen, G. G. (2008). Beyond polymer polarity: how the cytoskeleton builds a polarized cell. *Nature Reviews. Molecular Cell Biology*, 9(11), 860–73. doi:10.1038/nrm2522
- Liu, S.-L., May, J. R., Helgeson, L. a., & Nolen, B. J. (2013). Insertions within the actin core of actin-related protein 3 (Arp3) modulate branching nucleation by Arp2/3 complex. *The Journal of Biological Chemistry*, 288(1), 487–97. doi:10.1074/jbc.M112.406744
- Liu, S.-L., Needham, K. M., May, J. R., & Nolen, B. J. (2011). Mechanism of a concentration-dependent switch between activation and inhibition of Arp2/3 complex by coronin. *The Journal of Biological Chemistry*, 286(19), 17039–46. doi:10.1074/jbc.M111.219964

- Liverman, A. D. B., Cheng, H.-C., Trosky, J. E., Leung, D. W., Yarbrough, M. L., Burdette, D. L., Orth, K. (2007). Arp2/3-independent assembly of actin by Vibrio type III effector VopL. *Proceedings of the National Academy of Sciences of the United States of America*, 104(43), 17117–22. doi:10.1073/pnas.0703196104
- Luan, Q., & Nolen, B. J. (2013). Structural basis for regulation of Arp2/3 complex by GMF. *Nature Structural & Molecular Biology*, 20(9), 1062–8. doi:10.1038/nsmb.2628
- Ma, L., Rohatgi, R., & Kirschner, M. W. (1998). The Arp2/3 complex mediates actin polymerization induced by the small GTP-binding protein Cdc42. *Proc Natl Acad Sci U S A*, 95(26), 15362–15367. Retrieved from <http://www.pnas.org/cgi/content/full/95/26/15362>
- Machesky, L. M., Atkinson, S. J., Ampe, C., Vandekerckhove, J., & Pollard, T. D. (1994). Purification of a Cortical Complex Containing 2 Unconventional Actins from Acanthamoeba by Affinity-Chromatography on Profilin-Agarose. *Journal of Cell Biology*, 127(1), 107–115. doi:10.1083/jcb.127.1.107
- Machesky, L. M., & Insall, R. H. (1998). Scar1 and the related Wiskott–Aldrich syndrome protein, WASP, regulate the actin cytoskeleton through the Arp2/3 complex. *Current Biology*, 8(25), 1347–1356. doi:10.1016/S0960-9822(98)00015-3
- Machesky, L. M., Mullins, R. D., Higgs, H. N., Kaiser, D. a, Blanchoin, L., May, R. C., Pollard, T. D. (1999). Scar, a WASp-related protein, activates nucleation of actin filaments by the Arp2/3 complex. *Proceedings of the National Academy of Sciences of the United States of America*, 96(7), 3739–3744. doi:10.1073/pnas.96.7.3739
- Mannherz, H. G., & Hannappel, E. (2009). The beta-thymosins: intracellular and extracellular activities of a versatile actin binding protein family. *Cell Motility and the Cytoskeleton*, 66(10), 839–851. doi:10.1002/cm.20371
- Marchand, J. B., Kaiser, D. a, Pollard, T. D., & Higgs, H. N. (2001). Interaction of WASP/Scar proteins with actin and vertebrate Arp2/3 complex. *Nature Cell Biology*, 3(1), 76–82. doi:10.1038/35050590
- Martin, A. C., Welch, M. D., & Drubin, D. G. (2006). Arp2/3 ATP hydrolysis-catalysed branch dissociation is critical for endocytic force generation. *Nature Cell Biology*, 8(8), 826–833. doi:10.1038/ncb1443
- Martin, A. C., Xu, X. P., Rouiller, I., Kaksonen, M., Sun, Y., Belmont, L., ... Drubin, D. G. (2005). Effects of Arp2 and Arp3 nucleotide-binding pocket mutations on Arp2/3 complex function. *Journal of Cell Biology*, 168(2), 315–328. doi:10.1083/jcb.200408177
- Mullins, R. D., Heuser, J. a, & Pollard, T. D. (1998). The interaction of Arp2/3 complex with actin: nucleation, high affinity pointed end capping, and formation of branching networks of filaments. *Proceedings of the National Academy of Sciences of the United States of America*, 95(11), 6181–6186. doi:10.1073/pnas.95.11.6181
- Narayanan, A., LeClaire, L. L., Barber, D. L., & Jacobson, M. P. (2011). Phosphorylation of the Arp2 subunit relieves auto-inhibitory interactions for Arp2/3 complex

- activation. *PLoS Computational Biology*, 7(11), e1002226.
doi:10.1371/journal.pcbi.1002226
- Nolen, B. J., Littlefield, R. S., & Pollard, T. D. (2004). Crystal structures of actin-related protein 2/3 complex with bound ATP or ADP. *Proceedings of the National Academy of Sciences of the United States of America*, 101(44), 15627–15632.
doi:10.1073/pnas.0407149101
- Nolen, B. J., & Pollard, T. D. (2007). Insights into the Influence of Nucleotides on Actin Family Proteins from Seven Structures of Arp2/3 Complex. *Molecular Cell*, 26(3), 449–457. doi:10.1016/j.molcel.2007.04.017
- Nolen, B. J., & Pollard, T. D. (2008). Structure and biochemical properties of fission yeast Arp2/3 complex lacking the Arp2 subunit. *The Journal of Biological Chemistry*, 283(39), 26490–8. doi:10.1074/jbc.M802607200
- Oda, T., Iwasa, M., Aihara, T., Maeda, Y., & Narita, A. (2009). The nature of the globular- to fibrous-actin transition. *Nature*, 457(January), 441–446.
doi:10.1038/nature07685
- Otomo, T., Tomchick, D. R., Otomo, C., Panchal, S. C., Machius, M., & Rosen, M. K. (2005). Structural basis of actin filament nucleation and processive capping by a formin homology 2 domain. *Nature*, 433(7025), 488–494.
doi:10.1107/S0108767305096844
- Padrick, S. B., Cheng, H. C., Ismail, A. M., Panchal, S. C., Doolittle, L. K., Kim, S., ... Rosen, M. K. (2008). Hierarchical Regulation of WASP/WAVE Proteins. *Molecular Cell*, 32(3), 426–438. doi:10.1016/j.molcel.2008.10.012
- Padrick, S. B., Doolittle, L. K., Brautigam, C. a, King, D. S., & Rosen, M. K. (2011). Arp2/3 complex is bound and activated by two WASP proteins. *Proceedings of the National Academy of Sciences of the United States of America*, 108(33), E472–9.
doi:10.1073/pnas.1100236108
- Pan, F., Egile, C., Lipkin, T., & Li, R. (2004). ARPC1/Arc40 mediates the interaction of the actin-related protein 2 and 3 complex with Wiskott-Aldrich syndrome protein family activators. *Journal of Biological Chemistry*, 279(52), 54629–54636.
doi:10.1074/jbc.M402357200
- Panchal, S. C., Kaiser, D. a, Torres, E., Pollard, T. D., & Rosen, M. K. (2003). A conserved amphipathic helix in WASP/Scar proteins is essential for activation of Arp2/3 complex. *Nature Structural Biology*, 10(8), 591–8. doi:10.1038/nsb952
- Pollard, T. (1986). Rate constants for the reactions of ATP-and ADP-actin with the ends of actin filaments. *Journal of Cell Biology*, 103(6), 2747.
doi:10.1083/jcb.103.6.2747
- Pollard, T. D. (1986). Rate constants for the reactions of ATP-and ADP-actin with the ends of actin filaments. *Journal of Cell Biology*, 103(6), 2747.
doi:10.1083/jcb.103.6.2747
- Pollard, T. D. (2007). Regulation of actin filament assembly by Arp2/3 complex and formins. *Annual Review of Biophysics and Biomolecular Structure*, 36, 451–77.

doi:10.1146/annurev.biophys.35.040405.101936

- Pollard, T. D., & Cooper, J. A. (2009). Actin, a central player in cell shape and movement. *Science (New York, N.Y.)*, *326*(5957), 1208–1212. doi:10.1126/science.1175862
- Pruyne, D. (2002). Role of Formins in Actin Assembly: Nucleation and Barbed-End Association. *Science*, *297*(5581), 612–615. doi:10.1126/science.1072309
- Quinlan, M. E., Heuser, J. E., Kerkhoff, E., & Mullins, R. D. (2005). Drosophila Spire is an actin nucleation factor. *Nature*, *433*(7024), 382–8. doi:10.1038/nature03241
- Quinlan, M. E., Hilgert, S., Bedrossian, A., Mullins, R. D., & Kerkhoff, E. (2007). Regulatory interactions between two actin nucleators, Spire and Cappuccino. *Journal of Cell Biology*, *179*(1), 117–128. doi:10.1083/jcb.200706196
- Robinson, R. C., Turbedsky, K., Kaiser, D. a, Marchand, J., Higgs, H. N., Choe, S., & Thomas, D. (2001). Crystal Structure of Arp2 / 3 Complex. *Science*, *294*(November), 1679–1685. doi:10.1126/science.1066333
- Rodal, A. a, Sokolova, O., Robins, D. B., Daugherty, K. M., Hippenmeyer, S., Riezman, H., Goode, B. L. (2005). Conformational changes in the Arp2/3 complex leading to actin nucleation. *Nature Structural & Molecular Biology*, *12*(1), 26–31. doi:10.1038/nsmb870
- Rouiller, I., Xu, X.-P., Amann, K. J., Egile, C., Nickell, S., Nicastro, D., ... Hanein, D. (2008). The structural basis of actin filament branching by the Arp2/3 complex. *The Journal of Cell Biology*, *180*(5), 887–95. doi:10.1083/jcb.200709092
- Sept, D., & McCammon, J. a. (2001). Thermodynamics and kinetics of actin filament nucleation. *Biophysical Journal*, *81*(2), 667–674. doi:10.1016/S0006-3495(01)75731-1
- Sitar, T., Gallinger, J., Ducka, A. M., Ikonen, T. P., Wohlhoefer, M., Schmolter, K. M., Holak, T. a. (2011). Molecular architecture of the Spire-actin nucleus and its implication for actin filament assembly. *Proceedings of the National Academy of Sciences of the United States of America*, *108*(49), 19575–80. doi:10.1073/pnas.1115465108
- Smith, B. a., Padrick, S. B., Doolittle, L. K., Daugherty-Clarke, K., Corrêa, I. R., Xu, M. Q., Gelles, J. (2013). Three-color single molecule imaging shows WASP detachment from Arp2/3 complex triggers actin filament branch formation. *eLife*, *2013*(2), 1–25. doi:10.7554/eLife.01008
- Suetsugu, S. (2013). Activation of nucleation promoting factors for directional actin filament elongation: Allosteric regulation and multimerization on the membrane. *Seminars in Cell and Developmental Biology*, *24*(4), 267–271. doi:10.1016/j.semcdb.2013.01.006
- Sun, Y., Martin, A. C., & Drubin, D. G. (2006). Endocytic Internalization in Budding Yeast Requires Coordinated Actin Nucleation and Myosin Motor Activity. *Developmental Cell*, *11*(1), 33–46. doi:10.1016/j.devcel.2006.05.008

- Ti, S.-C., Jurgenson, C. T., Nolen, B. J., & Pollard, T. D. (2011). Structural and biochemical characterization of two binding sites for nucleation-promoting factor WASp-VCA on Arp2/3 complex. *Proceedings of the National Academy of Sciences of the United States of America*, *108*(33), E463–71. doi:10.1073/pnas.1100125108
- Urano, T., Liu, J., Li, Y., Smith, N., & Zhan, X. (2003). Sequential interaction of actin-related proteins 2 and 3 (Arp2/3) complex with neural Wiscott-Aldrich syndrome protein (N-WASP) and cortactin during branched actin filament network formation. *Journal of Biological Chemistry*, *278*(28), 26086–26093. doi:10.1074/jbc.M301997200
- Urano, T., Liu, J., Zhang, P., Fan Yx, Egile, C., Li, R., Zhan, X. (2001). Activation of Arp2/3 complex-mediated actin polymerization by cortactin. *Nature Cell Biology*, *3*(3), 259–266. doi:10.1038/35060051
- Wagner, A. R., Luan, Q., Liu, S.-L., & Nolen, B. J. (2013). Dip1 defines a class of Arp2/3 complex activators that function without preformed actin filaments. *Current Biology : CB*, *23*(20), 1990–8. doi:10.1016/j.cub.2013.08.029
- Welch, M. D., Iwamatsu, a, & Mitchison, T. J. (1997). Actin polymerization is induced by Arp2/3 protein complex at the surface of *Listeria monocytogenes*. *Nature*. doi:10.1038/385265a0
- Welch, M. D., & Mullins, R. D. (2002). Cellular control of actin nucleation. *Annual Review of Cell and Developmental Biology*, *18*, 247–88. doi:10.1146/annurev.cellbio.18.040202.112133
- Welch, M. D., Rosenblatt, J., Skoble, J., Portnoy, D. A., & Mitchison, T. J. (1998). Interaction of human Arp2/3 complex and the *Listeria monocytogenes* ActA protein in actin filament nucleation. *Science*, *281*(5373), 105–108. doi:10.1126/science.281.5373.105
- Winter, D., Podtelejnikov, a V, Mann, M., & Li, R. (1997). The complex containing actin-related proteins Arp2 and Arp3 is required for the motility and integrity of yeast actin patches. *Current Biology : CB*, *7*(7), 519–29. Retrieved from <http://www.ncbi.nlm.nih.gov/pubmed/9210376>
- Xu, X.-P., Rouiller, I., Slaughter, B. D., Egile, C., Kim, E., Unruh, J. R., Volkman, N. (2012). Three-dimensional reconstructions of Arp2/3 complex with bound nucleation promoting factors. *The EMBO Journal*, *31*(1), 236–47. doi:10.1038/emboj.2011.343
- Zalevsky, J., Lempert, L., Kranitz, H., & Mullins, R. D. (2001). Different WASP family proteins stimulate different Arp2/3 complex-dependent actin-nucleating activities. *Current Biology : CB*, *11*(24), 1903–13. Retrieved from <http://www.ncbi.nlm.nih.gov/pubmed/11747816>
- Zuchero, J. B., Coutts, A. S., Quinlan, M. E., Thangue, N. B. La, & Mullins, R. D. (2009). p53-cofactor JMY is a multifunctional actin nucleation factor. *Nature Cell Biology*, *11*(4), 451–9. doi:10.1038/ncb1852

REFERENCES CITED

CHAPTER II

1. Goley, E. D. & Welch, M. D. The ARP2/3 complex: an actin nucleator comes of age. *Nat Rev Mol Cell Biol* **7**, 713-726 (2006).
2. Rotty, J. D., Wu, C. & Bear, J. E. New insights into the regulation and cellular functions of the ARP2/3 complex. *Nat Rev Mol Cell Biol* **14**, 7-12, doi:10.1038/nrm3492 (2013).
3. Yi, K. *et al.* Dynamic maintenance of asymmetric meiotic spindle position through Arp2/3-complex-driven cytoplasmic streaming in mouse oocytes. *Nat Cell Biol* **13**, 1252-1258, doi:10.1038/ncb2320 (2011).
4. Achard, V. *et al.* A "primer"-based mechanism underlies branched actin filament network formation and motility. *Curr Biol* **20**, 423-428, doi:10.1016/j.cub.2009.12.056 (2010).
5. Marchand, J. B., Kaiser, D. A., Pollard, T. D. & Higgs, H. N. Interaction of WASP/Scar proteins with actin and vertebrate Arp2/3 complex. *Nat Cell Biol* **3**, 76-82 (2001).
6. Dayel, M. J., Holleran, E. A. & Mullins, R. D. Arp2/3 complex requires hydrolyzable ATP for nucleation of new actin filaments. *Proc Natl Acad Sci U S A* **98**, 14871-14876 (2001).
7. Martin, A. C. *et al.* Effects of Arp2 and Arp3 nucleotide-binding pocket mutations on Arp2/3 complex function. *J Cell Biol* **168**, 315-328 (2005).
8. Le Clainche, C., Didry, D., Carlier, M. F. & Pantaloni, D. Activation of Arp2/3 complex by Wiskott-Aldrich Syndrome protein is linked to enhanced binding of ATP to Arp2. *J Biol Chem* **276**, 46689-46692 (2001).
9. Wagner, A. R., Luan, Q., Liu, S.-L. & Nolen, B. J. WISH/DIP/SPIN90 proteins form a class of Arp2/3 complex activators that function without preformed actin filaments. *Curr Biol* **23**, 1990-1998 (2013).
10. Campellone, K. G. & Welch, M. D. A nucleator arms race: cellular control of actin assembly. *Nat Rev Mol Cell Biol* **11**, 237-251, doi:10.1038/nrm2867 (2010).
11. Moulding, D. A. *et al.* Unregulated actin polymerization by WASp causes defects of mitosis and cytokinesis in X-linked neutropenia. *The Journal of experimental medicine* **204**, 2213-2224, doi:10.1084/jem.20062324 (2007).
12. Devriendt, K. *et al.* Constitutively activating mutation in WASP causes X-linked severe congenital neutropenia. *Nature genetics* **27**, 313-317, doi:10.1038/85886 (2001).
13. Boettner, D. R. *et al.* The F-BAR protein Syp1 negatively regulates WASp-Arp2/3 complex activity during endocytic patch formation. *Curr Biol* **19**, 1979-1987, doi:10.1016/j.cub.2009.10.062 (2009).

14. Robinson, R. C. *et al.* Crystal structure of Arp2/3 complex. *Science* **294**, 1679-1684 (2001).
15. Nolen, B. J., Littlefield, R. S. & Pollard, T. D. Crystal structures of actin-related protein 2/3 complex with bound ATP or ADP. *Proc Natl Acad Sci U S A* **101**, 15627-15632 (2004).
16. Nolen, B. J. & Pollard, T. D. Insights into the influence of nucleotides on actin family proteins from seven structures of Arp2/3 complex. *Mol Cell* **26**, 449-457 (2007).
17. Luan, Q. & Nolen, B. J. Structural basis for regulation of Arp2/3 complex by GMF. *Nat Struct Mol Biol* **20**, 1062-1068, doi:10.1038/nsmb.2628 (2013).
18. Boczkowska, M. *et al.* X-Ray Scattering Study of Activated Arp2/3 Complex with Bound Actin-WCA. *Structure* **16**, 695-704 (2008).
19. Xu, X. P. *et al.* Three-dimensional reconstructions of Arp2/3 complex with bound nucleation promoting factors. *Embo J*, doi:10.1038/emboj.2011.343 (2011).
20. Rodal, A. A. *et al.* Conformational changes in the Arp2/3 complex leading to actin nucleation. *Nat Struct Mol Biol* **12**, 26-31 (2005).
21. Goley, E. D., Rodenbusch, S. E., Martin, A. C. & Welch, M. D. Critical conformational changes in the Arp2/3 complex are induced by nucleotide and nucleation promoting factor. *Mol Cell* **16**, 269-279 (2004).
22. Hetrick, B., Han, M. S., Helgeson, L. A. & Nolen, B. J. Small molecules CK-666 and CK-869 inhibit actin-related protein 2/3 complex by blocking an activating conformational change. *Chem Biol* **20**, 701-712, doi:10.1016/j.chembiol.2013.03.019 (2013).
23. Moreau, V., Madania, A., Martin, R. P. & Winson, B. The *Saccharomyces cerevisiae* actin-related protein Arp2 is involved in the actin cytoskeleton. *J Cell Biol* **134**, 117-132 (1996).
24. Liu, S. L., May, J. R., Helgeson, L. A. & Nolen, B. J. Insertions within the actin core of actin-related protein 3 (Arp3) modulate branching nucleation by Arp2/3 complex. *J Biol Chem* **288**, 487-497, doi:10.1074/jbc.M112.406744 (2013).
25. Daugherty, K. M. & Goode, B. L. Functional surfaces on the p35/ARPC2 subunit of Arp2/3 complex required for cell growth, actin nucleation, and endocytosis. *J Biol Chem* **283**, 16950-16959 (2008).
26. Narayanan, A., LeClaire, L. L., 3rd, Barber, D. L. & Jacobson, M. P. Phosphorylation of the Arp2 subunit relieves auto-inhibitory interactions for Arp2/3 complex activation. *PLoS Comput Biol* **7**, e1002226, doi:10.1371/journal.pcbi.1002226 (2011).
27. Suarez, C. *et al.* Profilin Regulates F-Actin Network Homeostasis by Favoring Formin over Arp2/3 Complex. *Developmental cell*, doi:10.1016/j.devcel.2014.10.027 (2014).

28. Martin, A. C., Welch, M. D. & Drubin, D. G. Arp2/3 ATP hydrolysis-catalysed branch dissociation is critical for endocytic force generation. *Nat Cell Biol* **8**, 826-833 (2006).
29. Ingerman, E., Hsiao, J. Y. & Mullins, R. D. Arp2/3 complex ATP hydrolysis promotes lamellipodial actin network disassembly but is dispensable for assembly. *J Cell Biol* **200**, 619-633, doi:10.1083/jcb.201211069 (2013).
30. Le Clainche, C., Pantaloni, D. & Carlier, M. F. ATP hydrolysis on actin-related protein 2/3 complex causes debranching of dendritic actin arrays. *Proc Natl Acad Sci U S A* **100**, 6337-6342 (2003).
31. Dayel, M. J. & Mullins, R. D. Activation of Arp2/3 Complex: Addition of the First Subunit of the New Filament by a WASP Protein Triggers Rapid ATP Hydrolysis on Arp2. *PLoS Biol* **2**, E91 (2004).
32. Muller, J. *et al.* Sequence and comparative genomic analysis of actin-related proteins. *Mol Biol Cell* **16**, 5736-5748, doi:10.1091/mbc.E05-06-0508 (2005).
33. Dalhaimer, P., Pollard, T. D. & Nolen, B. J. Nucleotide-mediated conformational changes of monomeric actin and Arp3 studied by molecular dynamics simulations. *J Mol Biol* **376**, 166-183 (2008).
34. Bahler, J. *et al.* Heterologous modules for efficient and versatile PCR-based gene targeting in *Schizosaccharomyces pombe*. *Yeast* **14**, 943-951 (1998).
35. Winter, D., Podtelejnikov, A. V., Mann, M. & Li, R. The complex containing actin-related proteins Arp2 and Arp3 is required for the motility and integrity of yeast actin patches. *Curr Biol* **7**, 519-529 (1997).
36. Rizvi, S. A. *et al.* Identification and characterization of a small molecule inhibitor of formin-mediated actin assembly. *Chem Biol* **16**, 1158-1168, doi:10.1016/j.chembiol.2009.10.006 (2009).
37. Morrell, J. L., Morpew, M. & Gould, K. L. A mutant of Arp2p causes partial disassembly of the Arp2/3 complex and loss of cortical actin function in fission yeast. *Mol Biol Cell* **10**, 4201-4215 (1999).
38. Cabrera, R., Suo, J., Young, E. & Chang, E. C. *Schizosaccharomyces pombe* Arc3 is a conserved subunit of the Arp2/3 complex required for polarity, actin organization, and endocytosis. *Yeast* **28**, 495-503, doi:10.1002/yea.1853 (2011).
39. Sirotkin, V., Beltzner, C. C., Marchand, J. B. & Pollard, T. D. Interactions of WASp, myosin-I, and verprolin with Arp2/3 complex during actin patch assembly in fission yeast. *J Cell Biol* **170**, 637-648 (2005).
40. Kaksonen, M., Toret, C. P. & Drubin, D. G. A modular design for the clathrin- and actin-mediated endocytosis machinery. *Cell* **123**, 305-320 (2005).
41. Sirotkin, V., Berro, J., Macmillan, K., Zhao, L. & Pollard, T. D. Quantitative analysis of the mechanism of endocytic actin patch assembly and disassembly in fission yeast. *Mol Biol Cell* **21**, 2894-2904, doi:10.1091/mbc.E10-02-0157 (2010).

42. Kaksonen, M., Sun, Y. & Drubin, D. G. A pathway for association of receptors, adaptors, and actin during endocytic internalization. *Cell* **115**, 475-487 (2003).
43. Basu, R. & Chang, F. Characterization of dip1p reveals a switch in Arp2/3-dependent actin assembly for fission yeast endocytosis. *Curr Biol* **21**, 905-916, doi:10.1016/j.cub.2011.04.047 (2011).
44. Kahraman, A., Malmstrom, L. & Aebersold, R. Xwalk: computing and visualizing distances in cross-linking experiments. *Bioinformatics* **27**, 2163-2164, doi:10.1093/bioinformatics/btr348 (2011).
45. Rouiller, I. *et al.* The structural basis of actin filament branching by the Arp2/3 complex. *J Cell Biol* **180**, 887-895 (2008).
46. Madania, A. *et al.* The *Saccharomyces cerevisiae* homologue of human Wiskott-Aldrich syndrome protein Las17p interacts with the Arp2/3 complex. *Mol Biol Cell* **10**, 3521-3538 (1999).
47. D'Agostino, J. L. & Goode, B. L. Dissection of Arp2/3 complex actin nucleation mechanism and distinct roles for its nucleation-promoting factors in *Saccharomyces cerevisiae*. *Genetics* **171**, 35-47 (2005).
48. Boczkowska, M., Rebowski, G., Kast, D. J. & Dominguez, R. Structural analysis of the transitional state of Arp2/3 complex activation by two actin-bound WCAs. *Nat Commun* **5**, 3308, doi:10.1038/ncomms4308 (2014).
49. Kreishman-Deitrick, M. *et al.* NMR analyses of the activation of the Arp2/3 complex by neuronal Wiskott-Aldrich syndrome protein. *Biochemistry* **44**, 15247-15256 (2005).
50. Kelly, A. E., Kranitz, H., Dotsch, V. & Mullins, R. D. Actin binding to the central domain of WASP/Scar proteins plays a critical role in the activation of the Arp2/3 complex. *J Biol Chem* **281**, 10589-10597 (2006).
51. Liu, S. L., Needham, K. M., May, J. R. & Nolen, B. J. Mechanism of a concentration-dependent switch between activation and inhibition of Arp2/3 complex by coronin. *J Biol Chem* **286**, 17039-17046, doi:10.1074/jbc.M111.219964 (2011).
52. Weaver, A. M. *et al.* Interaction of cortactin and N-WASp with Arp2/3 complex. *Curr Biol* **12**, 1270-1278 (2002).
53. Zalevsky, J., Grigorova, I. & Mullins, R. D. Activation of the Arp2/3 complex by the *Listeria acta* protein. Acta binds two actin monomers and three subunits of the Arp2/3 complex. *J Biol Chem* **276**, 3468-3475 (2001).
54. Padrick, S. B., Doolittle, L. K., Brautigam, C. A., King, D. S. & Rosen, M. K. Arp2/3 complex is bound and activated by two WASP proteins. *Proc Natl Acad Sci U S A* **108**, E472-479, doi:10.1073/pnas.1100236108 (2011).
55. Ti, S. C., Jurgenson, C. T., Nolen, B. J. & Pollard, T. D. Structural and biochemical characterization of two binding sites for nucleation-promoting factor

- WASp-VCA on Arp2/3 complex. *Proc Natl Acad Sci U S A* **108**, E463-471, doi:10.1073/pnas.1100125108 (2011).
56. Jurgenson, C. T. & Pollard, T. D. Crystals of the Arp2/3 complex in two new space groups with structural information about actin-related protein 2 and potential WASP binding sites. *Acta Crystallogr F Struct Biol Commun* **71**, 1161-1168, doi:10.1107/S2053230X15013515 (2015).
 57. Wen, K. K. & Rubenstein, P. A. Acceleration of yeast actin polymerization by yeast Arp2/3 complex does not require an Arp2/3-activating protein. *J Biol Chem* **280**, 24168-24174, doi:10.1074/jbc.M502024200 (2005).
 58. Nolen, B. J. & Pollard, T. D. Structure and biochemical properties of fission yeast ARP2/3 complex lacking the ARP2 subunit. *J Biol Chem* **283**, 26490-26498 (2008).
 59. Krissinel, E. & Henrick, K. Inference of macromolecular assemblies from crystalline state. *J Mol Biol* **372**, 774-797, doi:10.1016/j.jmb.2007.05.022 (2007).
 60. Chen, Q. & Pollard, T. D. Actin Filament Severing by Cofilin Dismantles Actin Patches and Produces Mother Filaments for New Patches. *Curr Biol* (2013).
 61. Rodal, A. A., Manning, A. L., Goode, B. L. & Drubin, D. G. Negative regulation of yeast WASp by two SH3 domain-containing proteins. *Curr Biol* **13**, 1000-1008 (2003).
 62. Humphries, C. L. *et al.* Direct regulation of Arp2/3 complex activity and function by the actin binding protein coronin. *J Cell Biol* **159**, 993-1004 (2002).
 63. Sato, M., Dhut, S. & Toda, T. New drug-resistant cassettes for gene disruption and epitope tagging in *Schizosaccharomyces pombe*. *Yeast* **22**, 583-591, doi:10.1002/yea.1233 (2005).
 64. Wu, J. Q., Kuhn, J. R., Kovar, D. R. & Pollard, T. D. Spatial and temporal pathway for assembly and constriction of the contractile ring in fission yeast cytokinesis. *Developmental cell* **5**, 723-734 (2003).
 65. Schneider, C. A., Rasband, W. S. & Eliceiri, K. W. NIH Image to ImageJ: 25 years of image analysis. *Nat Methods* **9**, 671-675 (2012).
 66. Edelstein, A., Amodaj, N., Hoover, K., Vale, R. & Stuurman, N. Computer control of microscopes using microManager. *Curr Protoc Mol Biol* **Chapter 14**, Unit14 20, doi:10.1002/0471142727.mb1420s92 (2010).
 67. Helgeson, L. A. & Nolen, B. J. Mechanism of synergistic activation of Arp2/3 complex by cortactin and N-WASP. *eLife* **2**, e00884, doi:10.7554/eLife.00884 (2013).
 68. Berro, J. & Pollard, T. D. Local and global analysis of endocytic patch dynamics in fission yeast using a new "temporal superresolution" realignment method. *Mol Biol Cell* **25**, 3501-3514, doi:10.1091/mbc.E13-01-0004 (2014).

69. Takeda, T. & Chang, F. Role of fission yeast myosin I in organization of sterol-rich membrane domains. *Curr Biol* **15**, 1331-1336, doi:10.1016/j.cub.2005.07.009 (2005).
70. Oda, T., Iwasa, M., Aihara, T., Maeda, Y. & Narita, A. The nature of the globular- to fibrous-actin transition. *Nature* **457**, 441-445, doi:10.1038/nature07685 (2009).
71. Afonine, P. V. *et al.* Towards automated crystallographic structure refinement with phenix.refine. *Acta Crystallogr D Biol Crystallogr* **68**, 352-367, doi:10.1107/S0907444912001308 (2012).

REFERENCES CITED

CHAPTER III

1. Campellone KG & Welch MD (2010) A nucleator arms race: cellular control of actin assembly. *Nat Rev Mol Cell Biol* 11(4):237-251.
2. Skau CT & Waterman CM (2015) Specification of Architecture and Function of Actin Structures by Actin Nucleation Factors. *Annual review of biophysics* 44:285-310.
3. Amann KJ & Pollard TD (2001) The Arp2/3 complex nucleates actin filament branches from the sides of pre-existing filaments. *Nat Cell Biol* 3(3):306-310.
4. Achard V, *et al.* (2010) A "primer"-based mechanism underlies branched actin filament network formation and motility. *Curr Biol* 20(5):423-428.
5. Wagner AR, Luan Q, Liu S-L, & Nolen BJ (2013) WISH/DIP/SPIN90 proteins form a class of Arp2/3 complex activators that function without preformed actin filaments. *Curr Biol* 23(20):1990-1998.
6. Rotty JD, Wu C, & Bear JE (2013) New insights into the regulation and cellular functions of the ARP2/3 complex. *Nat Rev Mol Cell Biol* 14(1):7-12.
7. Goley ED & Welch MD (2006) The ARP2/3 complex: an actin nucleator comes of age. *Nat Rev Mol Cell Biol* 7(10):713-726.
8. LeClaire LL, 3rd, Baumgartner M, Iwasa JH, Mullins RD, & Barber DL (2008) Phosphorylation of the Arp2/3 complex is necessary to nucleate actin filaments. *J Cell Biol* 182(4):647-654.
9. Marchand JB, Kaiser DA, Pollard TD, & Higgs HN (2001) Interaction of WASP/Scar proteins with actin and vertebrate Arp2/3 complex. *Nat Cell Biol* 3(1):76-82.
10. Kelly AE, Kranitz H, Dotsch V, & Mullins RD (2006) Actin binding to the central domain of WASP/Scar proteins plays a critical role in the activation of the Arp2/3 complex. *J Biol Chem* 281(15):10589-10597.
11. Hetrick B, Han MS, Helgeson LA, & Nolen BJ (2013) Small molecules CK-666 and CK-869 inhibit actin-related protein 2/3 complex by blocking an activating conformational change. *Chem Biol* 20(5):701-712.
12. Goley ED, Rodenbusch SE, Martin AC, & Welch MD (2004) Critical conformational changes in the Arp2/3 complex are induced by nucleotide and nucleation promoting factor. *Mol Cell* 16(2):269-279.
13. Rodal AA, *et al.* (2005) Conformational changes in the Arp2/3 complex leading to actin nucleation. *Nat Struct Mol Biol* 12(1):26-31.

14. Martin AC, *et al.* (2005) Effects of Arp2 and Arp3 nucleotide-binding pocket mutations on Arp2/3 complex function. *J Cell Biol* 168(2):315-328.
15. Xu XP, *et al.* (2011) Three-dimensional reconstructions of Arp2/3 complex with bound nucleation promoting factors. *Embo J*.
16. Higgs HN, Blanchoin L, & Pollard TD (1999) Influence of the C terminus of Wiskott-Aldrich syndrome protein (WASp) and the Arp2/3 complex on actin polymerization. *Biochemistry* 38(46):15212-15222.
17. Mullins RD, Heuser JA, & Pollard TD (1998) The interaction of Arp2/3 complex with actin: nucleation, high affinity pointed end capping, and formation of branching networks of filaments. *Proc Natl Acad Sci U S A* 95(11):6181-6186.
18. Martin AC, Welch MD, & Drubin DG (2006) Arp2/3 ATP hydrolysis-catalysed branch dissociation is critical for endocytic force generation. *Nat Cell Biol* 8(8):826-833.
19. Smith BA, *et al.* (2013) Three-color single molecule imaging shows WASP detachment from Arp2/3 complex triggers actin filament branch formation. *eLife* 2:e01008.
20. Robinson RC, *et al.* (2001) Crystal structure of Arp2/3 complex. *Science* 294(5547):1679-1684.
21. Nolen BJ, Littlefield RS, & Pollard TD (2004) Crystal structures of actin-related protein 2/3 complex with bound ATP or ADP. *Proc Natl Acad Sci U S A* 101(44):15627-15632.
22. Nolen BJ & Pollard TD (2007) Insights into the influence of nucleotides on actin family proteins from seven structures of Arp2/3 complex. *Mol Cell* 26(3):449-457.
23. Luan Q & Nolen BJ (2013) Structural basis for regulation of Arp2/3 complex by GMF. *Nat Struct Mol Biol* 20(9):1062-1068.
24. Rouiller I, *et al.* (2008) The structural basis of actin filament branching by the Arp2/3 complex. *J Cell Biol* 180(5):887-895.
25. Padrick SB, Doolittle LK, Brautigam CA, King DS, & Rosen MK (2011) Arp2/3 complex is bound and activated by two WASP proteins. *Proc Natl Acad Sci U S A* 108(33):E472-479.
26. Boczkowska M, Rebowski G, Kast DJ, & Dominguez R (2014) Structural analysis of the transitional state of Arp2/3 complex activation by two actin-bound WCAs. *Nat Commun* 5:3308.
27. Ti SC, Jurgenson CT, Nolen BJ, & Pollard TD (2011) Structural and biochemical characterization of two binding sites for nucleation-promoting factor WASp-VCA on Arp2/3 complex. *Proc Natl Acad Sci U S A* 108(33):E463-471.
28. Liu SL, Needham KM, May JR, & Nolen BJ (2011) Mechanism of a concentration-dependent switch between activation and inhibition of Arp2/3 complex by coronin. *J Biol Chem* 286(19):17039-17046.

29. Kreishman-Deitrick M, *et al.* (2005) NMR analyses of the activation of the Arp2/3 complex by neuronal Wiskott-Aldrich syndrome protein. *Biochemistry* 44(46):15247-15256.
30. Zalevsky J, Grigorova I, & Mullins RD (2001) Activation of the Arp2/3 complex by the Listeria acta protein. Acta binds two actin monomers and three subunits of the Arp2/3 complex. *J Biol Chem* 276(5):3468-3475.
31. Panchal SC, Kaiser DA, Torres E, Pollard TD, & Rosen MK (2003) A conserved amphipathic helix in WASP/Scar proteins is essential for activation of Arp2/3 complex. *Nature structural biology* 10(8):591-598.
32. Chereau D, *et al.* (2005) Actin-bound structures of Wiskott-Aldrich syndrome protein (WASP)-homology domain 2 and the implications for filament assembly. *Proc Natl Acad Sci U S A* 102(46):16644-16649.
33. Pan F, Egile C, Lipkin T, & Li R (2004) ARPC1/Arc40 mediates the interaction of the actin-related protein 2 and 3 complex with Wiskott-Aldrich syndrome protein family activators. *J Biol Chem* 279(52):54629-54636.
34. Jurgenson CT & Pollard TD (2015) Crystals of the Arp2/3 complex in two new space groups with structural information about actin-related protein 2 and potential WASP binding sites. *Acta Crystallogr F Struct Biol Commun* 71(Pt 9):1161-1168.
35. Britto PJ, Knipping L, & Wolff J (2002) The local electrostatic environment determines cysteine reactivity of tubulin. *J Biol Chem* 277(32):29018-29027.
36. Kahraman A, Malmstrom L, & Aebersold R (2011) Xwalk: computing and visualizing distances in cross-linking experiments. *Bioinformatics* 27(15):2163-2164.
37. Helgeson LA & Nolen BJ (2013) Mechanism of synergistic activation of Arp2/3 complex by cortactin and N-WASP. *eLife* 2:e00884.
38. Wen KK & Rubenstein PA (2005) Acceleration of yeast actin polymerization by yeast Arp2/3 complex does not require an Arp2/3-activating protein. *J Biol Chem* 280(25):24168-24174.
39. Yamaguchi H, *et al.* (2000) Two tandem verprolin homology domains are necessary for a strong activation of Arp2/3 complex-induced actin polymerization and induction of microspike formation by N-WASP. *Proc Natl Acad Sci U S A* 97(23):12631-12636.
40. Derry JM, *et al.* (1995) WASP gene mutations in Wiskott-Aldrich syndrome and X-linked thrombocytopenia. *Human molecular genetics* 4(7):1127-1135.
41. Dayel MJ, Holleran EA, & Mullins RD (2001) Arp2/3 complex requires hydrolyzable ATP for nucleation of new actin filaments. *Proc Natl Acad Sci U S A* 98(26):14871-14876.
42. Helgeson LA, Prendergast JG, Wagner AR, Rodnick-Smith M, & Nolen BJ (2014) Interactions with Actin Monomers, Actin Filaments, and Arp2/3 Complex

- Define the Roles of WASP Family Proteins and Cortactin in Coordinately Regulating Branched Actin Networks. *J Biol Chem* 289(42):28856-28869.
43. Uruno T, *et al.* (2001) Activation of Arp2/3 complex-mediated actin polymerization by cortactin. *Nat Cell Biol* 3(3):259-266.
 44. Huang C, *et al.* (1997) Down-regulation of the filamentous actin cross-linking activity of cortactin by Src-mediated tyrosine phosphorylation. *J Biol Chem* 272(21):13911-13915.
 45. Sirotkin V, Beltzner CC, Marchand JB, & Pollard TD (2005) Interactions of WASp, myosin-I, and verprolin with Arp2/3 complex during actin patch assembly in fission yeast. *J Cell Biol* 170(4):637-648.
 46. Kinley AW, *et al.* (2003) Cortactin interacts with WIP in regulating Arp2/3 activation and membrane protrusion. *Curr Biol* 13(5):384-393.
 47. Narayanan A, LeClaire LL, 3rd, Barber DL, & Jacobson MP (2011) Phosphorylation of the Arp2 subunit relieves auto-inhibitory interactions for Arp2/3 complex activation. *PLoS Comput Biol* 7(11):e1002226.
 48. Nolen BJ & Pollard TD (2008) Structure and biochemical properties of fission yeast ARP2/3 complex lacking the ARP2 subunit. *J Biol Chem* 283(39):26490-26498.
 49. Boczkowska M, Rebowski G, & Dominguez R (2013) Glia maturation factor (GMF) interacts with Arp2/3 complex in a nucleotide state-dependent manner. *J Biol Chem* 288(36):25683-25688.
 50. Liu SL, May JR, Helgeson LA, & Nolen BJ (2013) Insertions within the actin core of actin-related protein 3 (Arp3) modulate branching nucleation by Arp2/3 complex. *J Biol Chem* 288(1):487-497.

REFERENCES CITED

APPENDIX A

1. Oda T, Iwasa M, Aihara T, Maeda Y, Narita A. The nature of the globular- to fibrous-actin transition. *Nature*. 2009;457(7228):441-5.
2. Rouiller I, Xu XP, Amann KJ, Egile C, Nickell S, Nicastro D, et al. The structural basis of actin filament branching by the Arp2/3 complex. *J Cell Biol*. 2008;180(5):887-95.
3. Luan Q, Nolen BJ. Structural basis for regulation of Arp2/3 complex by GMF. *Nature structural & molecular biology*. 2013;20(9):1062-8.
4. Kahraman A, Malmstrom L, Aebersold R. Xwalk: computing and visualizing distances in cross-linking experiments. *Bioinformatics*. 2011;27(15):2163-4.
5. Murakami K, Yasunaga T, Noguchi TQ, Gomibuchi Y, Ngo KX, Uyeda TQ, et al. Structural basis for actin assembly, activation of ATP hydrolysis, and delayed phosphate release. *Cell*. 2010;143(2):275-87.
6. Martin AC, Xu XP, Rouiller I, Kaksonen M, Sun Y, Belmont L, et al. Effects of Arp2 and Arp3 nucleotide-binding pocket mutations on Arp2/3 complex function. *J Cell Biol*. 2005;168(2):315-28.
7. Anandakrishnan R, Aguilar B, Onufriev AV. H++ 3.0: automating pK prediction and the preparation of biomolecular structures for atomistic molecular modeling and simulations. *Nucleic Acids Res*. 2012;40(Web Server issue):W537-41.
8. Cavallo L, Kleinjung J, Fraternali F. POPS: A fast algorithm for solvent accessible surface areas at atomic and residue level. *Nucleic Acids Res*. 2003;31(13):3364-6.
9. Hetrick B, Han MS, Helgeson LA, Nolen BJ. Small molecules CK-666 and CK-869 inhibit actin-related protein 2/3 complex by blocking an activating conformational change. *Chem Biol*. 2013;20(5):701-12.

REFERENCES CITED

APPENDIX B

1. Rouiller I, *et al.* (2008) The structural basis of actin filament branching by the Arp2/3 complex. *J Cell Biol* 180(5):887-895.
2. Murakami K, *et al.* (2010) Structural basis for actin assembly, activation of ATP hydrolysis, and delayed phosphate release. *Cell* 143(2):275-287.
3. Kahraman A, Malmstrom L, & Aebersold R (2011) Xwalk: computing and visualizing distances in cross-linking experiments. *Bioinformatics* 27(15):2163-2164.
4. Hetrick B, Han MS, Helgeson LA, & Nolen BJ (2013) Small molecules CK-666 and CK-869 inhibit actin-related protein 2/3 complex by blocking an activating conformational change. *Chem Biol* 20(5):701-712.
5. Liu SL, May JR, Helgeson LA, & Nolen BJ (2013) Insertions within the actin core of actin-related protein 3 (Arp3) modulate branching nucleation by Arp2/3 complex. *J Biol Chem* 288(1):487-497.
6. Bahler J, *et al.* (1998) Heterologous modules for efficient and versatile PCR-based gene targeting in *Schizosaccharomyces pombe*. *Yeast* 14(10):943-951.
7. Liu SL, Needham KM, May JR, & Nolen BJ (2011) Mechanism of a concentration-dependent switch between activation and inhibition of Arp2/3 complex by coronin. *J Biol Chem* 286(19):17039-17046.
8. Wagner AR, Luan Q, Liu S-L, & Nolen BJ (2013) WISH/DIP/SPIN90 proteins form a class of Arp2/3 complex activators that function without preformed actin filaments. *Curr Biol* 23(20):1990-1998.
9. Helgeson LA, Prendergast JG, Wagner AR, Rodnick-Smith M, & Nolen BJ (2014) Interactions with Actin Monomers, Actin Filaments, and Arp2/3 Complex Define the Roles of WASP Family Proteins and Cortactin in Coordinately Regulating Branched Actin Networks. *J Biol Chem* 289(42):28856-28869.
10. Pollard TD (1986) Rate constants for the reactions of ATP- and ADP-actin with the ends of actin filaments. *J Cell Biol* 103(6 Pt 2):2747-2754.
11. Luan Q & Nolen BJ (2013) Structural basis for regulation of Arp2/3 complex by GMF. *Nat Struct Mol Biol* 20(9):1062-1068.
12. Ti SC, Jurgenson CT, Nolen BJ, & Pollard TD (2011) Structural and biochemical characterization of two binding sites for nucleation-promoting factor WASp-VCA on Arp2/3 complex. *Proc Natl Acad Sci U S A* 108(33):E463-471.
13. Boczkowska M, Rebowksi G, Kast DJ, & Dominguez R (2014) Structural analysis of the transitional state of Arp2/3 complex activation by two actin-bound WCAs. *Nat Commun* 5:3308.

14. Wang ZX (1995) An exact mathematical expression for describing competitive binding of two different ligands to a protein molecule. *FEBS Lett* 360(2):111-114.